

Innovative cutting materials for finish shoulder milling Ti-6Al-4V Aero-engine alloy

G.A. Oosthuizen

Supervisor: NF Treurnicht

**Thesis submitted in partial fulfilment of the
requirements for the degree Magister
Scientiae in Engineering**

March 2009



Declaration

I, the undersigned, hereby declare that the work contained in this thesis is my own original work and that I have not previously in its entirety or in part submitted it at any university for a degree.

.....
Signature

.....
Date



Acknowledgements

The author wishes to thank the following people for their contributions:

Mr Nico Treurnicht, for being a mentor, his idea that became the topic, motivation and technical inputs.

Prof Dimitri Dimitrov for his support that enabled the crucial visit to the Fraunhofer Institute in Germany and for the contract to make the completion of this thesis possible.

Dr Nedret Can, for organizing the collaboration with Element Six (Pty) Ltd and guidance throughout the project.

Dr Guven Akdogan, for his skilful guidance, enthusiasm and valuable criticism of my work at Element Six (Pty) Ltd.

Mr Mike Saxer, for his technical assistance during the experiments and his technical inputs.

Mr Norbert Leicher, Daliff Precision Engineering (Pty) Ltd, for hosting concept studies.

Mr Zaid Fakier, Daliff Precision Engineering (Pty) Ltd, for his excellent technical inputs.

Mr Aubrey Simon and Mr Werner Lombard, Denel Land Systems (Western Cape), for permission to use their product as the test bed for concept studies.

Hennie Joubert for creating an inspiring working atmosphere and for being a great friend.

Martin and Hendrinette Oosthuizen, for their never ending love and support.

My Heavenly Father for granting me the ability and grace to pursue my dreams.



Opsomming

Titaan allooie word wêreldwyd ge-implementeer in die lugvaart, mediese en voertuig vervaardigings-industrieë. Die verhoging in brandstofprys en die breë bevolking wat al hoe meer omgewingsbewus raak, stimuleer uiteindelik die vraag na hierdie materiaal met die gesogte belasting tot massa verhouding.

Tans is dit 'n groot uitdaging vir die masjinerings industrie om 'n hoë materiaal verwyderings tempo te handhaaf, sonder om die vorm en funksie van die onderdeel af te skeep. Terselfdertyd is vervaardigingsmaatskappye se doelwit om onderdele so vinnig en goedkoop as moontlik te vervaardig.

Tans word Ti-6Al-4V tussen 30 en 100 m/min gemasjineer. Hoër freestempo's is 'n uitdaging. Alhoewel titaan 'n baie gesogte materiaal is weens sy spesiale eienskappe, maak die sterkpunte masjinerie ook 'n besondere uitdaging.

In hierdie werk is die potensiaal van PCD in hoë spoed freeswerk van Ti-6Al-4V ondersoek en die fundamentele oorsake vir die faling van die snyvlakke bespreek. Die doel is om die huidige materiaal verwyderingstempo's te verbeter. Verskillende snystrategieë is ondersoek om snypunt leeftyd te verhoog.

Faling van die snyvlak gaan gepaard met 'n termo-meganiese hoë siklus swig verskynsel. 'n Moontlikheid om 'n hoër materiaal verwyderingstempo te handhaaf word bespreek en vergelyk met die swakker prestasie van 'n tungsten kARBIED snypunt.

Die werk toon verbetering in vergelyking met huidige resultate uit die literatuur. Die navorsing bevestig ook dat daar 'n gebied bestaan waar 'n spesifieke genereerde temperatuur in die sny area, snypunt leeftyd verbeter, gegee dat die snypunt die besonder veeleisende toestande, soos temperatuur en belasting kan weerstaan.



Synopsis

The titanium alloys have found wide application in the aerospace, biomedical and automotive industries. Soaring fuel prices and environmental concerns are the fundamental drivers that intensify the demand situation for titanium. From a machining viewpoint, one of the challenges companies face, is achieving high material removal rates while maintaining the form and function of the part. The ultimate aim for a machining business remains to make parts quickly.

Conventional cutting speeds range from 30 to 100 m/min in the machining of Ti-6Al-4V. Milling this alloy faster however is challenging. Although titanium is becoming a material of choice, many of the same qualities that enhance titanium's appeal for most applications also contribute to its being one of the most difficult materials to machine.

The author explored the potential for Polycrystalline diamond (PCD) inserts in high speed milling of Ti-6Al-4V, by trying to understand the fundamental causes of tool failure. The objective was to achieve an order of magnitude increase in tool life, while machining at high speed, simply by reducing some of the failure mechanisms through different cutting strategies.

Tool wear is described as a thermo-mechanical high-cycle fatigue phenomenon. The capability of a higher material removal per tool life is achieved in the case of PCD inserts compared to Tungsten carbide (WC). The average surface roughness produced was relatively low. The collected chips were also analyzed.

The work demonstrated progress over the performance reported in current literature. The work confirms that there is a region where a sufficiently high temperature in the cutting zone may contribute to extended tool life, provided that the tool material can withstand these extreme conditions.



Table of Contents

Declaration	i
Acknowledgements	ii
Opsomming	iii
Synopsis	iv
LIST OF FIGURES	ix
LIST OF TABLES	xi
Glossary	1
1. Introduction	4
2. The market for titanium machining	6
2.1 The evolving market	6
2.1.1 Introduction	6
2.1.2 Growing demand	7
2.1.3 Greener skies	8
2.2 Aero-engines	10
2.2.1 Introduction	10
2.2.2 Superalloys	11
2.2.2.1 Types of superalloys	11
2.2.2.2 Applications	12
2.2.3 Machinability of Aero-engine alloys	12
3. Titanium and its machinability characteristics	14
3.1 Introduction	14
3.2 Titanium and its alloys	15
3.2.1 Alpha phase alloys	16
3.2.2 Alpha-Beta alloys	16
3.2.3 Beta phase alloys	17
3.3 Characteristics of Titanium	17
3.4 Titanium in the industry	18
3.4.1 Aerospace sector	19



3.4.1.1	Commercial aerospace	19
3.4.1.2	Military aerospace	20
3.4.2	Automotive applications	21
3.4.3	Biomedical applications	22
3.4.4	Consumer Applications	24
3.4.4.1	Marine markets	24
3.4.4.2	Industrial	24
3.4.4.3	Sport equipment	25
3.4.4.4	Architecture and Construction	25
3.5	Cutting behaviour of Titanium	25
3.6	Ti-6Al-4V alloy	25
3.6.1	Introduction	25
3.6.2	Chemical composition	26
3.6.3	Basic physical and chemical properties	26
3.6.4	Chip Formation	27
3.6.5	Machining challenges	27
3.6.5.1	Poor conductor of heat	28
3.6.5.2	Strong alloying tendency or chemical reactivity	30
3.6.5.3	Low modulus of elasticity	30
3.6.5.4	Small contact area	31
3.6.6	Applications	32
4.	Milling considerations for Ti-6Al-4V	34
4.1	Introduction	34
4.2	Influence of different cutting parameters	35
4.2.1	Cutting speeds (V_c)	35
4.2.2	Feed per tooth (f_z)	36
4.2.3	Influence of axial cut (a_p)	37
4.2.4	Influence of radial cut (a_e)	37
4.2.5	Coolant	37
4.3	Temperature	39
4.4	Cutting forces	41
4.5	Milling strategy	42
5.	Cutting materials and Insert configurations	45
5.1	Introduction	45
5.2	Overall insert geometry	46
5.2.1	Round inserts	46
5.2.2	Square inserts	46
5.2.3	Triangular inserts	47
5.3	Insert properties	47
5.3.1	Transverse Rupture Strength	47
5.3.2	Hardness	48
5.3.3	Fracture toughness	49



5.3.4	Thermal expansion	50
5.3.5	Thermal conductivity	50
5.3.6	Thermal shock resistance	51
5.4	Polycrystalline diamond	52
5.4.1	Introduction	52
5.4.2	CMX 850 (Fine)	53
5.4.3	CTB 010 (Medium)	53
5.4.4	CTM 302 (Coarse)	54
5.4.5	Machining with PCD	54
5.5	Machining with CBN	55
5.6	Machining with Carbide Tools	55
5.7	Summary	56
6.	Machining performance assessment	58
6.1	Tool life	58
6.2	Tool wear	60
6.2.1	Failure Modes	60
6.2.1.1	Temperature failure	60
6.2.1.2	Fracture	61
6.2.1.3	Gradual wear	62
6.2.2	Types of tool wear	62
6.2.2.1	Crater wear	63
6.2.2.2	Flank wear	64
6.2.2.3	Notch wear	64
6.2.2.4	Nose radius wear	64
6.2.3	Mechanisms of tool wear	65
6.2.3.1	Abrasion	65
6.2.3.2	Adhesion	65
6.2.3.3	Diffusion	65
6.2.3.4	Chemical reactions	66
6.2.3.5	Plastic deformation	66
6.3	Surface finish	67
6.3.1	Geometric factors	67
6.3.2	Work material factors	68
6.3.3	Vibration and machine tool factors	69
6.4	Overview of performance assessment considerations	70
7.	Aims and objectives	71
8.	Experimental Setup and Design	72
8.1	Introduction	72
8.2	Background study 1: Palletised work holding to emulate 5-axis machining	73



8.3	Background study 2: Turning PM steels with experimental PCBN	74
8.3.1	Introduction	74
8.3.2	Background to the test	74
8.3.3	Wear Measurement	74
8.3.4	Summary of results	75
8.3.5	Conclusion	75
8.4	Pilot test 1: Influence of different milling parameters	75
8.4.1	Background to test	75
8.4.2	Experimental setup and procedure	75
8.4.3	Results	77
8.5	Background study 3: Cutting strategy for missile hanger	77
8.6	Pilot study 2: Roll-in strategy for PCD materials	78
8.7	Experimental setup, design and procedure for final experiments	80
8.7.1	Experimental setup	80
8.7.2	Material specifications	85
8.7.3	Test Equipment	86
8.7.4	Experimental design	87
8.7.5	Test Procedure	88
8.7.6	Collected Data	88
8.7.7	Wear Measurement	88
9.	Results and discussion	91
9.1	Wear measurements	91
9.1.1	CTM302	91
9.1.2	CTB010	93
9.1.3	CMX850	95
9.1.4	Summary of performance	97
9.2	Wear scar	99
9.3	The performance of CMX850	103
10.	Conclusion	108
11.	References	110
Appendix A:	High Performance machining of titanium: Charting the challenge	I
Appendix B:	Work holding	XIII
Appendix C:	Experimental machine programmes	XXXI



LIST OF FIGURES

FIGURE 2-1: INNOVATION CHANGE THE WORLD, INNOVATION NEEDS CHANGES [2]	6
FIGURE 2-2: ROLLS ROYCE ENGINE ORDER FORECAST [8]	8
FIGURE 2-3: INCREASE IN JET FUEL (US\$/BARREL) [12]	9
FIGURE 2-4: TYPICAL COMMERCIAL AERO-ENGINE MATERIAL CONTENT [14]	10
FIGURE 3-1: PRICES OF U.S. TITANIUM INGOT [28]	14
FIGURE 3-2: WORLD MILL PRODUCT TITANIUM CONSUMPTION BY MAJOR INDUSTRY [41]	18
FIGURE 3-3: TITANIUM USAGE IN GE-90 AERO-ENGINE [30]	19
FIGURE 3-4: TITANIUM IN COMMERCIAL AIRCRAFT [19 & 28]	20
FIGURE 3-5: POTENTIAL AUTOMOTIVE APPLICATIONS OF TITANIUM [30]	22
FIGURE 3-6: BONE PLATE IMPLANT [30]	23
FIGURE 3-7: SCHEMATIC OF ARTIFICIAL HIP-JOINT [30]	24
FIGURE 3-8: Ti-6AL-4V PRODUCING A SERRATED CHIP [53]	27
FIGURE 3-9: THERMAL CONDUCTIVITY (W/M.K) OF DIFFERENT ALLOYS	28
FIGURE 3-10: AREA-WEIGHTED AVERAGE CUTTING TEMPERATURE AS A FUNCTION OF CUTTING SPEED FOR K68 CARBIDE INSERT (CHIP LOAD, 0.127 MM/REV) [56]	29
FIGURE 3-11 TENSILE PROPERTIES OF Ti-6AL-4V AT ROOM AND ELEVATED TEMPERATURES [58]	29
FIGURE 3-12: ELASTIC MODULUS OF DIFFERENT MATERIALS [17 & 19]	31
FIGURE 3-13: CONTACT AREA OF (A) A CONTINUOUS CHIP, AND (B) SERRATED Ti-6AL-4V CHIP [53]	32
FIGURE 4-1: CLIMB (DOWN) AND CONVENTIONAL (UP) MILLING [66]	34
FIGURE 4-2: VARIOUS MILLING OPERATIONS [66]	35
FIGURE 4-3: INFLUENCE OF FEED RATE ON TOOL LIFE [66]	36
FIGURE 4-4: HEAT GENERATED DISTRIBUTION AS A FUNCTION OF THE THERMAL CONDUCTIVITY OF THE TOOL [71]	38
FIGURE 4-5 TEMPERATURE GENERATED FOR DIFFERENT CUTTING CONDITIONS [74]	40
FIGURE 4-6: EFFECT OF CUTTING SPEED ON TOOL LIFE ($F_z = 0.025\text{MM/Z}$, $A_e = 0.25\text{MM}$, FORGED Ti6AL4V, A50) [56]	41
FIGURE 4-7: EFFECT OF CUTTING SPEED ON CUTTING FORCE. (FORGED, $H_x=0.025\text{MM}$, $A_e=0.25\text{MM}$, A50) [56]	42
FIGURE 4-8: ROLL-IN MACHINING STRATEGY [66]	43
FIGURE 5-1: PRIMARY ASPECTS ASSOCIATED WITH ADVANCING CUTTING TECHNOLOGY [76]	45
FIGURE 5-2: DIFFERENT TOOL SHAPES [75 & 77]	46
FIGURE 5-3: THE EFFECT OF TRANSVERSE RUPTURE STRENGTH ON TOOL LIFE [56]	47
FIGURE 5-4: TRANSVERSE RUPTURE STRENGTH OF DIFFERENT CUTTING MATERIALS	48
FIGURE 5-5: HARDNESS OF DIFFERENT CUTTING MATERIALS	49
FIGURE 5-6: FRACTURE TOUGHNESS OF DIFFERENT CUTTING MATERIALS	49
FIGURE 5-7: THERMAL EXPANSION COEFFICIENT OF DIFFERENT CUTTING MATERIALS	50
FIGURE 5-8: THERMAL CONDUCTIVITY OF DIFFERENT CUTTING MATERIALS [75]	51
FIGURE 5-9: EFFECT OF THERMAL SHOCK RESISTANCE (R_T) ON TOOL LIFE [56]	52
FIGURE 5-10: TRANSVERSE RUPTURE STRENGTH AND FRACTURE TOUGHNESS OF DIFFERENT PCD MATERIALS [79]	54
FIGURE 6-1: TOOL LIFE	58
FIGURE 6-2: AVERAGE FLANK WEAR (V_B) FOR DIFFERENT CUTTING SPEEDS [101]	59
FIGURE 6-3: RELATIONSHIP BETWEEN THERMAL CRACK RESISTANCE AND THERMAL EXPANSION COEFFICIENT [75]	61
FIGURE 6-4: RELATIONSHIP BETWEEN CHIP RESISTANCE AND TRANSVERSE RUPTURE STRENGTH [75]	62
FIGURE 6-5: TYPES OF TOOL WEAR	63
FIGURE 6-6: RELATIONSHIP BETWEEN FLANK WEAR RESISTANCE AND HARDNESS [75]	64
FIGURE 6-7: TYPES OF TOOL WEAR [20]	65
FIGURE 6-8: RELATIONSHIP BETWEEN PLASTIC DEFORMATION RESISTANCE AND HARDNESS	67
FIGURE 6-9: THE EFFECTS OF NOSE RADIUS AND FEED OF SURFACE ROUGHNESS [19]	68
FIGURE 6-10: AVERAGE SURFACE ROUGHNESS (R_A) FOR WC AND PCD INSERTS [101]	69
FIGURE 8-1: RESEARCH PROCEDURE FLOW DIAGRAM	72



FIGURE 8-2: INFLUENCE OF DIFFERENT CUTTING PARAMETERS ON TOOL LIFE.....	77
FIGURE 8-3: MISSILE HANGER	78
FIGURE 8-4: CONVENTIONAL ROLL-IN MILLING STRATEGY FOR PCD.....	79
FIGURE 8-5: RESULTS OF CUTTING STRATEGY USING PCD.....	80
FIGURE 8-6: MACHINERY AND EQUIPMENT FOR EXPERIMENTS.....	83
FIGURE 8-7: EXPERIMENTAL TEST PROCEDURE	88
FIGURE 8-8: ACID (HCL - 32 VOL %) CLEANING PROCESS OF SOME PCD SAMPLES	89
FIGURE 9-1: CTM302 WEAR (V_B) MEASUREMENTS FOR DIFFERENT CONDITIONS	91
FIGURE 9-2: FLANK AND CRATER WEAR OF CTM302 AT HIGH CUTTING SPEEDS	92
FIGURE 9-3: ESTIMATED PERFORMANCE OF CTM302 FOR CERTAIN CONDITIONS	92
FIGURE 9-4: CTB010 WEAR (V_B) MEASUREMENTS FOR DIFFERENT CONDITIONS	93
FIGURE 9-5: FLANK AND CRATER WEAR OF CTB010 AT HIGH CUTTING SPEEDS	94
FIGURE 9-6: ESTIMATED PERFORMANCE OF CTB010 FOR CERTAIN CONDITIONS	94
FIGURE 9-7: CMX850 WEAR (V_B) MEASUREMENTS FOR DIFFERENT CONDITIONS	95
FIGURE 9-8: FLANK AND CRATER WEAR OF CMX850 AT HIGH CUTTING SPEEDS	96
FIGURE 9-9: ESTIMATED PERFORMANCE OF CMX850 FOR CERTAIN CONDITIONS	96
FIGURE 9-10: PERFORMANCE OF DIFFERENT INSERTS.....	97
FIGURE 9-11: INFLUENCE OF CUTTING SPEED (V_C) AND FEED RATE (F_z)	98
FIGURE 9-12: INFLUENCE OF DIFFERENT PARAMETERS.....	98
FIGURE 9-13: PCD WEAR SCAR	100
FIGURE 9-14: BUILD-UP ANALYZED USING THE SEM.....	101
FIGURE 9-15: EDM SECTIONED WEAR SCAR.....	102
FIGURE 9-16: TOOL LIFE OF CMX850 AT DIFFERENT CUTTING SPEEDS ($F_z=0.05\text{MM/Z}$).....	103
FIGURE 9-17: TOOL LIFE OF CMX850 COMPARED TO THE VP15TF AT ELEVATED CUTTING SPEEDS.....	104
FIGURE 9-18: TOOL LIFE OF CMX850 AND VP15TF ($F_z = 0.05\text{MM/Z}$)	104
FIGURE 9-19: SURFACE ROUGHNESS (R_a) PRODUCED IN DIFFERENT CONDITIONS.....	106
FIGURE 9-20: CHIP FORMATION FOR CMX850 AT DIFFERENT CUTTING SPEEDS	107



LIST OF TABLES

TABLE 2-1: ENGINE DELIVERIES PER SECTOR [9].....	8
TABLE 4-1: DIFFERENT CUTTING CONDITIONS FOR TEMPERATURE MEASUREMENTS	40
TABLE 8-1: EXPERIMENTAL EQUIPMENT AND MACHINING SPECIFICATIONS FOR PILOT TESTS WITH WC	76
TABLE 8-2: EXPERIMENTAL PILOT TEST CONDITIONS AND RESULTS	76
TABLE 8-3: INSERT SPECIFICATIONS AND CUTTING CONDITIONS FOR CUTTING STRATEGY EXPERIMENT	79
TABLE 8-4: INSERT SPECIFICATIONS AND CUTTING CONDITIONS FOR FINAL EXPERIMENTS	81
TABLE 8-5: INSERT PROPERTIES COMPARISON [79]	84
TABLE 8-6: COMPOSITION (WT %) OF Ti-6AL-4V [32].....	85
TABLE 8-7: MECHANICAL AND PHYSICAL PROPERTIES OF THE Ti-6AL-4V SAMPLE AT ROOM TEMPERATURE.....	86
TABLE 8-8: MACHINERY AND EQUIPMENT	86
TABLE 8-9: EXPERIMENTAL DESIGN	87
TABLE 9-1: INFLUENCE OF THE DIFFERENT PARAMETERS	99
TABLE 9-2: TYPICAL BREAKDOWN (%WT) ON A SPECTRUM OF THE BUILD-UP ON THE PCD INSERTS	101



Glossary

Abrasion wear	A wear pattern that occurs due to the chips rubbing across the surface of the tool.
Adhesiveness	A term that describes the stickiness of a material.
a_e	Working engagement
Allotropy	The property by which certain elements may exist in more than one crystal structure. An allotrope is a specific crystal structure of the metal.
Alloy system	A complete series of compositions produced by mixing in all proportions any group of two or more components, at least of which is metal.
Alpha	The low temperature allotrope of titanium with a hexagonal, close-packed crystal structure.
Alpha-beta structure	A microstructure containing α and β as the principal phases at a specific temperature.
Annealing	A generic term denoting a treatment, consisting of heating to, and holding at, a suitable temperature followed by cooling at a suitable rate.
ANSI	An organization founded in 1918 that developed standards for industrial products in the United States.
a_p	Cutting depth
Beta	The high temperature allotrope of titanium with a body-centered cubic crystal structure that occurs above the β transus.
Binder	A substance added to the powder to increase the strength of the compact and cement together powder particles that alone would not sinter into a strong object.
Brinell hardness number (HB)	A number related to the applied load and to the surface area of the permanent impression made by a ball indenter.
Brittleness	The tendency of a material to fracture without first undergoing significant plastic deformation. Contrast with ductility.
Built-up edge	It is a condition where some of the work piece material welds to the cutting edge.
CBN	Cubic Boron Nitride
Cemented carbide	Material that is manufactured by combining tungsten carbide (WC) powders and binder cobalt powders (Co).
Ceramics	Cutting materials that offers high mechanical and thermal properties.
Cermets	Sintered alloy that is comprised of titanium carbide (TiC), titanium nitride (TiN) and nickel (Ni) binder.
CIS	Standards developed by Japan Cemented Carbide Tool Manufacturers Association.
Coarse grains	Grains larger than normal for the particular wrought metal or alloy or of



	a size that produces a surface roughening known as alligator skin in wrought metals.
Compact	An object produced by compression of metal powder, generally while confined in a die, with or without the inclusion of non-metallic constituents.
Corrosion	The deterioration of a metal by a chemical or electrochemical reaction with its environment.
Corrosive wear	Wear in which chemical or electrochemical reaction with the environment is significant
Depth of cut	Describe the thickness of the work piece material that is to be removed by the cutting edge when machining.
Ductility	The ability of a material to deform plastically before fracturing. Measured by elongation or reduction of area in a tension test
EDM	Electric Discharge Machining
Fatigue	The phenomenon leading to fracture under repeated or fluctuating stresses having a maximum value less than the tensile strength of the material. Fatigue fractures are progressive, beginning as minute cracks that grow under the action of fluctuating stress.
Feed (v_f)	The distance a tool moves in a given time period.
Feed per tooth (f_z)	The amount of movement of the table from when one tooth comes to the cutting position to when another tooth comes to the cutting position.
Fracture toughness	Term that is used as a measure of resistance of a material to failure from fracture from a pre-existing crack.
Hardness	A measure of the resistance of a material to surface indentation or abrasion; may be thought of as a function of the stress required to produce some specified type of surface deformation. There is no absolute scale for hardness.
Impurities	Undesirable elements or compounds in the material.
Inclusion	A particle of foreign material in a metallic matrix. The particle is usually a compound (oxide, sulphide).
ISO	International Organization for Standardization
Machinability	The relative ease of machining a metal.
Megatrends	Long-term processes of transformation with a broad scope and a dramatic impact. They are considered to be powerful factors which shape future markets.
Melting point	The temperature at which a pure metal, compound, or eutectic changes from solid to liquid. The temperature at which the liquid and solid are in equilibrium.
Microstructure	Refers to the phases and grain structure present in a metallic component.
MRR	Material removal rate
Oxidation	A reaction in which there is an increase in valence resulting from a loss of electrons. Contrast with reduction.



Passes	Term given to the number of times the cut needs to be carried out.
PCBN	Polycrystalline Cubic Boron Nitride
PCD	Polycrystalline diamond
PM	Powder Metallurgy
Residual stress	Stress remaining in a structure or member as a result of thermal or mechanical treatment or both. Stress arises in fusion welding primarily the weld metal contracts on cooling from the solidus to room temperature.
Rockwell hardness number (HR)	A number derived from the net increase in depth of impression as the load of the indenter is increased and decreased from a fixed load. The numbers are always quoted with a scale symbol.
Rupture stress	The stress at failure. Also known as breaking or fracture stress.
SEM	Scanning Electron Microscope
Shoulder milling	A machining process (milling) in which 90° walls can be achieved.
Sintering	A process of heating a material and bonding its powder particles or compressed powder particles.
Spindle	A rotation axis of a machine, on which a cutting tool is mounted.
Surface Hardening	A generic term covering several processes applicable to a suitable ferrous alloy that produces, by quench hardening only, a surface layer that is harder or more wear resistant than the core.
V_b	Average flank wear [This comes from the German "Verschleißmarkbreite" (wear width)]
V_c	Cutting speed
Vickers Hardness number	An indentation hardness test employing a 136° diamond pyramid indenter (Vickers) and variable loads, enabling the use of one hardness scale for all ranges of hardness.
WC	Tungsten Carbide
XRD	X-Ray Diffraction



1. Introduction

The purpose of this project is to determine how to exploit the high performance milling approach on titanium.

The global trend is towards faster, greener results. Aircraft manufacturing is in a growth phase, and as a result, the demand for titanium components in aircraft manufacture is experiencing significant growth. It holds the key to mass reduction where load bearing or performance under moderately elevated temperatures is required. The superior mass to strength ratio results in reduced fuel consumption and emissions.

The South African government has successfully included counter trade clauses into recent aircraft acquisition transactions. To support future counter trade opportunities, the Department of Science and Technology (DST) has embarked on a manufacturing capability enhancement programme. Manufacturing processes of light metals with an emphasis on titanium machining is one of the research initiatives supported by the DST.

The current business perspective for success is to take global megatrends into consideration to deduce a unique custom company focus. Soaring fuel prices, environmental concerns and increased air travel demand are drivers that intensify the demand situation for titanium. A growing market niche for high value titanium machined components is perceived. Ti-6Al-4V is one of the most popular titanium alloys. Machining is a major cost contributor. It creates an opportunity for a supplier to gain a competitive advantage. Tool materials able to withstand high temperatures, such as PCD, is shown to have potential to last significantly longer at higher cutting speeds. Cutting strategy is another potential focus area to achieve effective improvements.

Hypothesis

PCD cutting materials will yield cost and lead time benefits for titanium machining.

This document contains the different machining challenges of Ti-6Al-4V and indicates the opportunities for effectiveness improvement. This study explores the potential for



innovative cutting materials to mill Ti-6Al-4V at high speeds. Studies of the wear modes and mechanisms were the point of departure to establish performance criteria.



2. The market for titanium machining

“Give me six hours to chop down a tree and I will spend the first four sharpening the axe.” - Abraham Lincoln, US President (1861-65)

2.1 The evolving market

2.1.1 Introduction

The one word that characterises good business in our time is speed. Thomas Friedman states in his book, *The World is Flat*, the twenty-first century will be remembered not for military conflicts or political events, but as the new age of globalization and the “flattening of the world”. The explosion of advanced technologies now means that knowledge, skills and resources have connected all over the planet, levelling the playing field as never before, so that each of us as individuals, businesses, industries or as countries are potentially an equal and a competitor of the other [1]. Think global, act local.

Today the trend is towards Megatrends. Nottbohm [2] mentioned that megatrends are a guide for innovation, which became a relevant strategic issue in many corporate headquarters (figure 2-1).

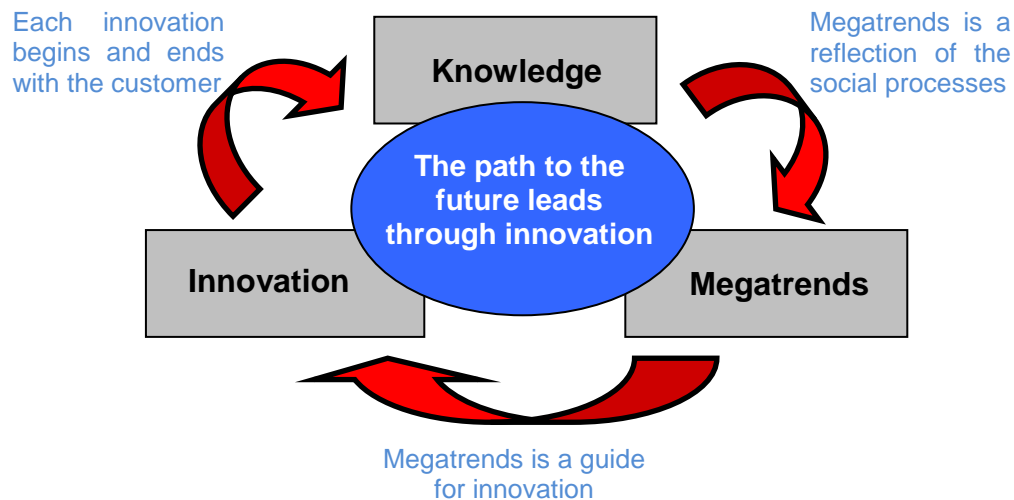


Figure 2-1: Innovation change the world, innovation needs changes [2]

Companies can gain valuable insights if information on a megatrend is translated into a company’s very own context. Globalization, energy and resource reversal, climate



change and environmental impacts are some of the main megatrends [3 & 4] in the manufacturing industry. Climate change and global environmental concern guided aerospace companies to introduce methods to move to greener skies. These megatrends are also directing innovations to the efficient manufacturing of energy resources, like wind- and sea energy turbines. The increase of Russians, Indians and Brazilians that want to fly is a reflection of the new patterns of mobility [3], which is globally increasing.

Outsourcing is enabled by the massive investment in technology of the last decade and now goods, services and skills are sourced easily from almost any part of the globe [5]. The Aerospace industry makes use of outsourcing to a large extent in order to keep costs down and stay competitive. This trend caused a shift of technology development towards the suppliers. Technology development to supply the product faster, cheaper and technologically superior is now a challenge shared by the system integrator and the supplier network.

2.1.2 Growing demand

“Air transportation is definitely a growing industry contributing to economic development and generating wealth around the world.” - Airbus Chief Operating Officer (COO)

Customers, John Leahy.

The global civil aviation industry is estimated to contribute 8% of the world's gross domestic product (GDP), or \$3.5 trillion [6]. The Airbus Global Market Forecast anticipates a demand for 24,300 new passenger and freighter aircraft between 2007 and 2026, creating an average delivery rate of some 1,215 airliners annually during this 20-year period valued at US\$ 2.8 trillion [7]. The aerospace and defence industries are currently experiencing substantial growth (figure 2-2), however it is questionable whether they have sufficient capacity to meet future demands.



Rolls Royce forecast [8] that engine orders will increase from 35 000 in the period 1996-2005 to about 55 000 in 2006-2015 (57% growth).

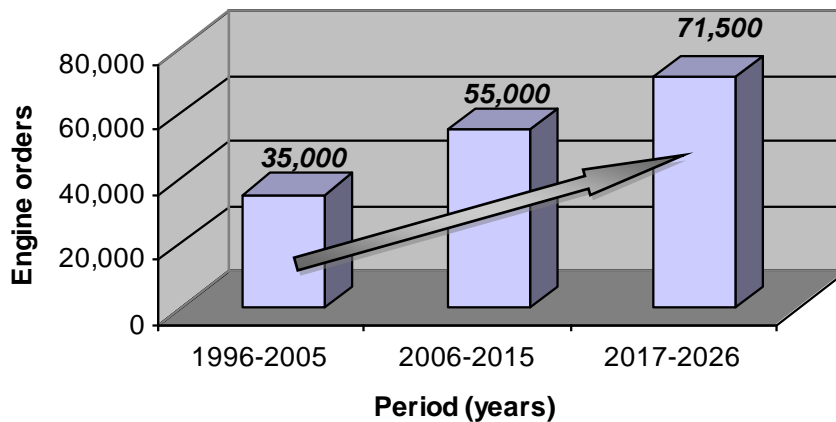


Figure 2-2: Rolls Royce engine order forecast [8]

The latest outlook report forecasts that engine deliveries units are estimated to be 71, 500 in 2017-2026. Engine demand over the next 20 years could be worth US\$ 701 billion as indicated in table 2-1 [9]. Additionally, world traffic is expected to increase by 4.9% p.a. [6, 7 & 9] Since 1970, air traffic has doubled every 15 years, and Airbus expects it to double again in the next 15 years [6]. These high growth rates together with the highly competitive environment in which aerospace companies operate, will necessitate an accompanying increase in effectiveness and capacity. The largest aircraft customers over the next decade will be China and India, and as a result many aircraft components that traditionally would be made in Europe, the US, and Canada are instead being manufactured in these emerging markets [10].

Table 2-1: Engine deliveries per sector [9]

Sector	Units	Value (\$bn)
<i>Business Jets</i>	63,816	93
<i>Regional Aircrafts</i>	14,427	43
<i>Mainline Aircraft</i>	51,126	528
<i>Freighters</i>	2,244	36
Total	131,613	701

2.1.3 Greener skies

April 2008, leaders from across the global aviation industry, the big four Western commercial aircraft manufacturers and the Western aero-engine makers, affirmed their and their companies' commitment to combating global climate change. This will pursue



the development and deployment of new technologies, cleaner fuels and to further improve aircraft fuel efficiency [6]. Fuel is the largest cost for all airlines and a major priority for profitable airline operation.

Figure 2-3 indicate the definite increased trend in jet fuel cost. For some carriers the fuel bill can account for up to 50% of direct operating costs. For most carriers fuel expense grew from 15% to more than 25% of total airline operating costs (2003-2006) [9 & 11]. The market need for approximately 24,300 new aircraft during the next 20 years represents a combined order book value of US\$2.8 trillion, and will be driven by the need for more fuel and eco-efficient aircraft to cope with traffic growth, as well as for the replacement of older-generation equipment [7]. The industry's main emissions are CO₂, H₂O and Nitrogen oxides. The CO₂ emissions are directly proportional to the amount of fuel burnt. According to the UN Intergovernmental Panel on Climate Change, aviation accounts for 2% of global CO₂ emissions [6]. Therefore the drive for fuel efficiency is vital in all airlines operations. This is also reflected in the orders for newer type, fuel efficient airplanes.

By 2026, the fuel consumption of the average world fleet is expected to be at three litres per 100 passenger kilometres (km), similar to the benchmark that the A380 set recently [7]. Cars currently marketed in Europe have an average of 6.5 litres per person per 100 km, while the average for US cars is 9.6 litres [6].

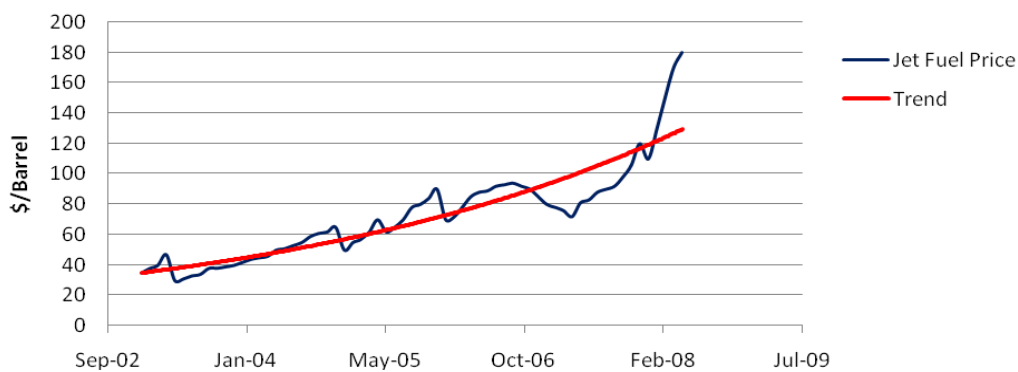


Figure 2-3: Increase in jet fuel (US\$/barrel) [12]

Alternative fuels are also being investigated, such as gas-to-liquids-produced synthetic fuels and possible second-generation non-food bio-fuels. Second generation bio-fuels



might be available by 2020, and the fuels mix including 30% bio-fuels might be in service by 2030 [13].

Whether if the fuel price will fall in the long term only time will tell, however fuel efficiency will remain important to many airlines and fleet renewal is essential part of this. The future trend is to fight climate change and to get our skies greener. Reducing the weight of the aircrafts can contribute a great deal.

2.2 Aero-engines

2.2.1 Introduction

The components of an aero-engine must withstand a highly demanding operating environment. Clearly these conditions place great demands on the materials used in engine construction. The important properties include high temperature, high strength-to-weight ratio and corrosion resistance. The structures must also withstand wide range of thermal and g-force conditions. The maximum operating temperatures could well exceed the melting point of most metals.

Driven by a competitive consumer's market to keep airfares and shipping rates low, aerospace manufacturers need to reduce costs from 5 to 10% annually [10]. This makes the application of the materials used in the aero-engine and efficiency of the manufacturing processes critical. The material for one of the titanium split-fan cases cost \$30 000 per part in 2007 compared to \$5 000 in 2004 [10]. Aero-engines are generally manufactured of alloys of steel, nickel, titanium and aluminium as shown in Figure 2-4 [14].

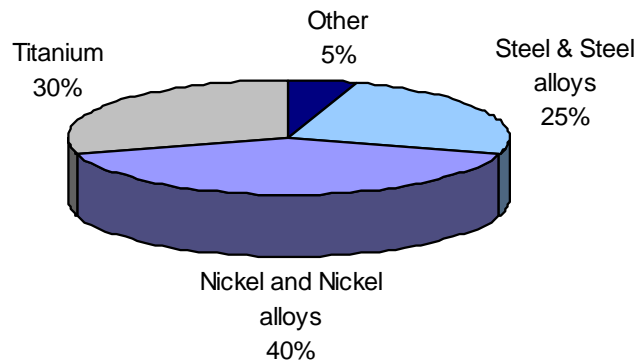


Figure 2-4: Typical commercial aero-engine material content [14]



These materials offer an economical benefit by ensuring efficient fuel consumption and longer operation life because of their properties. Titanium and Nickel-based alloys best satisfy this criterion. There was also an increase in the use of titanium and nickel-based up till the end of the 20th century, suggesting their dominant and competitive use in aerospace engines [15]. Their machinability is however poor, currently limiting their use.

2.2.2 Superalloys

The term superalloy is derived from the especially tough and demanding operational applications where these alloys are used [15]. These applications require high tolerance to extreme temperatures. Superalloys are not only employed in turbine applications, but are also utilized in petrochemical equipment and nuclear reactors [16]. Superalloys represent a category that overlaps the ferrous and nonferrous metals. Some of them are based on iron while others are based on nickel and cobalt. These metals are commercially important as they are rather costly and of technological importance, because of their extraordinary characteristics. The high costs associated with the machining of these materials can be credited to the fact that cutting speeds for superalloys are only 5 to 10% of those used for steel [17].

Nevertheless, in many instances, although superalloys have significant oxidation resistance, it is not sufficient enough for some extreme applications. Therefore many applications at temperatures above 760°C, as in aircraft turbines, the superalloy must be coated [17]. Nickel-based turbine blades can operate at temperatures up to 520°C [13].

2.2.2.1 Types of superalloys

These alloys typically have an austenitic face-centered cubic crystal structure. A superalloy's base alloying element is usually nickel, cobalt, or nickel-iron [17]. These alloys are divided into three groups according to their principal constituent.

1. Iron-based

Iron-based have been developed from austenitic stainless steels. Iron is the main ingredient of this alloy, although it is less than 50% in some cases. Some have very low thermal expansion coefficients which make them especially suited for shafts, rings and casings. However, they have the poorest hot strength properties of the three groups.

Common types: *Inconel 909, A286 and Greek Ascology*

2. Nickel-based



Nickel-based alloys are the most widely used and accounts for about 50 wt% of materials used in an aerospace engine. This is mainly in the gas turbine compartment [13]. The base metal is nickel as the name indicates and this material generally has better high temperature strength than alloy steels. The principal alloying elements are chromium and cobalt. Lesser elements include aluminium and titanium. Inconel 718 is the most popular of the nickel-based alloys, accounting for 25% and 45 % of the annual volume production for cast and wrought nickel-based alloys, respectively [18].

Common types: *Inconel 718 and Inconel 625*

3. Cobalt-based

Cobalt-based alloys display superior hot corrosion resistance at high temperatures, but are more expensive and more difficult to machine compared to nickel-based alloys. Therefore their use in turbines is restricted to combustion parts in the hottest engine areas. They are also used for components in nuclear reactors and surgical implants. The main elements in these alloys are cobalt and chromium [19].

Common types: *Haynes 25 and Stellite 31*

2.2.2.2 Applications

The aerospace industry consumes roughly two-thirds of all the superalloys produced [17]. This industry uses the superalloy to manufacture jet engines and associated components, mainly in the hot end of aircraft engines and land-based turbines. The material's ability to retain high mechanical and chemical properties at elevated temperatures makes it ideal to use in both rotating and stationary components in the hot end of jet engines [20]. The remaining third of superalloy consumption is used by the chemical, medical and structural industries, due to their high temperature properties and exceptional corrosion resistance [21].

2.2.3 Machinability of Aero-engine alloys

Machinability rating depends on tool life, surface finish and power consumed during the operation. Component forces and chip shape also provide a good assessment of the machinability of the material [22]. The poor machinability of super- and titanium alloys are due to their inherent characteristics [23].



These characteristics subject cutting tool materials to extreme thermal and mechanical stresses close to the cutting edge [15]. Titanium alloys reaction with most tool materials at elevated temperatures conditions also results in accelerated tool wear [20].

Although these high-performance alloys are able to withstand extreme temperatures that would destroy conventional metals like steel and aluminium, the low thermal conductivity of titanium alloy (about 15 W/m.°C) and nickel alloy (about 11 W/m.°C) [17], relative to conventional steels or cast iron, leads to significant increase in temperature at the cutting edge during machining [24]. Aero-engine alloys retain most of their strength at these increased cutting temperatures, which also generate additional heat in the shear zone. This leads to rapid tool failure [25]. Typical tool failure includes notching at the nose, flank wear, crater wear and chipping [15].



3. Titanium and its machinability characteristics

3.1 Introduction

In 1791 a priest and part-time chemist, William Gregor, discovered a new chemical element in the mineral Menachanite [26]. Gregor named the new element Menachite.

In 1795 the German Chemist M.H. Klaproth rediscovered the element, naming it Titanium after the Titans. The pure element was first isolated by Liebig from Rutile in 1831. Rutile is pure Titanium Dioxide [27].

Titanium as a metal was first isolated in 1910 [27]. For many years the element titanium remained a chemical curiosity because any attempt to smelt the metal from its ore led to an extremely brittle material with no practical usage.

In the 1940s and 50s, Kroll and Hunter were able to eliminate the source of fragility by avoiding the absorption of elements like oxygen, nitrogen, carbon and hydrogen in titanium with the Kroll process. This process is nowadays the used system for prime smelting of metallic titanium [26]. As indicated in Figure 3-1 [28], the price of titanium was relatively stable until 1998.

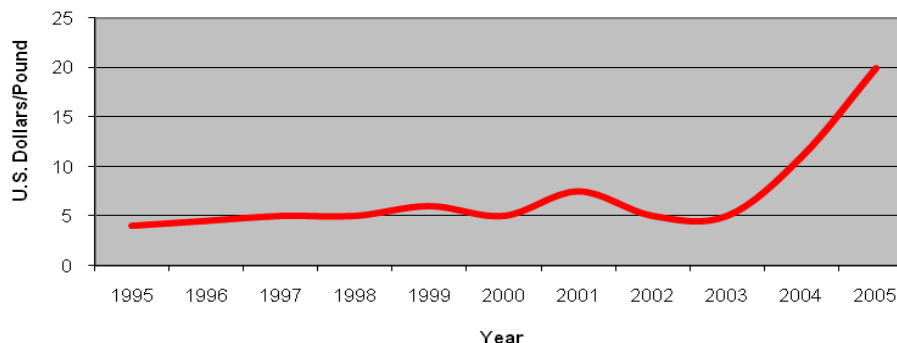


Figure 3-1: Prices of U.S. Titanium ingot [28]

Increased industrial, medical, sporting goods and other commercial application demand drove higher prices in 2001. Prices dropped 33% in 2002 after the 9/11 events and a steep decline in the commercial aerospace sector, causing titanium mills to slow production significantly. In early 2003, global titanium demand began to increase rapidly



primarily due to the recovery of the commercial aerospace sector, driving up prices for finished titanium, as well as for titanium scrap and raw materials. The price of titanium ingot doubled in 2004 and doubled again in 2005 [28].

Titanium ingot is produced by three U.S. companies: Timet (Titanium Metals Corporation), Allegheny Technologies Incorporated, and RMI Titanium. These three companies produce 54 percent of the world's titanium ingot [28].

3.2 Titanium and its alloys

Titanium is an allotropic element; it exists in more than one crystallographic form [15 & 17]. The properties of titanium alloys are determined by their metallurgy and alloy content, and the particular heat treatment to which they have been exposed. Titanium exists in an alpha-form with a hexagonal close packed (HCP) structure at a lower temperature, but in the region of 950°C and above, this change to a beta body-centred cubic (BCC) formation [29]. The inherent properties of these two allotropes are quite different, and the physical properties and machining behaviour of the titanium depend greatly on how much each phase is present. Titanium alloys are available in three varieties depending on the structures and alloying types present, which include alpha, beta and alpha-beta. These categories denote the general type of microstructure after processing. Crystal- and grain structure are not synonymous terms and both must be specified to completely identify the alloy and its expected mechanical, physical and corrosion behaviour [30]. Titanium is able to maintain good strength properties at temperatures above 500 °C (although some modern alloys can operate at 820°C) and apart from their good anti-corrosion properties, titanium also has good creep properties. [31]. While grain shape and size affect behaviour, the crystal structure changes (alpha to beta or vice versa) that occur during processing play a major role in defining titanium properties [32].

A summary of these alloy groups is provided in this chapter, but for a detailed description of titanium alloys and their properties, the reader is referred to Honnarat [29 & 30].



3.2.1 Alpha phase alloys

Alpha (α) alloys are alloys with relatively high amounts of alpha stabilizer and low concentrations of beta stabilizers. The alpha phase is known as Commercially Pure (CP) titanium; it is relatively soft and can be machined at high speeds. These alloys are generally more resistant to creep at high temperature than Alpha-Beta or Beta alloys. [30]. This material presents no significant machining problems, but the material lacks the beneficial properties of the other alloys. It is primarily the strength and flexibility that limits its uses. The minimum yield strength ranges from 170 to 480 MPa [33].

Grain structure changes in alpha and super alpha alloys are made by inducing recrystallization through cold work and annealing [30]. Residual stresses induced by cold working of alpha and super alpha alloys are relieved by stress-relief annealing or recrystallization annealing [32]. Alpha alloys have inherently good weldability, which stems from the fact that alpha alloys generally are insensitive to heat treatment. These alloys however have poorer forgeability and narrower forging temperature ranges than the other alloys [32]. This ductile alloy is being used extensively in the biomedical field.

3.2.2 Alpha-Beta alloys

Alpha-Beta ($\alpha+\beta$) alloys are the most common titanium alloys. When a blend of beta-favouring and alpha-favouring alloy elements is added to titanium, the alloy structures in the alpha-beta range are formed. These alloys are moderately difficult to machine, and relatively short tool life can be a problem because alpha-beta chips are difficult to break and abrasive [15, 30 & 32]. These alloys show higher strength than the near alpha alloy, and have a good combination of properties that ensure better operations at about 315-400°C [33].

Mixed $\alpha+\beta$ alloys, in which a mixture of both classes are present accounts for the majority of titanium alloys employed today [30 & 32]. A wide variety of microstructures can be generated in alpha-beta alloys by adjusting the thermo-mechanical process parameters. Ti-6Al-4V, the most widespread Alpha-Beta alloy, is used extensively in the aerospace, medical and chemical industries [34 & 35].



3.2.3 Beta phase alloys

Beta (β) phase titanium alloys do not have the toughness of the Alpha-Betas, but are harder and more brittle due to the higher percentage vanadium, molybdenum and chromium present in the phase [30 & 32]. Therefore these alloys are difficult to machine, but extremely lightweight and strong. Push rods and valve stems in auto racing and components for jet engines are applications areas for this material.

3.3 Characteristics of Titanium

Titanium is a material used extensively in aerospace frame structural parts, where the operating temperature exceeds 130°C, which is the conventional maximum operating temperature for aluminium alloys [33]. Titanium alloys account for 30% of the total engine mass as shown in figure 2-4 in commercial and 40% in military projects [29]. Apart from this major application titanium is also used in the automotive, medical, micro-component and petro-chemical industry, due to its superior characteristics [30 & 32]. Titanium has a density which is only about half of steel, therefore weighing roughly half of steel parts. But its strength 551 MPa (80, 000 psi) for pure titanium and 1240 MPa (180, 000 psi) for its alloys are far greater than the strength of many alloy steels [30].

This relatively lightweight and high strength gives titanium an extremely high strength-to-weight ratio. In fact, titanium possesses the highest strength to weight ratio of any modern structural metal, a feature which was spurred its widespread in aerospace frames. Titanium also has nearly twice the elasticity of steel, making it an ideal choice for applications that require flexible materials that do not crack or rupture [30]. It also resists corrosion and oxidation which provide savings on protective coating like paints that will otherwise be used in the case of steel [33]. These properties and machining characteristics can be modified and carefully controlled through alloying, and in some cases, by heat treatment [32]. A significant part of current machining centre technology development is focused on maximizing material removal rates (MRR) and thereby reducing machining time of titanium components. Cutting titanium alloys quicker, however is challenging. Although titanium is becoming a material of choice, many of the same qualities that enhance titanium's appeal for most applications also contribute to its being one of the most difficult to machine materials [35-40].



3.4 Titanium in the industry

Figure 3-2 [41] provides the consumption and expected output of mill products for 2004-2010. This is estimated by Timet (Titanium Metals Corporation) based on information from various sources and assumptions. The aircraft build rate estimated by The Airline Monitor in July 2005 was used to estimate the commercial aerospace titanium requirements. The decline in demand for titanium by the commercial aerospace market is not currently expected until 2009. Military aerospace demand is based on numbers from the Teal Group. Industrial market demand is estimated to grow by 3% per year as the Far East and China continue to build power plants to support internal growth. The emerging market demand is estimated to grow at competitive rates fuelled significantly by demand from the oil and gas markets. Figure 3-2 indicates that the consumption of titanium products is expected to continue to grow from the record in 2004 of 61,800 metric tons to 86,000 metric tons in 2010 [41].

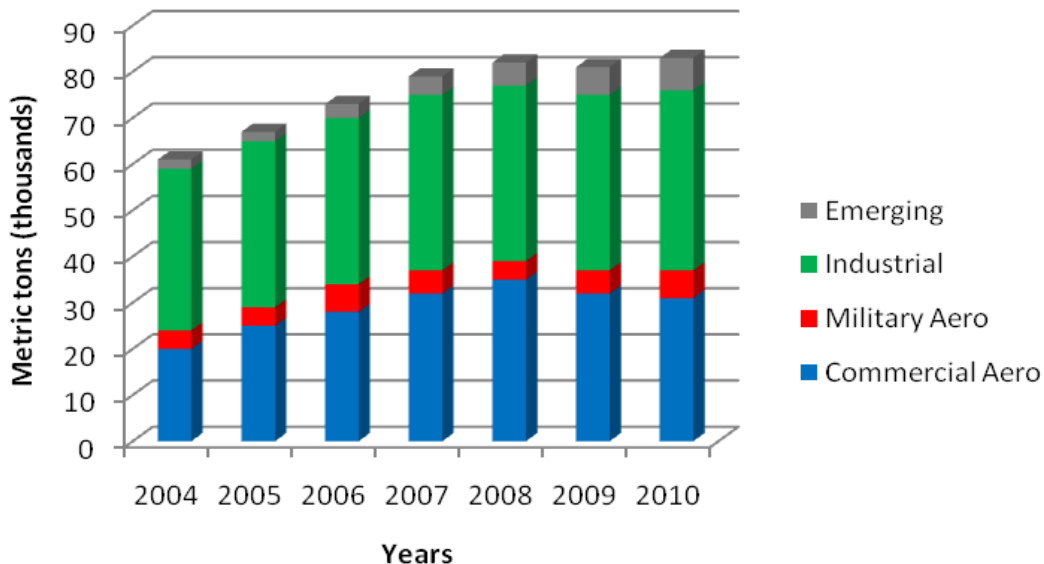


Figure 3-2: World Mill Product Titanium consumption by mayor industry [41]

If this demand occurs as projected, then the titanium industry will have an extended up-cycle during which it should have the financial resources to invest capital to improve the production process and develop low-cost sponge capabilities. Extensive research in different manufacturing aspects of titanium and its alloys are therefore important. This includes machining and specifically milling of the material.



3.4.1 Aerospace sector

In both military and commercial aircraft, the classical application areas for titanium alloys are airframes and aero-engines.

3.4.1.1 Commercial aerospace

Titanium can be utilised in the flow rotors, compressor wheels and other forged items in large high-performance engines as indicated in figure 3-3 [30]. This is due to their high tensile strength-to-weight ratio, high corrosion resistance [17, 30] and ability to withstand moderately high temperatures without creeping, that titanium alloys are used in aerospace. A large proportion as indicated in figure 3-4, of all titanium metal produced is used in aircraft engines and frames [30].

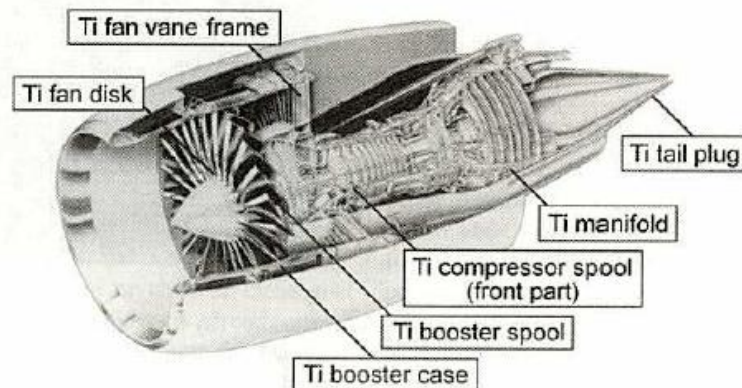


Figure 3-3: Titanium usage in GE-90 aero-engine [30]

Due to the alloy's low density it is employed in compressor blades which operate at extremely high peripheral speeds. Alloys that have a high Young modulus (E) and a low density (ρ) have a high specific modulus (E/ρ) within an extended temperature range (-250°C to 500°C) which is ideal [42].



Approximately 10% of the Boeing 777 airframe weight is titanium and the total amount of the aircraft is more than 45 tons (100 000 lbs) as indicated in figure 3-4 [19 & 28].

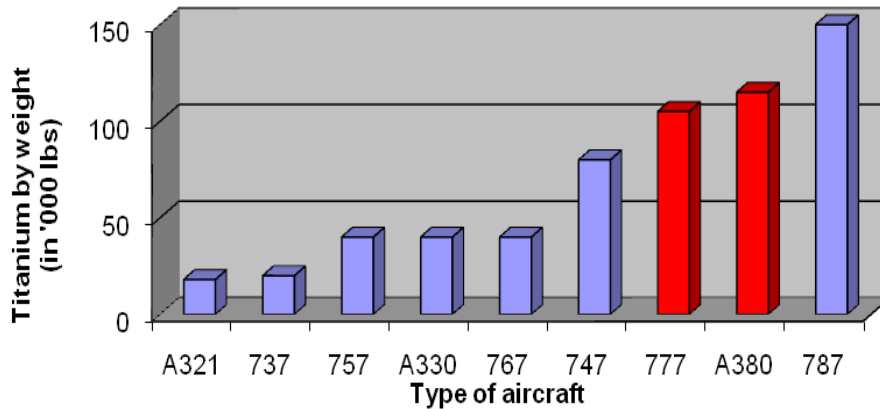


Figure 3-4: Titanium in commercial aircraft [19 & 28]

The decline of titanium use in the 767 can be attributed to the perceived shortage in titanium supply. The engines alone of the Airbus A380 use about 11 tons of titanium, but the total weight of titanium in this aircraft is more than 50 tons (110 000 lbs).

3.4.1.2 Military aerospace

The difference between military aircraft and commercial aircraft are in their airframes. Military aircrafts use a higher percentage of titanium than commercial airliners. This is due to considerably higher dynamic and static loading of the airframe in military class aircrafts. The typical aluminium structural technology used in a commercial aircraft is simply insufficient to meet current military standards. The principle reason for the increased use of titanium is that each generation of aircraft needs to fly higher, faster and be more manoeuvrable than its predecessor. Global, military use of titanium is expected to increase significantly between now and 2015 [28]. The high-thrust military engines are possible through advanced engineering developments in the use of titanium alloys that have elevated fatigue strength, creep resistance and high temperature strength.

Over the past 20 years [41] military aircraft demand declined from more than 500 units per year in the late 1980's to about 150 in 2000 and 2001. This is largely due to the end of the cold war and downsizing of military arsenals and budgets. Corresponding to the



previously mentioned decline in aircraft shipments, there has been decline in titanium consumption.

However, the potential for conflicts has ushered in a renewed need for air superiority and with the fleet aging and new aircraft poised to replace the old, the trend is reversing. The outlook is for growth in the military aerospace segment. Projected manufacture improved to over 200 in 2003-2006 and it is expected to be over 300 in 2007 - 2010. Most of these new aircraft will be cargo aircrafts and fighters, rather than bombers [41].

In 1959, the SR-71 "Blackbird" was one of the first aircraft to make extensive use of titanium within its structure, paving the way for its use in modern fighter and commercial aircraft [30]. Its titanium airframe helped it withstand the 260°C (500°F) heat generated by air friction in sustained Mach 3 flight [30].

The F-4 Phantom was the first production fighter to make extensive use of titanium. The upcoming F-22 Raptor and the Eurofighter, calls for around 40%wt titanium [30]. It is the highest proportion of titanium of any current US fighter [28]. The Eurofighter's first production deliveries occurred in 2002 and 409 are expected to be built in the period from 2003 to 2010. The F-22's deliveries were scheduled for 2003 [28].

The military aircraft production is definitely on the increase with many current programs that use more titanium than their predecessors. Therefore this market should remain a significant part of total world consumption of titanium.

3.4.2 Automotive applications

Although Titanium seems compatible for the use in several components in passenger cars, the high price of Titanium prevented the realization of these applications in mass-produced passenger cars [43]. The different alloys can be used for the applications indicated in Figure 3-5 [30]. Titanium based materials could be used for the valves and turbocharger rotors, because it combines high temperature capability and low density. Alpha phase titanium sheets would be appropriate for the exhaust system, because of outstanding weld ability and formability.



Beta phase titanium alloys are the best choice for suspension springs, because of high strength and low modulus of elasticity [30]. Ti-LCB, a new low cost β -alloy, has been pointed out to have the potential to be used as spring material for mass-produced passenger cars [32].

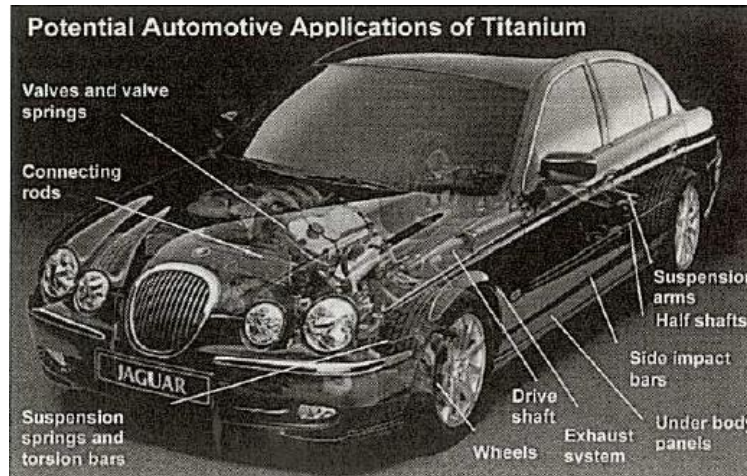


Figure 3-5: Potential Automotive applications of Titanium [30]

Volkswagen equipped the LUPO FSI model with rear suspension springs made out of this low cost Beta alloy Ti-LCB [32]. The Mitsubishi Lancer GSR model introduced a titanium inter-metallic component in their passenger car by casting the rotor head of the turbocharger rotor with a γ -alloy. The advantage of using a γ -material is the low weight of the rotor which minimizes the time required to spin up the turbocharger and therefore reducing the lag [30].

The current cost structure severely limits the use of titanium in the automotive industry. There are however several examples where the application of titanium yielded significant performance benefits. It can be expected that the motor industry will develop into a major market for titanium and titanium machining once prices are reduced.

3.4.3 Biomedical applications

Ductile Alpha-titanium is being employed extensively in the biomedical field. Corrosion resistance, bio-adhesion (bone in growth), bio-compatibility (non-toxic and is not rejected by the body), modulus of elasticity, fatigue strength, and good process ability are all properties which are of interest for biomedical implications [45]. The modulus of elasticity should be as close as possible to the modulus of bone which is in the range of 10-30 GPa [30].



The use of titanium in the biomedical field has become well known, for the reason that titanium fulfils the mentioned property requirements better than any competing material. Competing materials include stainless steels, commercially pure (CP) tantalum and Co-Cr-alloys [44]. The exceptional corrosion resistance and biocompatibility of Titanium gives the material the edge over its competing materials. According to the authors [45] there are a range of different medical devices using titanium. These devices include hip joint implants, heart valves, bone plates and screws. The material can also be used for the surgical instruments used in image-guided surgery, wheelchairs, and products where high strength-to-weight ratio is essential.

Fractures can be repaired by stabilizing the fractured bones with small titanium plates and screws as shown in Figure 3-6 [30]. Commercially pure titanium (CP-Ti) is the material of choice for bone plates which does not have such a high strength requirement. Depending on the complexity and shape of the individuals needs, various grades of CP titanium can be used. If fairly straight plates of higher strength is essential, either Ti-6Al-4V or Ti-6Al-7Nb alloys is used [32].

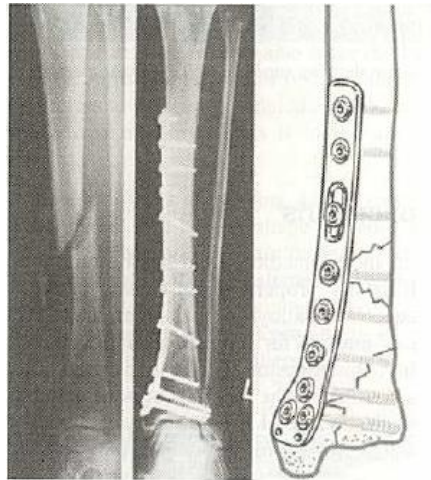


Figure 3-6: Bone plate implant [30]

The stem of a hip joint implant is the most demanding biomedical implant application and requires high fatigue strength. The stem which is manufactured of titanium has a ceramic head which can rotate in a cup made out of ultra-high molecular weight polyethylene (UHMWPE) (Figure 3-7 [30]). This combination of materials results in a very low friction coefficient. The cup is held in a metal backed shell. The metal backed shell and the screws are also made out of titanium, usually Ti-6Al-4V or CP-Ti [30]. The



surface of the stem is essential to facilitate better bone in growth (bio-adhesion). Bone adhesion improves with increasing roughness of the surface stem.

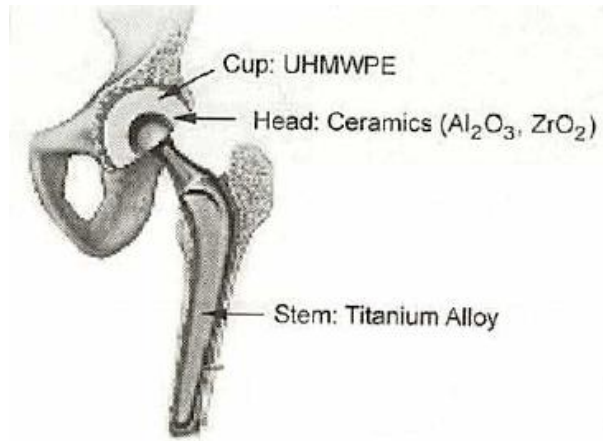


Figure 3-7: Schematic of artificial hip-joint [30]

Since titanium is non-ferromagnetic, patients with titanium implants can be safely examined with magnetic resonance imaging [30]. Preparing titanium for implantation in the body involves subjecting it to a high-temperature plasma arc which removes the surface atoms, exposing fresh titanium that is instantly oxidized [32].

3.4.4 Consumer Applications

3.4.4.1 Marine markets

Due to its high corrosion resistance to sea water, titanium is used extensively in the marine world. The material is used in the heat exchangers of desalination plants [46], heater-chillers for salt water aquariums, and to make propeller shafts. Titanium is used to manufacture the housings and other components of ocean-deployed surveillance and monitoring devices for scientific and military use [32].

3.4.4.2 Industrial

Titanium is used in welded pipes and process equipment such as heat exchangers, tanks, process vessels and valves in the chemical and petrochemical industries [30]. The pulp and paper industry uses titanium in process equipment exposed to corrosive media such as sodium hypochlorite or wet chlorine gas [32].



3.4.4.3 Sport equipment

Equipment such as golf clubs, lacrosse stick shafts, helmet grills and bicycle frames are made from titanium [30 & 32]. Almost everything on expensive racing bikes can be made from this material [47]. Although it is slightly more expensive than traditional alternatives, these products can be considerably lighter without compromising strength.

3.4.4.4 Architecture and Construction

Titanium has occasionally been used in architectural applications. The 40m memorial to Yuri Gagarin (the first man to travel in space) in Moscow, is made of titanium for the metal's attractive colour and association with rocketry [30]. The Guggenheim Museum, Bilbao and the Cerritos Millennium Library were the first buildings in Europe and North America respectively to be covered in titanium panels [32].

3.5 Cutting behaviour of Titanium

The machinability of titanium alloys is poor compared to both general steels and stainless steels, which imposes particular demands on the cutting tools employed for machining [19 & 22]. Titanium alloys requires cutting forces only slightly higher, but do have metallurgical characteristics that make them more difficult and more expensive to machine than steels with equivalent hardness [30]. Despite the obvious desirability of such a low density and high strength metal as an engineering material, other properties have historically conspired to present difficulties when machining titanium alloys. Until modern cutting tools and methods were developed it was considered to be extremely difficult to machine efficiently [32 & 48].

3.6 Ti-6Al-4V alloy

3.6.1 Introduction

Ti-6Al-4V is one of the most popular titanium alloys and comprises about 45–60% of the total titanium products in practical use [30, 33 & 34]. This alloy is formed by a blend of alpha- and beta favouring alloying elements and form part of the Alpha-Beta alloys. The α (hexagonal close packed) is hard, brittle with strong hardening tendency. The β (body centred cubic) is ductile, easily formed with strong tendency to adhere [42]. Ti-6Al-4V is available in wrought, cast and powder metallurgy and the properties depend on the interstitial contents and thermal-mechanical processing.



3.6.2 Chemical composition

Ti-6Al-4V can be produced in a variety of formulations, depending on the application. The aluminium content may reach up to 6.75% (by weight) and vanadium 4.5%. The oxygen content may vary from 0.08 to more than 0.2% and the nitrogen may be adjusted up to 0.5%. Raising the content of these elements, especially oxygen and nitrogen, will help to increase the strength. Equally, the lower additions of oxygen, nitrogen and aluminium will improve ductility, stress-corrosion resistance, fracture toughness and resistance against crack growth [32].

Ti-6Al-4V is designed primarily for high strength at low to moderate temperatures. The material has a high specific strength (strength/density), stability at temperatures up to 400°C and good corrosion resistance [42].

3.6.3 Basic physical and chemical properties

Ti-6Al-4V is not as corrosion-resistant as commercially pure titanium alloys, but still excellent compared to other alloy systems. This exceptional corrosion resistance is due to the oxide-film formation.

The oxidation behaviour of the material is very similar to that of unalloyed titanium. The reaction rate laws, range from logarithmic (at 300-500°C) to parabolic (at 500-750°C) to linear (above 750°C) with increasing temperatures of oxidation. Ti-6Al-4V alloy is universally used for compressor blades operating up to 350°C [42].

Hydrogen damage of the material is manifested as a loss of ductility (embrittlement) and a reduction in the stress-intensity threshold for crack propagation. The damage is caused by hydrides, which form as hydrogen diffuses into the material during exposure with gaseous or cathodic hydrogen. The phenomenon depends on both hydrogen diffusion and hydride formation and therefore there may be a peak in hydrogen embrittlement as a function of temperature [32].

The authors of “Influence of heat treatment and cutting parameters on chip formation and cutting forces” [49], indicated that chip formation and cutting forces depends essentially on the work piece material.



3.6.4 Chip Formation

The chip segmentation is very distinct in titanium alloys [50 & 51]. Ti-6Al-4V is known to form serrated (segmented or shear-localized) chips [52]. The theory of catastrophic thermoplastic shear [53] and periodic crack formation [54] were formulated to explain the formation of this chip type. The first stage of segment formation involves upsetting of the wedge shaped volume of material immediately ahead of the tool. This is illustrated in figure 3-8.

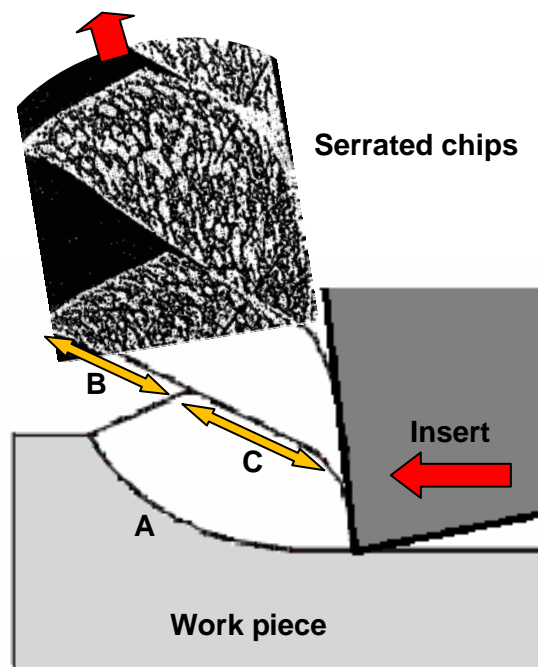


Figure 3-8: Ti-6Al-4V producing a serrated chip [53]

Once a critical shear strain is attained along “A”, there is an intense localized deformation in this primary shear zone. This leads to separation of the surfaces “B” and “C” due to catastrophically shear. These chips are semi-continuous in the sense that they possess a saw-tooth appearance that is produced by a cyclical chip formation of alternating high shear strain followed by low shear strain [49 & 53].

3.6.5 Machining challenges

The machinability of material significantly depends on the low thermal conductivity [42] of (7 W/m.K), which is very low (86% lower) compared to that of AISI 1045 steel (50 W/m.K) [34]. This low thermal conductivity coupled with a high melting point (1650°C /



1930°K) concentrates high cutting temperatures at low cutting speeds near the tool cutting edge [56]. Consequently, besides the thermal stresses there are very high mechanical stresses on the cutting edge which is known conditions for extensive tool wear [42].

3.6.5.1 Poor conductor of heat

Ti-6Al-4V is a poor conductor of heat. The thermal conductivity of Ti-6Al-4V (7 W/m.K) is approximately one twenty fifth of that of Aluminium (6061: 177 W/m.K) and one eighth of that of steel (1018: 59 W/m.K) [19, 22 & 32]. It is less than a third of the corresponding value for stainless steel (SS422B: 24 W/m.K) and only half of the value for even Inconel (718: 15 W/m.K) [15 & 17]. The low thermal conductivity of this alloy is compared to other aero-engine materials in figure 3-9.

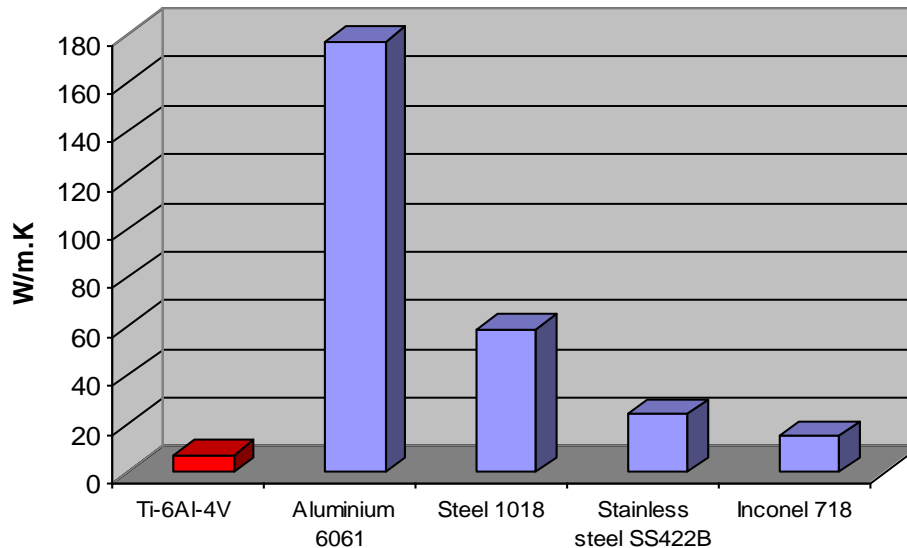


Figure 3-9: Thermal conductivity (W/m.K) of different alloys

Heat generated during the cutting does not dissipate through the part and machine structure, but concentrates in the cutting edge and tool area. This cause a concentration of the heat build-up in the cutting zone, causing the characteristically high tool wear for which titanium is known [42].

Figure 3-10 shows the results from a study to measure the cutting temperature of titanium.



The cutting temperature ($^{\circ}\text{K}$) is plotted relative to the increase in cutting speed.

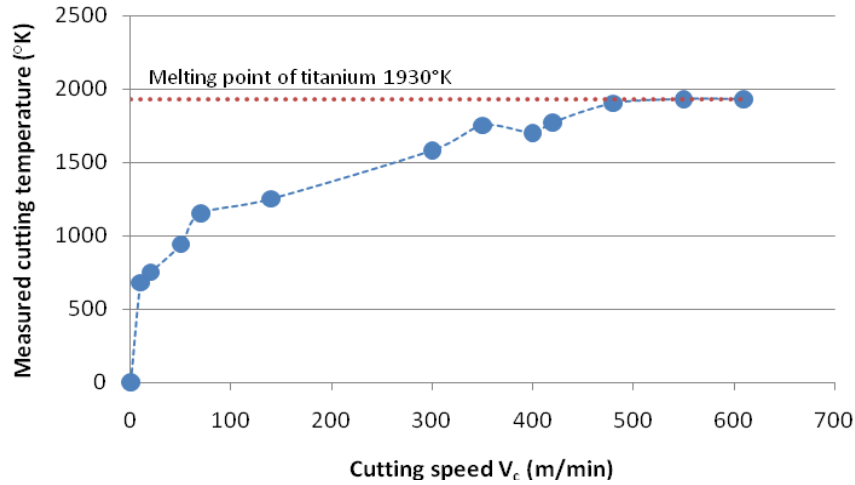


Figure 3-10: Area-weighted average cutting temperature as a function of cutting speed for K68 carbide insert (chip load, 0.127 mm/rev) [56]

From this figure, it can be seen that increasing the cutting speed beyond 250 m/min will increase the cutting temperature too significantly over 1000°C . Temperatures of 900°C have been measured at a cutting speed of 75 m/min [57]. If exposed to temperatures above approximately 450°C [30], Ti-6Al-4V strength decreases very rapidly. As shown in figure 3-11 the strength of this alloy drops from 1000 MPa (room temperature) to below 550 MPa (above 500°C) under elevated temperature conditions.

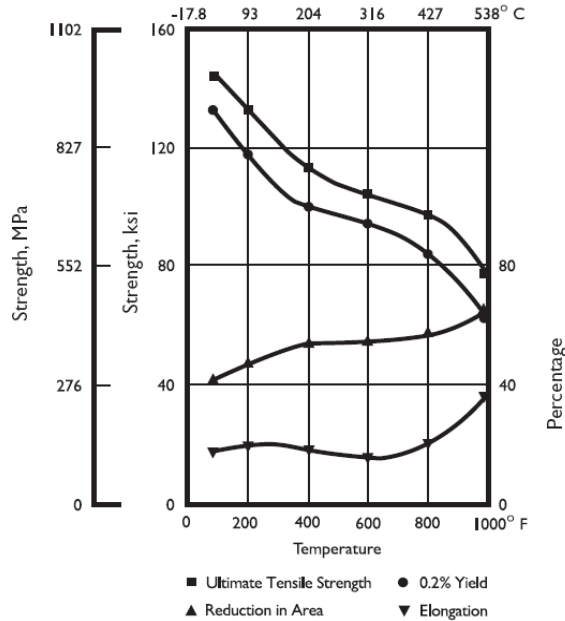


Figure 3-11 Tensile properties of Ti-6Al-4V at room and elevated temperatures [58]



These excessive temperatures can lead to cutting edge chipping and deformation if the insert is not able to withstand the tough conditions. Dull edges on tools generate even more heat and further reduce tool life [32]. Cutting temperatures can get so high that titanium chips could spontaneously ignite. This high temperature generated during the cutting process also causes a work hardening phenomenon that affects the surface integrity of titanium. This phenomenon could lead to geometric inaccuracies in the part and severe reduction in its fatigue strength. The critical temperature by which steady machining of titanium can occur is 700°C [59].

3.6.5.2 Strong alloying tendency or chemical reactivity

Ti-6Al-4V has a strong alloying tendency or chemical reactivity with materials in the cutting tools at tool operating temperatures. The alloy become chemical active with most tool materials at cutting temperature in excess of 500°C leading to a high diffusion wear rate [60, 61 & 62]. Chemical reaction between the cutting tool material and the work piece could lead to notching wear. In contrast, during the machining process, deposits of titanium work materials tend to accumulate on the rake face of the insert [32]. The high pressure developed in this area can weld these particles to the cutting edge, forming a built-up edge phenomenon. Once a built up edge develops, tool failure follows rapidly according to Kirk [31]. According to the author over successively shorter intervals these particles are inclined to peel off the cutting edge, pulling some carbide content from the cutting insert away with it. This causes galling, welding, and smearing along with rapid destruction of the cutting tool.

A practical manifestation of this chemical reactivity problem is that chips can spontaneously ignite as they react with oxygen. Recently, a 5-axis machine was destroyed by fire in this way in the Western Cape, South Africa.

3.6.5.3 Low modulus of elasticity

Ti-6Al-4V has a relative low elastic modulus and consequently more “springiness” than superalloys and steels which is desirable and beneficial for finished parts. This low Young’s modulus (114 GPa) coupled with a high strength however encourages deflection, chatter and movement away from the tool. This can result in the rubbing of the edges rather than cutting [32]. This rubbing process generates heat, compounding problems caused by the material’s poor thermal conductivity.



Pushing and deflecting the part, rather than cutting, makes it difficult to cut to size and cause tolerance problems. As the material moves away from the cutting edge it deforms plastically, instead of elastically. The elasticity of different materials are compared in figure 3-12.

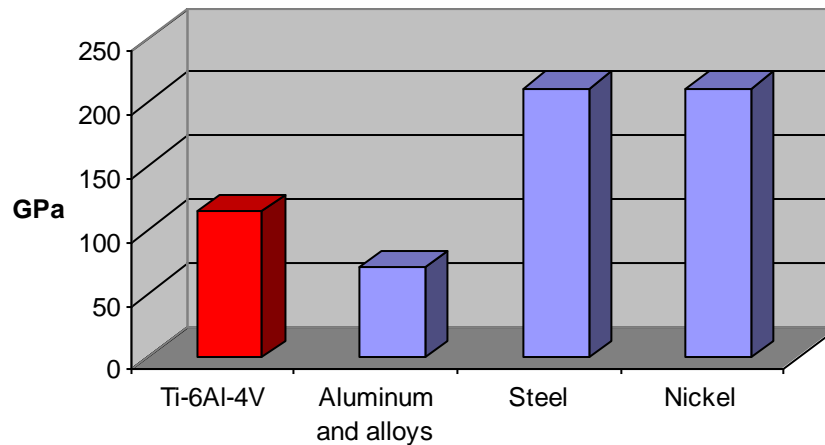


Figure 3-12: Elastic modulus of different materials [17 & 19]

Proper back-up and special attention to appropriate work holding are required to improve the stiffness. Rigidity of the entire system is consequently critical, as is the use of sharp, properly shaped cutting tools. Greater clearances of cutting tools are also required due to the reflections [22].

3.6.5.4 Small contact area

This titanium alloy's metallic characteristics cause high shearing angle to be formed ahead of the cutting edge. This in turn causes the chip to contact a relatively small area on the cutting tool face and results in high bearing loads per unit area [53].

Titanium exhibits segmented chip formation and has been cited to cause much confusion in interpreting cutting data pre 1980's [56] to steel being machined at the same rate, this contact area is only a third for titanium as shown in figure 3-13 (a) [53].

This small contact area together with the low thermal conductivity, result in a high rate of temperature increase with cutting speed and wear occurring closer to the tool cutting edge [31].

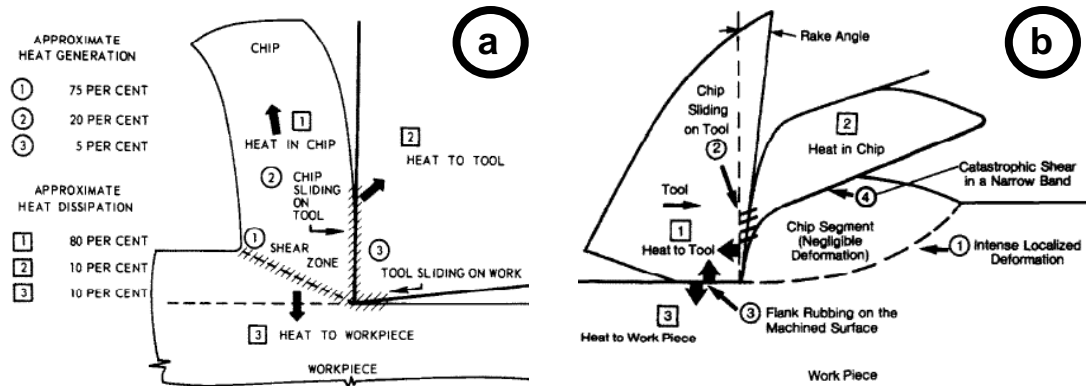


Figure 3-13: Contact area of (a) a continuous chip, and (b) serrated Ti-6Al-4V chip [53]

In machining steel, it was found [63] that most (about 75%) of the heat is generated in the primary shear zone, while for Ti-6Al-4V owing to rapid flank wear and almost no secondary deformation on the rake face, the significance of zones 2 and 3 (Figure 3.13 b) is virtually opposite. This means that a significant portion of heat is generated for Ti-6Al-4V at the clearance face (due to rapid flank wear) as a result of rubbing between the flank and the machined surface. An insignificant portion of heat is generated between the sliding chip and rake face.

According to the Pettifor, [64] Ti-6Al-4V is also a strong carbide-forming element, which can influence the machinability. During these studies it was realized that the affinity of a metal to carbide can be determined by the material's enthalpy. The more negative the enthalpy, the greater the affinity of the metal to carbon. Titanium has a very low enthalpy and will therefore, according to the studies, have a high affinity to carbon [42].

3.6.6 Applications

Wrought Ti-6Al-4V is used in the aerospace industry, especially for airframe applications and turbine engines. The engine components include blades, discs and wheels. According to the author the alloy accounts for almost 50% of all alloys used in aircraft applications [32]. The Boeing 777 is the first commercial airplane, for which β titanium alloys outweigh the classical Ti-6Al-4V alloy. This is primarily because most of the landing gear is made out of the β alloy Ti-10-2-3 [33].



It is used in the biomedical field because of its low modulus, good tensile, fatigue strength and biological compatibility. Ti-6Al-4V is also used in the automotive industry in special applications in high performance and racing cars where weight is critical. These special applications, which are all part of the reciprocating and rotating parts, include valves, valve springs, connecting rods and rocker arms [30]. This alloy could be used for connecting rods, because of high fatigue strength and sufficient temperature capability

Casting applications include water-jet inducers for hydrofoil propulsion and seawater ball valves for nuclear submarines [32].



4. Milling considerations for Ti-6Al-4V

4.1 Introduction

Milling is characterised by the fact that interruption of the cut is almost inevitable. When considering a material like a high strength titanium alloy interrupted cutting, and the related shock loading, is the key phenomenon that distinguishes it from other machining practises, for example turning [22].

There are two basic types of milling operations; conventional (up) and climb (down) milling [65]. Climb milling (figure 4-1 a) starts at the top of the work piece with a maximum chip width and decreases. Less machine power is required and climb milling exerts a downward force on the work piece for which a simple and less costly fixture is suitable [22 & 65].

In conventional milling (figure 4-1 b) the tool meets the work piece at the bottom of the cut where the thickness of the chip starts from zero and increases. More power is required due to the rubbing provoked by the chip beginning at minimum width. The surface finish is also marred due to the chips being carried upwards.

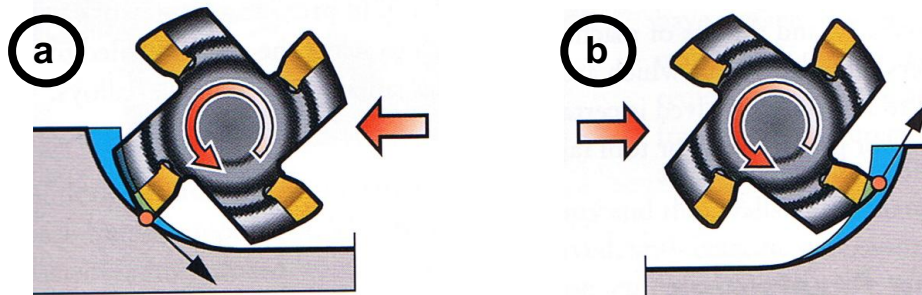


Figure 4-1: Climb (down) and conventional (up) milling [66]

As shown in figure 4-2 [66] several forms of milling evolved from these types. Thermal shock and mechanical overload are mechanisms that may act in parallel. The largest component of mechanical load will act as the insert enters the cut, while thermal shock will act as the insert leaves the cut and enters the coolant. The cutting speed represents the magnitude of the thermal load, while the radial immersion represents the duration of exposure to the thermal load.



Increased immersion increases the exposure of the tool to high temperatures, while increased chip thickness increase the mechanical shock load on the tool [56]. Increasing the fracture resistance of the insert due to this mechanical shock (impact) can increase the tool's life for milling operations [67].

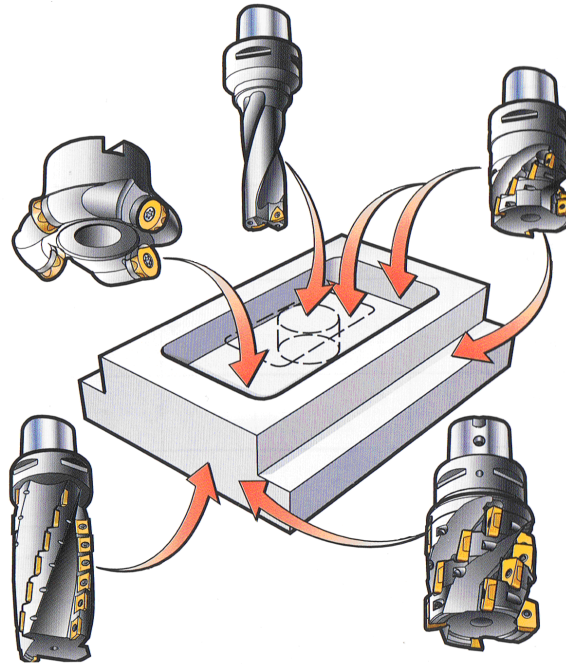


Figure 4-2: Various milling operations [66]

4.2 Influence of different cutting parameters

Understanding these different parameters can help to machine Ti-6Al-4V efficiently. Cutting speed (V_c) and feed rate (f_z) are two of the most important variables. Speed and feed rate have a direct influence on tool life and therefore it is desirable to have charts and graphs available for different combinations, which is not likely. Consequently research studies are important to obtain this knowledge. These variables can be used to increase the metal removal rate (cm^3/min) cost effectively. Reasonable production rates for machining titanium can be achieved at acceptable cost levels if the machining conditions are selected properly for a specific alloy and processing sequence [32].

4.2.1 Cutting speeds (V_c)

The cutting speed strongly affects the tool tip temperature; hence it is the most influential to tool life. Ti-6Al-4V requires lower speeds than for unalloyed titanium [30]. A low cutting speed helps to minimize tool edge temperature and maximizes tool life with tools that



are temperature sensitive. According to Kitagawa et al conventional cutting of titanium with sintered carbide tools is in the range of 30 m/min [68]. Che-Haron [69] reports that advisable industry practice cutting speeds (V_c) for titanium are limited to about 45 m/min. This agrees with the recommendations made in the titanium machining application guide of Sandvik [66]. Compared to a 20-100 times higher cutting speed for Aluminium and 4-8 times higher for hardened steel, this cutting speeds for Ti-6Al-4V results in a relative low productivity [66 & 75].

An increase in cutting speed will not only reduce the cutting forces, but also a chip formation transition from continuous to segmented chips [49]. High speed machining offers advantages over conventional machining such as higher material removal rate, increased machining accuracy and better surface finish [70].

4.2.2 Feed per tooth (f_z)

The temperature at the cutting edge is less affected by the feed rate than by the speed. Material removal rate is directly proportional to feed rate; hence it is desirable to use the highest feed rate possible. Experiments conducted at Sandvik [66] are shown in figure 4-3. A CoroMill Plura ($D_c=12\text{mm}$, $a_p=10\text{mm}$, $a_e=0.5\text{mm}$) was used to machine Ti-6Al-4V.

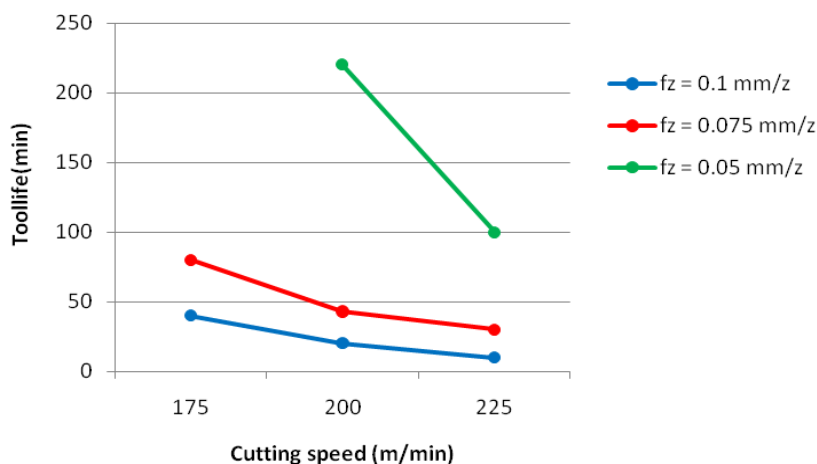


Figure 4-3: Influence of feed rate on tool life [66]

As shown in figure 4-3 there is a definite increase in tool life, with a decrease in feed rate and cutting speed. A feed rate of 0.05mm/z show promising results at a cutting speed of 200m/min. For feed rates (f_z) below 0.051 mm, chipping becomes less of an issue [56].



The depth of cut should also be greater than the work-hardened layer formed from the previous cut [30]. Therefore it is important to keep the tool feeding during machining to prevent smearing and seizing which can lead to tool breakdown [32]. It is also better to stay as long as possible in the cut, as every fresh entry into Ti-6Al-4V can induce vibrations, which in the long run will reduce tool life.

4.2.3 Influence of axial cut (a_p)

High axial immersion cut strategies also hold promise for advances in titanium machining. Machining guidelines by Sandvik [66] show that a decrease in tool life is only weakly correlated with an increase in axial immersion. It is essential that the depth of cut should be greater than the work-hardened layer formed from the previous cut [56]. Although round and 45° inserts have limited depth of cut, the 90° has a cutting depth as deep as the cutter diameter and a length that allows for stable cutting [75].

4.2.4 Influence of radial cut (a_e)

The radial cut can influence both the removal rate and the life of the tool. Although a high radial immersion increases the removal rate, Sandvik [66] advises that the relationship of a_e / D_c is critical. The best balance for a high removal rate and economic tool life need to be established for new insert entrants. Barnett-Ritcey confirmed that radial immersion values must be kept below 0.05 mm to achieve reasonable tool life [56].

4.2.5 Coolant

The low thermal conductivity of Ti-6Al-4V causes a concentration of the heat build-up in the cutting zone [42]. Together, the low thermal conductivity and heat concentration on a small contact area account for high tool wear. According to figure 4-4, roughly 80% of this heat is retained in the tool, while only 20% is removed by means of the chip machining Ti-6Al-4V [71].



The figure indicates that for an increase in thermal conductivity of the tool, there is a decrease in the percent of heat removed by the chips.

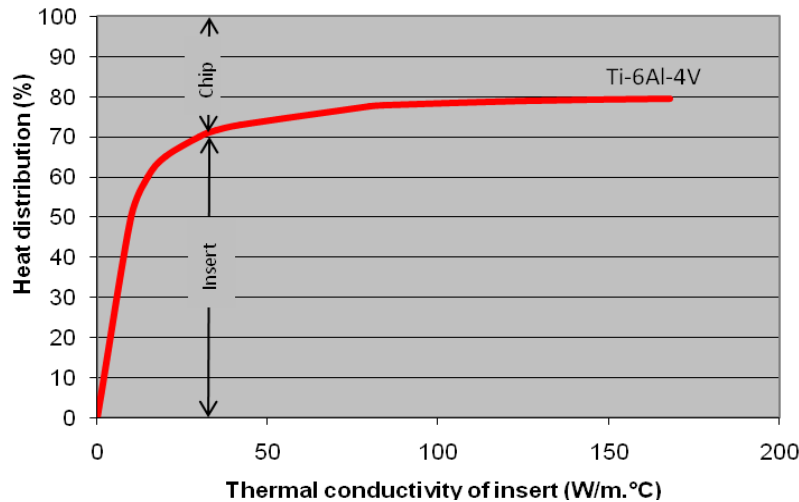


Figure 4-4: Heat generated distribution as a function of the thermal conductivity of the tool [71]

In interrupted cutting the tool is subjected to cyclic heating and cooling, causing thermal shock. When the rate of cooling is increased significantly, the result is crack formation causing premature tool failure [72]. Su et al [73] connects cyclic thermal shock directly with thermal crack initiation. It logically follows that indiscriminate high power cooling will yield diminishing returns.

Coolant is always recommended to assist in chip removal and prevent re-cutting of the chips. A generous quantity improves tool life by providing more effective heat transfer, a reduction in cutting forces and washing away of the chips [32]. Application to exactly where the heat build-up is concentrated, thermal shock and heat transfer at elevated tool temperatures are the constraint factors. Titanium machining requires high application pressures to penetrate to the localized heat generation zone. When the cutting zone is shielded from the lubricant stream such as in cutting with deeper axial immersion (roughing), the coolant needs to be focused on the cutting edge [72].

At high tool temperatures, typically above 550°C, the heat transfer mechanism between the cooling fluid and the tool surface changes to two phase high speed flow [56]. The coolant is vaporized on contact with the heated tool surface, forming an isolating



boundary layer on the tool surface. Quantifying the phenomenon, the heat transfer coefficient for water is reduced almost ten-fold from a value of $13\,500\text{ W/m}^2\text{K}$ at 380°C to $1470\text{ W/m}^2\text{K}$ above 830°C [56]. The phenomenon is also described as delayed surface wetting in the heat transfer literature. The relevance to titanium machining is that cooling becomes ineffective at higher heat loading on the tool surface. The design of efficient cooling systems specifically for titanium machining is considered an area that holds potential for significant improvement.

Implementing a cooling system with too high cooling power will promote thermal shock. Even with the low, unpredictable power of flood cooling thermal shock has been described often in the literature [56 & 72] as well as encountered in practice. The author is of the opinion that through spindle application, high pressures (50 bar +) as well as customized, possibly even under dynamic control, of gas/fluid mixtures for “soft” or controlled heat exchange rate cooling holds key to significantly increased machining effectiveness.

4.3 Temperature

The cutting temperature influences both the cutting forces of the milling operation and the tool life (TL) of the insert. At elevated temperatures (1000°C - 1500°C) Ti-6Al-4V (melting point 1650°C) becomes softer and therefore easier to machine [56]. If a cutting material can be found that can withstand these elevated temperatures dynamically this could yield an optimum cutting condition.

The cutting material is submitted to cyclic heating and cooling at the corners through the contact with the work piece during milling operations. The cyclic process occurs as the tool enters and exits the work piece material, which could lead to a phenomenon known as thermal fatigue [72]. Due to the higher thermal conductivity of PCD ($\lambda = 500\text{W/mK}$), thermal fatigue is not as influential on the tool. This temperature increase could initiate thermal softening in the shear zone of Ti-6Al-4V, if the insert can withstand the impact related wear at these high material removal rate conditions.

Studies conducted by Kikuchi [74] estimated the temperature for milling Ti-6Al-4V by measuring the thermal electromotive force of the tool thermocouple.



Temperature is estimated to be around 750°C [74] for different milling conditions as indicated in figure 4-5.

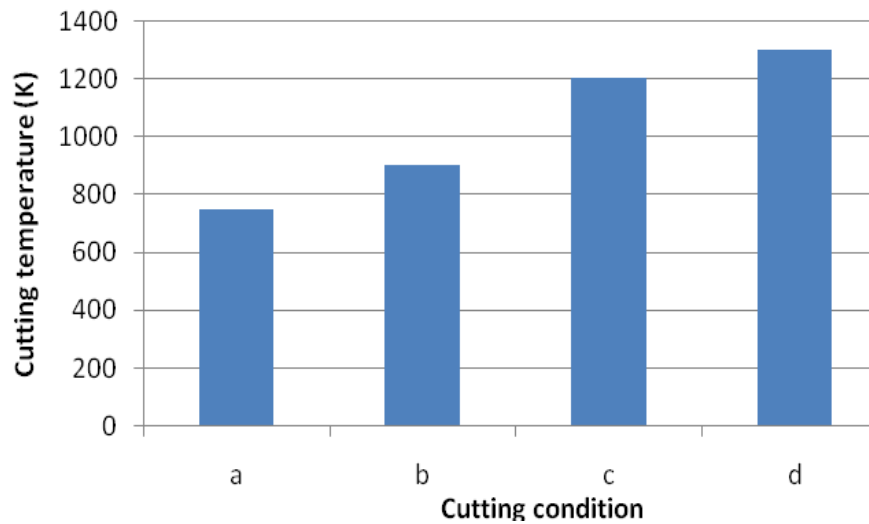


Figure 4-5 Temperature generated for different cutting conditions [74]

Kikuchi estimated the generated temperature, during the milling of Ti-6Al-4V, by measuring the thermal electromotive force of the tool thermocouple. The generated heat is calculated to be around 750°C [figure 4-5] for the different milling conditions indicated in table 4-1.

Table 4-1: Different cutting conditions for temperature measurements

Condition	V_c (m/min)	Feed (mm/s)	Depth of cut (mm)	MRR (mm^3/s)
A	50	1	0.2	0.6
B	50	1	0.4	1.2
C	100	2	0.2	1.2
D	100	2	0.4	2.4

Withstanding elevated temperatures, especially of fast cyclic thermal loading, such as milling, will depend basically on the thermal diffusivity [56].



Figure 4-6 [56] shows that a cutting material able of withstanding temperatures in the region of 1000 to 1500°C will be able support cutting speeds in excess of 200 m/min.

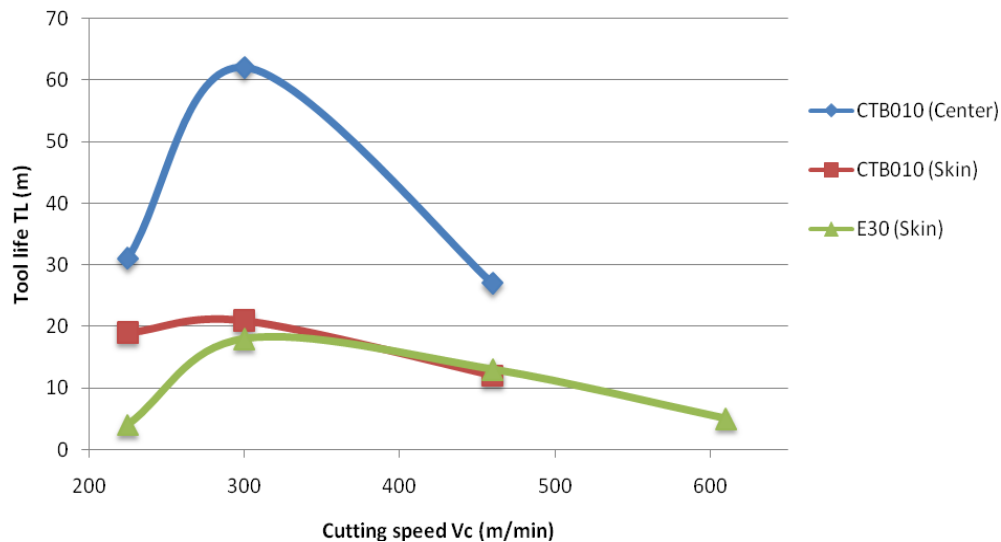


Figure 4-6: Effect of cutting speed on tool life ($f_z = 0.025\text{mm/z}$, $a_e = 0.25\text{mm}$, forged Ti6Al4V, A50) [56]

The tool life recorded with the CTB 010 PCD insert is doubled when the cutting speed is increased from 229 m/min to 305 m/min. In the same figure it can be seen that tool material E30, which is a more conventional tungsten carbide, did not perform well.

A cutting material with a relative high thermal conductivity and transverse rupture strength creates a distinct potential for withstanding high temperatures combined with increased mechanical shock resistance.

4.4 Cutting forces

Machining of titanium requires cutting forces only slightly higher than those needed to machine steels. This is due to the high stresses at the cutting edge caused by the small contact area (2-3½ times less than when machining steel). [53] Reasonable production rates and excellent surface finish can be obtained with conventional machining methods if the unique characteristics of the metal are taken into account [70].



Cutting forces will increase, with an increase in chip thickness (feed rate) and decrease with an increase in cutting speed as shown in figure 4-7 [56].

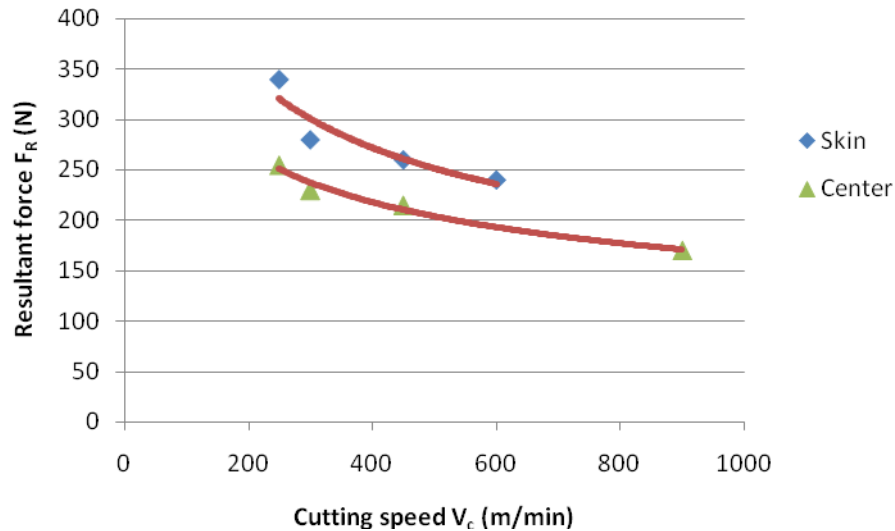


Figure 4-7: Effect of cutting speed on cutting force. (Forged, $h_x=0.025\text{mm}$, $a_e=0.25\text{mm}$, A50) [56]

Cutting forces and chip thickness are also affected by the cutting strategy. Decreasing the initial entrance cut reduces the impact on the insert. A roll-in strategy (figure 4.7) produces a smaller entering angle which provides a more gradual entry into the cut, reducing radial pressure and protecting the cutting edge [66].

4.5 Milling strategy

The choice of a tool, insert and machining path should be determined with care in order to have an efficient and productive machining operation. This will be influenced by a variety of considerations arising from both the desired end result and the available resources.

The potential for significant advances in Ti-6Al-4V machining, lie in the utilisation of the insert characteristics of superhard cutting materials. Carbides in their extreme hard form are rather susceptible to thermal shock [66]. Due to high TRS the material is however relatively immune to mechanical shock loading. The combination of these two parameters lead to the machining strategy focus that should minimise both forms of shock but placing an emphasis on reducing thermal shock if it is a trade-off between the



two factors. Figure 4-8 [66] shows a roll-in strategy to minimise shock loading on the cutting edge.

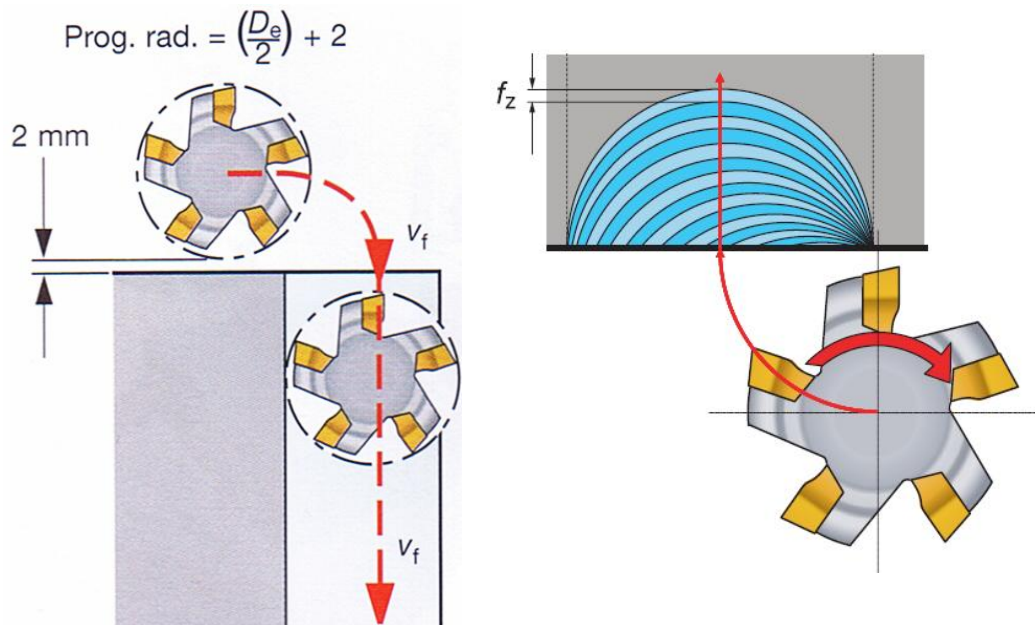


Figure 4-8: Roll-in machining strategy [66]

This work needs to be analysed fundamentally and applied to the new generation PCD tool materials. PCD is for example relatively susceptible to mechanical shock due to lower TRS values, but is much more resistant to thermal shock.

Conventional (Up-milling) can be used to minimise the mechanical shock on the PCD inserts. It gives us a very small chip thickness starting at zero on entry gradually growing through the cut. The cutter exists while the chip is relatively thick compared to the entry thickness, resulting in some thermal shock. Climb milling results in a sudden entry with a relatively large chip thickness, gradually tapering to zero on exit may work well for tungsten carbide as a cutting strategy. This will create the situation of substantial mechanical shock on entry, and very little thermal shock on exit.

High axial immersion cut strategies also holds promise for titanium machining effectiveness advances. Research by Sandvik [66] has shown that a decrease in tool life is only weakly correlated with an increase in axial immersion. The correlation of tool life with maximum chip thickness (f_z) is stronger, while the correlation with cutting speed



is extremely strong. It is therefore possible to tailor the cutting process parameters to maintain tool life, while increasing the material removal rate. There are further possibilities to apply these principles to the considerably different set of material characteristics of the synthetic diamond family of cutting materials.



5. Cutting materials and Insert configurations

5.1 Introduction

While the history of cutting tools date back to the Stone Age, the invention (1898) of high-speed steel (HSS) could still be associated to a dramatic development of cutting materials. In the 1920's, Dr Schroter (German), invented cemented carbide that was much harder than HSS. Friedlich Krupp, a German company, successfully merchandised cemented carbide and started selling these products in 1926. General Electric marketed cemented carbide products in 1928 under the name of "Carbology". As new technologies are developed we have seen an increase in the quality of cutting tools, leading to an increase in production [75].

The drivers of change in cutting technology are summarized in figure 5-1. Byrne et al found that the key drivers include: reduction of component size, enhanced surface quality, tighter tolerances and manufacturing accuracies, minimizing costs, reduction of weight and smaller batch sizes. These drivers towards change have a direct influence on the primary inputs to the cutting process of which the cutting tool material and configurations form part.

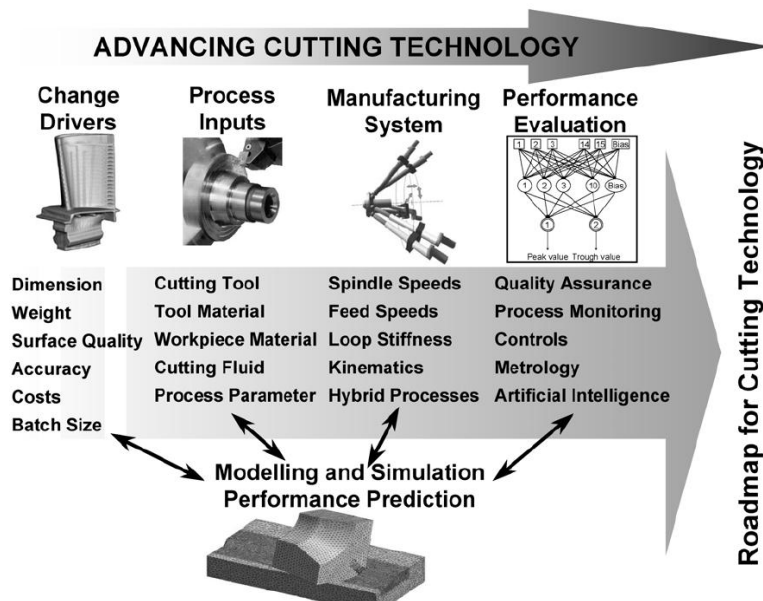


Figure 5-1: Primary aspects associated with advancing cutting technology

[76]



Currently a wide range of inserts are available with varying levels of application support. The modern machining industry is therefore one of many possibilities, with the capability in the hands of the machining company to position themselves in the competitiveness race.

5.2 Overall insert geometry

The insert geometry, tolerance and dimensions are based on ISO standards, which are also the foundation for other standards like ANSI (America) and JIS, CIS (Japan). The strength of any insert edge is affected by the basic shape of the tool. Standard inserts are available in different shapes. Although there are different insert shapes, it is important to select the correct one for the application in order to machine the work piece to its preferred form. As overall width and depth of the tool shape is improved from the triangle on the right to a circle on the left (figure 5-2), the overall strength of the tool increases.

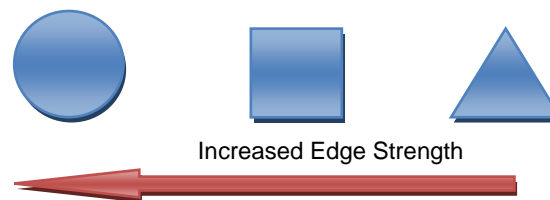


Figure 5-2: Different tool shapes [75 & 77]

The most common standard insert shapes available in the industry are discussed below.

5.2.1 Round inserts

These inserts are by far the strongest, because they don't have corners. Round inserts provide more cutting edges per side. This number of cutting edges will depend on the depth of cut and the way of indexing the insert. The problem is that these inserts can only be used to machine work pieces that do not require sharp corners. The biggest depth of cut which can be taken with round inserts is half the insert diameter [75 & 79].

5.2.2 Square inserts

These inserts are the most popular, although they have fewer cutting edges and less corner strength than round inserts. Square inserts produce a wide variety of corner shapes and can be set to almost any lead angle [75 & 77]



5.2.3 Triangular inserts

These inserts have longer cutting edges than other inserts, but are weaker. Triangular inserts are the most versatile shape, because they can be used to produce a wide range of shapes on the work piece [77 & 79].

5.3 Insert properties

Different properties enable materials to have their respective suitable applications and work piece materials. Machado et al [62] discovered through their machining research on titanium alloys, that the cutting inserts require the following properties in order to machine these alloys competitively:

- a. High Transverse rupture strength
- b. Reduced tendency to react with titanium
- c. High hardness at elevated temperatures
- d. Toughness and fatigue resistance to withstand the chip segmentation process
- e. High thermal conductivity to minimize thermal shock on the tool

5.3.1 Transverse Rupture Strength

The transverse rupture strength (TRS) can be defined as the resistance to crack initiation. To avoid rake face chipping from mechanical overload, this property of the tool material should be greater than the applied load. Studies (figure 5-3) on the machining of Ti-6Al-4V with PCD indicated that an increase in TRS enabled a longer tool life [56].

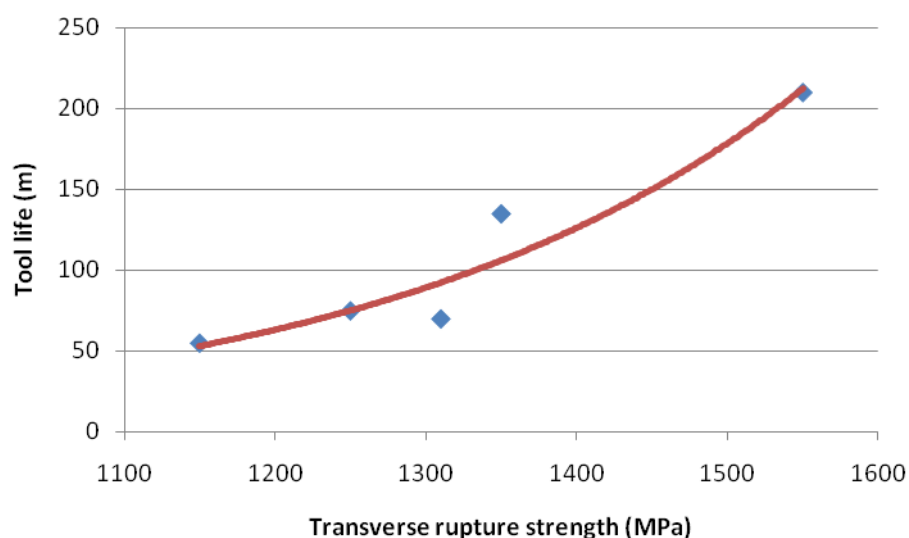


Figure 5-3: The effect of transverse rupture strength on tool life [56]



Lammer [78] studied the transverse rupture strength of PCD by a three point bend test. The data were analyzed based on particle size, Co-WC content, and the interaction of crack front and the Co-WC. Huang et al [80] investigated the influence of particle size on transverse rupture strength.

In order to do a comprehensive machining performance assessment, the transverse rupture strength of various cutting materials was collected from diverse sources. [66, 75 & 79]. Figure 5-4 compares the TRS of various cutting materials used in industry.

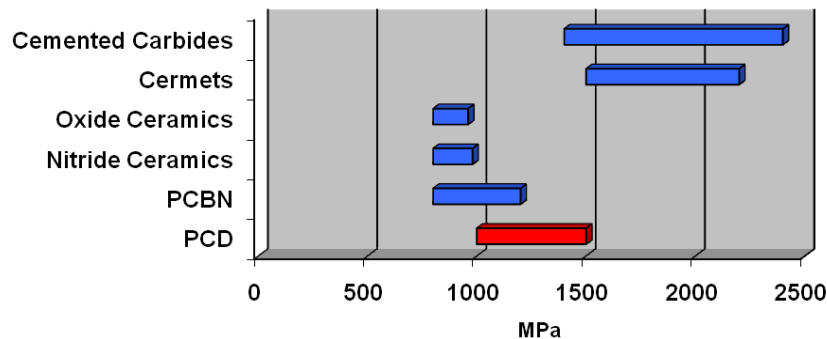


Figure 5-4: Transverse rupture strength of different cutting materials

TRS is the ability to withstand brittle fracture (chipping). Chipping is a dominant wear mechanism in superhard cutting materials. Therefore it is an important performance characteristic. The figure clearly shows that carbide has much higher transverse rupture strength than PCD.

5.3.2 Hardness

Hardness is the measure of a material's resistance to deformation by surface indentation or by abrasion [63]. According to Nabhani [81] diamond has hardness higher than 49GPa. In order to do a comprehensive machining performance assessment, the hardness of various cutting materials was collected from diverse sources [66, 75 & 79].



Figure 26 compare the hardness of various cutting materials used in industry.

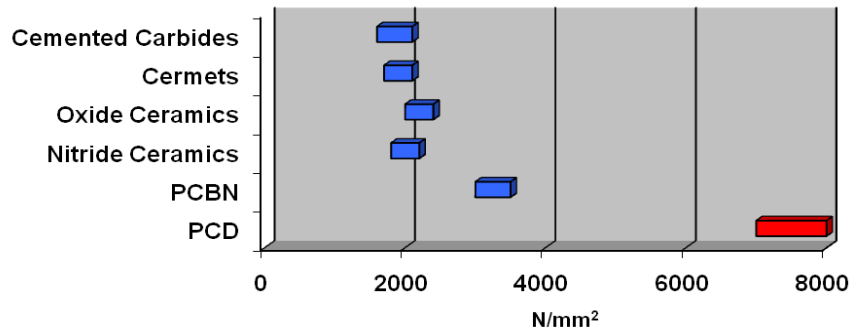


Figure 5-5: Hardness of different cutting materials

This comparison clearly indicates the superior hardness of PCD, followed by PCBN.

5.3.3 Fracture toughness

Fracture toughness is the property of a material to withstand rapid crack propagation. Various subscripts are used to denote different loading conditions or fracture toughness.

Lammer [78] also studied the fracture toughness of PCD, using a compression test. However, the fracture toughness values obtained from this method consisted of contributions from both crack initiation (TRS) and crack propagation. In order to provide a more direct measurement, the author has employed a single-edge pre-crack beam test to evaluate the fracture toughness. Fracture toughness of various cutting materials was collected from assorted sources [66 & 79] and compared in figure 5-6.

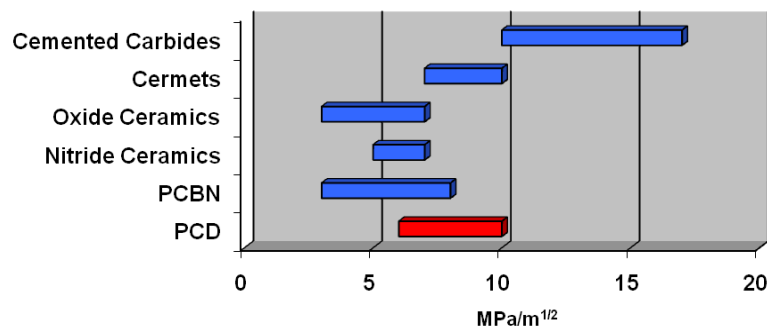


Figure 5-6: Fracture toughness of different cutting materials

Research indicated that the fracture toughness of polycrystalline diamond (PCD) increased with increasing diamond particle size. This may be attributed to increasing



tensile components of the internal stresses occurred in PCD with decreasing particle size due to thermal mismatch between sintered diamond and Co-WC. In addition, it has also been found that increasing Co-WC alone in PCD did not result in significant increase of fracture toughness [80].

5.3.4 Thermal expansion

Thermal expansion is the change in volume as a function of temperature [9]. As computed by means of finite-difference method, the maximum temperature between the chip and tool can reach 1400°C when machining Ti-6Al-4V at a cutting speed of 120m/min [82]. The coefficient of thermal expansion of various cutting materials is shown in figure 5-7 [75 & 79].

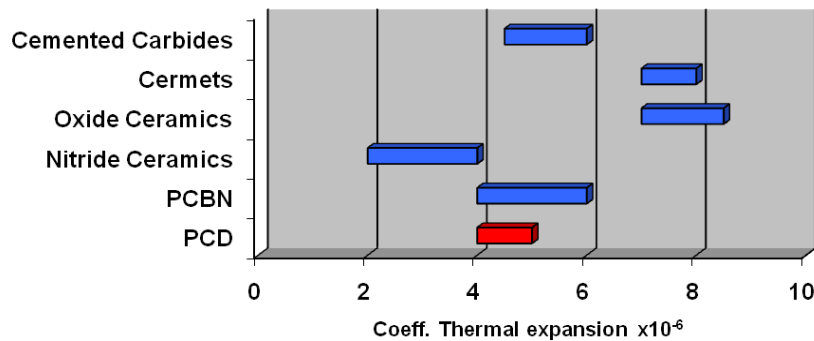


Figure 5-7: Thermal expansion coefficient of different cutting materials

PCD has a relative low thermal expansion coefficient compared to other cutting materials.

5.3.5 Thermal conductivity

Thermal conductivity is a property characterizing the ability of both the machined-, and cutting material to conduct heat [63]. According to Ownby [83] and Flauhaut [84] PCD can reach a very good thermal conductivity of 550 W/m.K at 300°C. Ceramic tools have similar thermal conductivity as Ti-6Al-4V (around 7 W/m.K).



Figure 5-8 compare the thermal conductivity of various cutting materials.

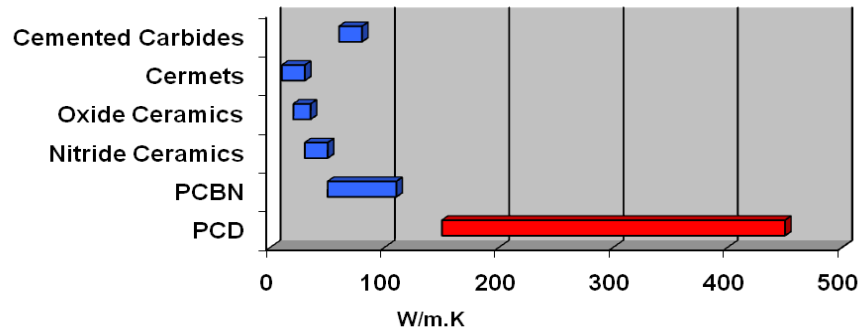


Figure 5-8: Thermal conductivity of different cutting materials [75]

The figure illustrates PCD's advanced thermal conductivity properties. Thermal conductivity play a critical role for efficient machining of titanium [42 & 56].

5.3.6 Thermal shock resistance

Thermal shock is an additional cause of wear and as a result it is essential to evaluate. Depending on heat flow conditions, Bulk transient (R) or Local transient (R_v) thermal shock factors are relevant.

$$R = TRS (1 - \nu) / E\alpha \quad (1)$$

$$R_v = \gamma (R) \quad (2)$$

TRS is seen to increase both factors, but increased thermal diffusivity (γ) also acts to increase the transient thermal shock factor. In relation to equation 1 & 2, Cemented tungsten carbide have a better bulk thermal shock resistance, while PCD has a better local thermal shock resistance. To avoid fracture by thermal shock, the TRS and thermal diffusivity or conductivity needs to be as high as possible, while E and thermal expansion should be kept at a low. R_v is more relevant to machining than R , because only the tip of the insert is heated and the gradient at the surface may be region of primary interest [56].



The effect of thermal shock resistance (R_T) on tool life is shown in figure 5-9.

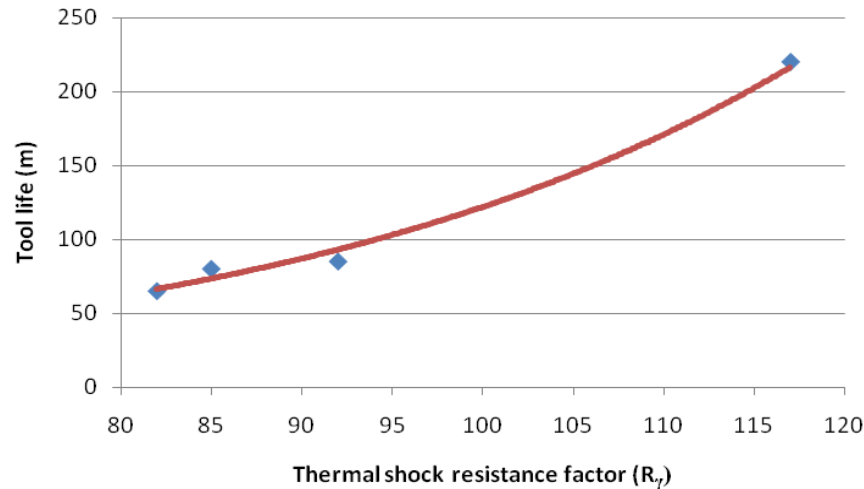


Figure 5-9: Effect of thermal shock resistance (R_T) on tool life [56]

Barnett-Ritchey et al [56] discovered that maximizing both the transverse rupture strength and R_T values will produce a robust tool capable of longer tool life.

5.4 Polycrystalline diamond

5.4.1 Introduction

Syndite (PCD) is produced by sintering together micron-sized diamond particles at ultra high pressure and temperature in the presence of a metallic catalyst. The binder can be added as a powder or as a coating on the diamonds [85]. The presence of the metal in the PCD structure, together with the tungsten carbide substrate, present a degree of toughness and electrical conductivity not found in single crystal diamond products [79].

PCD can be produced in relatively large blocks, because the sintering process avoids problems involved in the growing of large single crystals [86]. The manufactured blanks can be used as is, or after mechanical-, wire EDM-, or laser cutting, to produce cutting tools, mining bits or wear resistant part blanks [85].

The finer the diamond grain size, the better the cutting edge and surface produced [56]. The coarser the particle size, the greater the wear resistance, which is also reflected in the machinability. Coolant is usually used with these tools, but dry cutting can also be employed. Syndite can be regarded as a composite material which combines the



hardness, abrasion resistance and thermal conductivity of diamond, with the toughness of tungsten carbide.

Interesting to note is that ferrous alloys chemically attack the diamond, leading to an increased tool wear [67]. Especially for titanium the inserts should be able to restrain the generated heat from the operation, while conducting it away from the cutting edge, to attain higher cutting speeds [87]. PCD's relative high thermal conductivity combined with a appropriately designed cutting strategy might be the reason for the material to hold undiscovered potential for this operation.

Ownby [83] indicated that diamond reacts at high temperatures with titanium to form its own carbides known as TiC. Diamond is metastable and therefore its phase changes very slowly at ambient pressure and temperature and it transforms into graphite, while a high temperature combined with a low pressure can strongly accelerate graphitization [88].

5.4.2 CMX 850 (Fine)

According to the manufacturers this PCD product combines a high chip and abrasion resistance with good process ability, which makes it an ideal utility grade for many different applications on a variety of work piece materials.

The use of one micron sized diamond particles as the base material together with a proprietary manufacturing process, led to a polycrystalline material that displays a well sintered, homogeneous structure. This fine grain size gives CMX850 both relative high fracture toughness and TRS properties, which is an ideal combination for cutting tool materials. Its abrasion resistance is comparable to coarse grain materials and the material is suitable for finish and rough machining operations [79].

5.4.3 CTB 010 (Medium)

This product has a 10 micron average grain size and is available in a range of PCD layers and overall thicknesses. Being the general purpose grade, this includes standard, thin or thick PCD layers. This allows the manufacture of a wide range of general, precision and roughing tools as well as wear parts. This material has the best combination of tool fabrication and application performance characteristics.

It also has the lowest fracture toughness as indicated in figure 5-9.

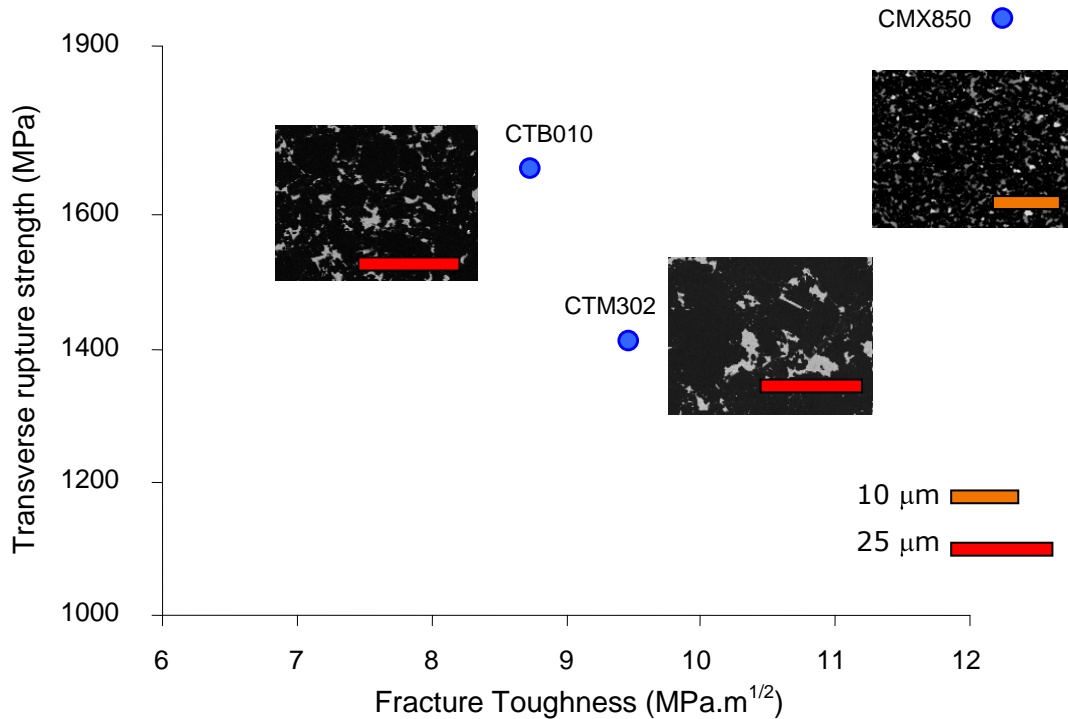


Figure 5-10: Transverse rupture strength and fracture toughness of different PCD materials [79]

5.4.4 CTM 302 (Coarse)

CTM302 contains a mix of micron diamond particles sizes between 30 and 2 μ m. A combination of this mix and controlled sintering conditions increases the diamond packing density, which increases wear resistance. Optimisation of microstructure and hence mechanical properties also result in a more continuous ground cutting edge, enhancing work piece surface finish. The coarse particles impart excellent abrasion resistance and improve thermal stability. The fine particles improve packing density and give high cutting-edge quality for a low work piece surface roughness. Although it has the lowest TRS, the high fracture toughness of the material imparts good chip resistance. According to the manufacturers the CTM302 is the optimum material for machining compacted graphite cast irons.

5.4.5 Machining with PCD

According to studies by König and Neises, PCD represents a substitute tool material for turning titanium alloys [89]. In 2001, more work on finish turning indicated that the PCD



produced a better work piece surface integrity [90]. Regardless of all these positive findings in turning, very little data exists on finish milling titanium alloys and even less, if any at all, on the rough milling of titanium alloys using PCD.

Barnett-Ritcey reported a tool life of 215 min ($V_c=457\text{m/min}$), concluding that high speed milling of Ti-6Al-V4 is possible with PCD [56]. Kuljanic et al also reported a very long tool life ($T=381\text{min}$) with good surface finish and geometrical accuracy, finish milling titanium compressor blades with PCD at a relatively slower cutting speed ($V_c=110\text{m/min}$) [42]. Konig and Neises [89] found that the diffusion and dissolution processes were worsened by the high local temperature resulting from the poor thermal conductivity of the Ti-6Al-4V.

5.5 Machining with CBN

Ezugwu et al [91] evaluated the cutting performance of different Cubic Boron Nitride (CBN) tool grades when finish turning Ti-6Al-4V alloy under cutting conditions of up to 250 m/min and various coolant supplies. They studied the wear of the tool, failure modes and cutting forces. The surface roughness of the machined surfaces were also monitored and used to assess the performance of the cutting tools. Bhaumik et al [71] also investigated the wear mechanism of wBN-cBN composite tools on the same material as O. Ezugwu et al. In 2000, Zoya and Krishnamurthy [59] studied CBN tools under finishing conditions (feed rate= $0,05\text{m/min}$ and $a_p=0,5\text{mm}$) at speeds up to 350m/min. They evaluated the turning performance of titanium alloys and concluded that it's a thermally dominant process and a critical temperature of 700°C can be a decisive factor for tool life. They also mentioned that the prominent wear of CBN tools is diffusion.

Despite the relative good cutting performance of CBN, ceramic tools are generally preferred for high speed machining of aero-engine materials, because of their much lower cost [15]. Ezugwu et al also confirmed that for machining Ti-6Al-4V alloy with different grades of CBN tools gave lower performance, in terms of tool life, compared to uncoated carbide tools for different turning conditions [91].

5.6 Machining with Carbide Tools

An uncoated Carbide (K10) was used by Li et al [92] for high speed milling of Ti6Al4V. They observed the effects of the cutting speed on the temperature. They came to a



conclusion that the cutting temperature increase with cutting speed and also perceived that there is no reduction of cutting temperature at higher cutting speeds.

In an additional study the performance of various tool materials in machining titanium alloys were examined. According to Bryant [93] titanium alloys are very reactive with the cutting tool materials at 500°C. Straight tungsten carbide (WC–Co) tools are reported to have superiority in performance in machining titanium alloys in interrupted cutting [94]. Although the application of the appropriate WC–Co alloys were satisfactory, machining performance could not be achieved under room temperature conditions in view of the fact that the cutting speeds are limited ($V_c=45\text{m/min}$). Uncoated carbide (WC) inserts were used for orthogonal continuous and interrupted cutting by Wang et al. at conventional cutting speeds [95]. They studied the cutting performances under dry cutting, minimal quality lubrication (MQL) and flood coolant. According to them, MQL was an effective alternative approach for flood coolant during high speed turning of Ti-6Al-4V.

The authors [69] confirmed that $V_c=45\text{m/min}$ is the usual cutting speed for machining titanium with uncoated straight grade cemented carbide (WC-Co). Abrasion wear is the major cause of flank wear when machining aero-engine alloys with carbide tools at lower speeds conditions [87]. In another study on the dry end milling of Ti-6242S, the following optimum cutting conditions were obtained, $V_c=88\text{m/min}$ ($f_z=0.20\text{ mm/z}$), $V_c=113.5\text{ m/min}$ ($f_z=0.15\text{ mm/z}$) and $V_c=163\text{ m/min}$ ($f_z=0.10\text{ mm/z}$), as the best compromise among cutting speed, MRR (cm^3/min) and TL (min) [96].

5.7 Summary

Turning Ti-6Al-V4, Hoffmeister et al revealed that Element Six PCD (CTB010) could achieve a 3 fold increase in tool life over tungsten carbide at a speed of 200 m/min ($f_z=0.05\text{ mm/rev}$) [97]. In another study on turning TA48, Nabhani achieved a 4 fold increase in tool life over KC850 carbide at a speed of 75 m/min ($f_z =0.25\text{ mm/rev}$) using similar PCD tooling [98]. Kramer [99] reported that CBN tools retain their strength at temperatures in excess of 1100°C while carbide tools encounter plastic deformation at this temperature range. Turning Ti-6Al-V4, Klocke et al also evaluated PCD, HW-K10 cemented carbide, PCBN and oxide ceramic (alumina). They found PCD was subject to a much lower level of crater wear compared to the other tools.



Narutaki and Murakoshi [87] showed that natural diamond tools used dry at $V_c=100\text{m/min}$ lasted longer than carbide tools used with a cutting fluid at the same speed. When used with a cutting fluid at $V_c=200\text{m/min}$, the diamond tool had the same wear rate as during dry machining at $V_c=100\text{m/min}$. This, in a way, corresponds with the findings of Sharman et al. [100] on the machining of $\gamma\text{-TiAl}$ intermetallic alloys. Their study showed that with a low pressure fluid supply, $2\ \mu\text{m}$ and $10\ \mu\text{m}$ grain size PCD produced similar tool life to that of using WC with a high pressure fluid supply. Nurul Amin et al studied the effectiveness of polycrystalline diamond inserts (PCD) and compared it to uncoated tungsten carbide–cobalt inserts machining Ti–6Al–4V. They compared the inserts with respect to the applicable cutting speed ranges, metal removal (MR) per tool life and tool wear rates, tool wear morphology, surface finish, chip segmentation and chatter phenomena [101]. The authors concluded that PCD inserts can be used effectively up to cutting speeds of $160\ \text{m/min}$, as the wear rate is quite low and the amount of metal removal per tool life quite reasonable.

To conclude, PCD exhibits a higher thermal conductivity and hardness, but lower TRS which can be ideal for finish milling Ti-6Al-4V at elevated speeds if the correct milling strategy is applied.



6. Machining performance assessment

6.1 Tool life

Tool life (TL) is defined as the length of cutting time that the tool can be used or operating time of the tool until catastrophic failure. TL is usually defined by flank wear due to the significant influence this parameter has on the surface finish and dimensional accuracy of the machined part [22]. Surface roughness increases as flank wear increases, while crater wear has a strong influence on process reliability as it can lead to instantaneous failure due to chipping the tool. The authors [42] discovered a definite relationship between tool wear and surface roughness.

The typical wear growth curve (figure 6-1) [19] can be divided into different regions. The break-in-period is at the beginning of tool use. Initially the sharp cutting edge wears rapidly. This region is followed by a relatively uniform wear (steady-state region). The slope of the tool wear is affected by work material and cutting conditions. The harder the material, the more inclined the slope. Before failure, the rate begins to accelerate which marks the beginning of the failure region [19].

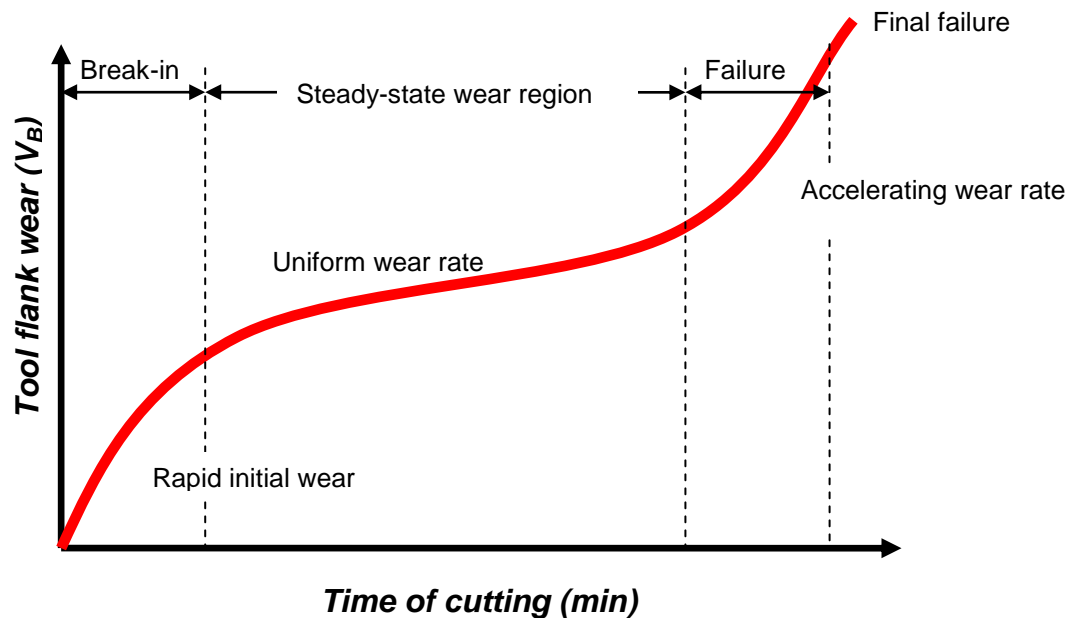


Figure 6-1: Tool life



A failed insert causes large problems with surface quality. It is suggested that a tool wear band width (V_B) is identified, which signifies the end of the tool. The failed tool can be switched as the wear reaches this width. Literature recommends a flank wear scar limit of 0.3 mm [101] for experimental studies. The cutting distance or time in cut can be measured accordingly.

F.W. Taylor formulated an equation (3) that determines tool life as a function of cutting speed. This is widely known as the Taylor tool life equation:

$$vT^n = C \quad (3)$$

with v = cutting speed (m/min), T = tool life (min) and n , C constants [19]. Barnett-Ritcey [56] expanded this Taylor equation to make it suitable for the machining of titanium to:

$$TL = C_{TL} V^{nv} a_e^{nae} h_x^{nhx} \quad (4)$$

Where nv , nae , nhx and C_{TL} are constants and found experimentally for a given tool diameter (D) and axial immersion (a_p).

Comprehensive experiments with PCD inserts, milling Ti-6Al-4V [101], enabled the authors to calculate the tool life for different cutting speeds [figure 6-2].

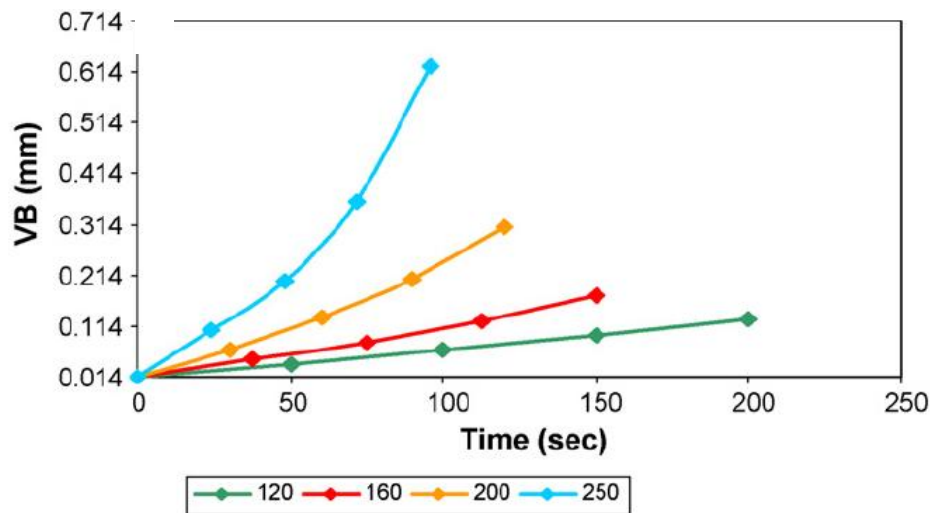


Figure 6-2: Average flank wear (V_B) for different cutting speeds [101]

The total volume of material removed during the life of the tool (with average actual or extrapolated flank wear, $V_B=0.3$ mm) was calculated for different cutting speeds. The maximum metal removed ($59.87 \times 10^3 \text{ mm}^3$) is at $V_c=120$ m/min and the minimum



($16.72 \times 10^3 \text{ mm}^3$) at $V_c=250 \text{ m/min}$. PCD inserts can be used effectively up to cutting speeds of 160 m/min.

6.2 Tool wear

There are a number of possible modes by which a cutting tool can fail [19]. Gradual and expected degradation of tool wear are the only accepted forms within the machining industry. Premature tool failures are minimized by careful analysis of work piece materials, operating parameters and tool preparation practices. Different interactions can occur between the tool and work piece during the machining of titanium. These alloys react with most tool materials at elevated temperatures conditions, which results in accelerated tool wear [23]. Inserts employed for machining titanium alloys traditionally have a short tool life, mainly due to the generated high temperatures near the cutting edge [22].

6.2.1 Failure Modes

6.2.1.1 Temperature failure

Temperature failure occurs when the cutting temperature is too high for the inserts. It softens the tip of the insert, which leads to plastic deformation and loss of the sharp edge. Failure is also due to changes in temperature at the cutting edge. This temperature cycling mainly derives from interrupted cutting. The failure is recognized by its thermal cracks that occur on the cutting edge [19].



In figure 6-3 the relationship between thermal crack resistance and thermal expansion coefficient is illustrated.

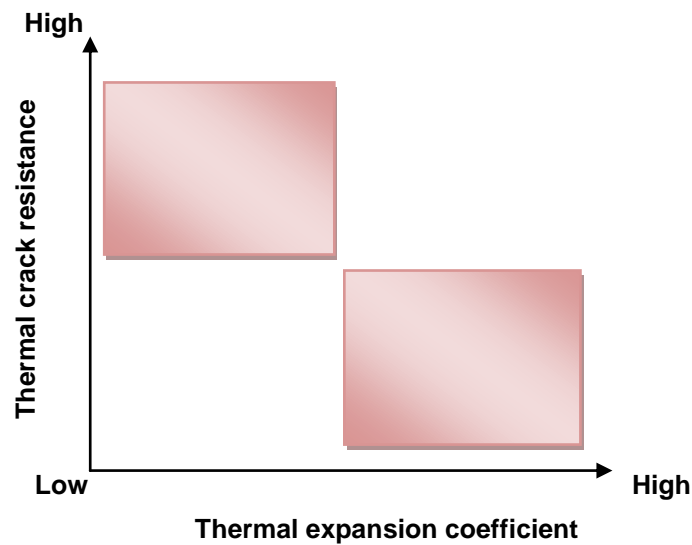


Figure 6-3: Relationship between thermal crack resistance and thermal expansion coefficient [75]

A high thermal expansion coefficient is correlated with a low thermal crack resistance and vice versa, is shown [75].

6.2.1.2 Fracture

This impact failure refers to the breakdown of the insert's cutting edge. This occurs when mechanical loading exceeds the fracture strength (TRS) of the insert [56]. This mechanical overload causes the tool to fail suddenly.



In figure 6-4 the relationship between chip resistance and transverse rupture strength is shown.

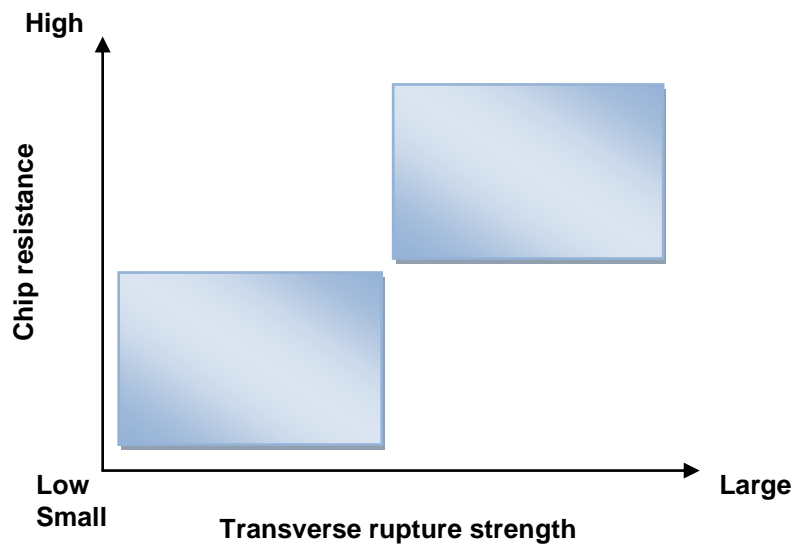


Figure 6-4: Relationship between chip resistance and transverse rupture strength [75]

Large transverse rupture strength is correlated with a high chip resistance and vice versa, is shown [75].

6.2.1.3 Gradual wear

Gradual wear causes loss of tool shape and reduction in cutting efficiency. The wear scar's growth accelerates as the tool becomes heavily worn. Similarly to temperature failure the tool fails. This type of failure occurs on the top rake face and the flank.

Premature failure is primarily thermal, chemical or impact related, which is undesirable [64]. Gradual wear is preferred, because it leads to a longer TL and economic benefits. According to Nurul Amin et al a cutting speed beyond 120 m/min will initiate an intensive tool wear on PCD [101].

6.2.2 Types of tool wear

Wear types described and shown in figures 6-5 & 6-7 [19, 20 & 75] can be distinguished into crater- and flank wear. Flank wear can also be divided into two features according to the condition.



6.2.2.1 Crater wear

This wear is formed by the action of chips sliding against the surface. It consists of a concave section on the rake face of the tool. High temperatures and stresses characterize the tool-chip contact interface. This contributes to the wearing action shown in figure 6-5. Most of the heat during the machining of titanium is restricted in the primary zone, causing rapid chemical reactions on the flank face. In continuous to slight interrupted mode, the inserts experience failure due to chipping as a result of excessive crater wear [62]. It is expected that any reduction in crater wear will result in longer tool life.

Hartung et al compared different cutting materials in a crater wear rate (wear/min) study. [102]. The authors determined that machining Ti-6Al-4V at $V_c=61\text{m/min}$, the PCD ($1.4\mu\text{m/min}$) outperformed both Carbide ($2.2\text{--}8\mu\text{m/min}$) and PCBN ($30\mu\text{m/min}$). Machado et al documented rake face temperatures in the area of 900°C at a cutting speed of 75m/min when machining Ti-6Al-4V. This caused rapid crater wear due to dissolution and diffusion [62]. According to another research study [57] coated carbides should not perform well with Ti-6Al-4V due to rapid crater wear (diffusion driven) of the ceramic coating in turning. Figure 6-5 illustrates the main types of tool wear.

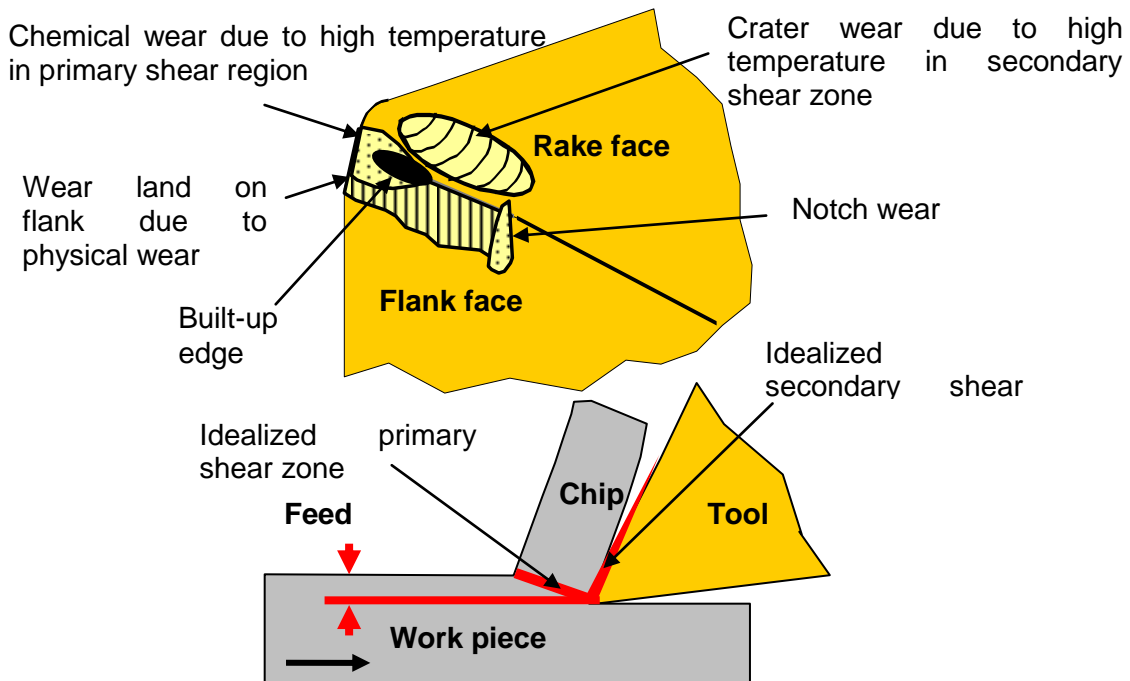


Figure 6-5: Types of tool wear



6.2.2.2 Flank wear

Flank wear results from rubbing between the newly generated work surface and the flank face nearby the cutting edge. This wear occurs on the flank insert and is measured by the average width of the wear band (V_B) which is occasionally called the flank wear land (FW). According to the authors the V_B involve adhesion, pull-out, abrasion and dissolution wear if titanium alloys are machined [94].



Figure 6-6: Relationship between flank wear resistance and hardness [75]

The relationship between flank wear resistance and hardness, namely that high hardness is correlated with a high flank wear resistance and vice versa, is shown [75].

6.2.2.3 Notch wear

Notch wear is an extreme condition of flank wear and often appears on the cutting edge. This wear occurs because the original surface is harder and/or more abrasive than the internal material. This could be due to work hardening from cold drawing or machining.

6.2.2.4 Nose radius wear

Nose radius wear occurs on the nose radius of the tool. This usually leads into the end of the cutting edge.



Nose and notch wear are indicated in figures 6-5 & 6-7 [19, 20 & 75].

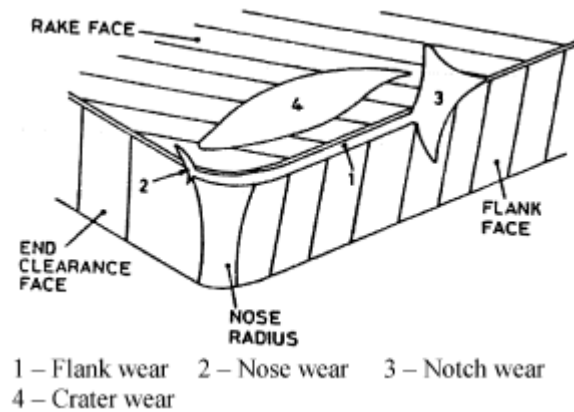


Figure 6-7: Types of tool Wear [20]

6.2.3 Mechanisms of tool wear

6.2.3.1 Abrasion

The friction generated between the flank and work piece due to the action of sliding chips in the shear, cause abrasion. This wear happens primarily due to hard inclusions of work material or separated small particles of tool material that scratch the contact surface [87]. Abrasion is compounded by the part's hardness and strength properties, which is also an indication of appropriate machining speeds. This mechanism occurs gradually on the flank (make it possible to estimate the tool life) and after the crater is weakened due to diffusion, crater wear is accelerated by abrasion [19 & 101].

6.2.3.2 Adhesion

This is when two materials are forced into contact under high pressure and temperatures until they weld together. These conditions are present between the chip and rake face of the insert. This results in a form of abrasion, as the sticky chips break away small particles on the surface [42 & 75]. The critical temperature for adhesion to occur machining with PCD and CBN are 760°C and 900°C respectively and the nominal pressures about 0.142 and 0.146 GPa [81].

6.2.3.3 Diffusion

Crater wear on the rake face of a cutting tool is due to the interaction between the underside of the chip and the tool face [19 & 75]. This happens under high contact



stresses, high temperature and interface thermo chemical reactions. Wear at high cutting speed can be regarded as a consequence of a diffusion effect.

Diffusion of the tool material at 700°C [59] assists in the decision to regard this temperature as critical for machining titanium alloys with CBN tools. Diffusion is the main contributor to wear at HS conditions [22 & 75]. Titanium can react with the Nitrogen in the CBN at temperature above 1100°C when inter-atomic diffusion of titanium and CBN accelerate significantly. This was confirmed by Nabhani [98] machining TA48 with CBN and PCD tools. The cutting edge of the tool was bonded to the underside of the chips.

6.2.3.4 Chemical reactions

Chemical wear can be considered as a thermally activated process. It's due to a reaction between the insert and work piece. The insert and work piece material react, removing the material from the insert on an atomic scale. The rate of this chemical wear increases with an increase in temperature [19 & 75]. This can result in chemical reactions like oxidation. As mentioned are premature failures primarily caused by thermal, chemical or impact factors [19, 56 & 75].

6.2.3.5 Plastic deformation

The cutting forces acting on the edge at high temperature cause the edge to deform plastically, which makes it more vulnerable to abrasion. Thermal softening, oxidation and chemical reactions weaken the inter-granular bonds which cause the grains to tear apart under the action of the machining shear stress. The grains are dislodged out of the matrix; hence Pull-out [56, 66 & 75].



In figure 6-8 the relationship between plastic deformation resistance and hardness is shown.

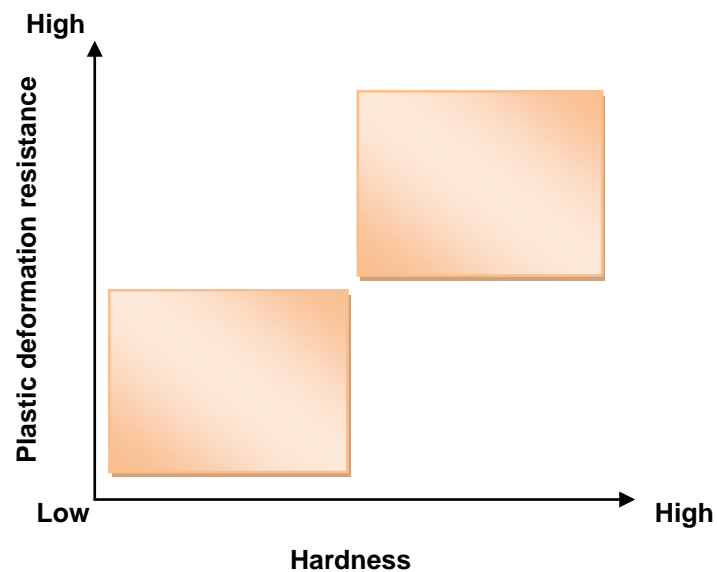


Figure 6-8: Relationship between plastic deformation resistance and hardness

High hardness is correlated with a plastic deformation wear resistance and vice versa, is shown [19, 22 & 75].

6.3 Surface finish

Machined components for aerospace are subjected to rigorous surface analysis to detect surface damages that will be detrimental [104]. Machining is often the manufacturing process that determines the part's surface texture as it is usually the final process. Average surface roughness (R_a) and geometry are important in determining the functional performance of machined components. Sub-surface characteristics like residual stress and surface defects (porosity, micro-cracks) are also critical. The R_a depends on the geometric, material, vibration and machine tool factors [19].

6.3.1 Geometric factors

Geometric factors include the machining parameters. These include the type of operation, insert geometry, feed and nose radius. Surface geometry is referred to as the theoretical surface roughness.



Tool geometry and feed combine to form the surface geometry. The effects can be seen for a single-point tool in figure 6-5.

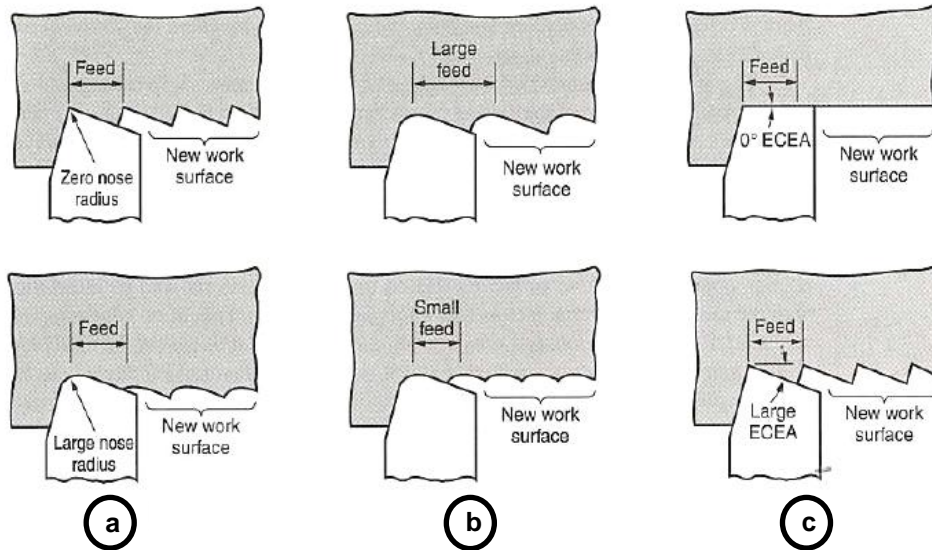


Figure 6-9: The effects of nose radius and feed of surface roughness [19]

With the same feed, a larger nose radius causes the feed marks to be less pronounced, thus leading to a better finish (figure 6-9 a). If two feeds are compared with the same nose radius, the larger feed increases the separation between the feed marks, leading to an increase in the value of ideal surface roughness (figure 6-9 b). Thiele and Melkote [105] experimented with steel and realized feed is the primary influence on surface roughness, followed by edge geometry. If feed rate is large enough and the nose radius is small enough so that the end cutting edge participates in creating the new surface, then the end cutting-edge angle (ECEA) will affect surface geometry as shown in figure 6-9 (c).

6.3.2 Work material factors

The ideal surface finish mentioned above is highly unlikely due to factors related to the work material and its interaction with the insert. Built-up-edge (BUE) causes the surface to have a rough sandpaper texture. If the BUE is large and unstable, the surface finish degrades, which leads to surface roughness.

Chips curling back into the work damage the surface. It is affected by the tearing of work surface during chip formation. As the tool wears, the edge may chip which worsens the



situation. This is further degraded by plastic deformation. Tool wear causes an increase in cutting forces which worsen surface finish.

$$R_a = r_{ai} \times R_i \quad (4)$$

Machined surfaces often require the actual surface roughness (R_a) to be below a certain limit. An empirical ratio (r_{ai}) [19] and equation (4) helps to convert the ideal SR (R_i) into an estimate of the actual surface roughness. Nowadays a surface roughness machine is used to measure the actual value.

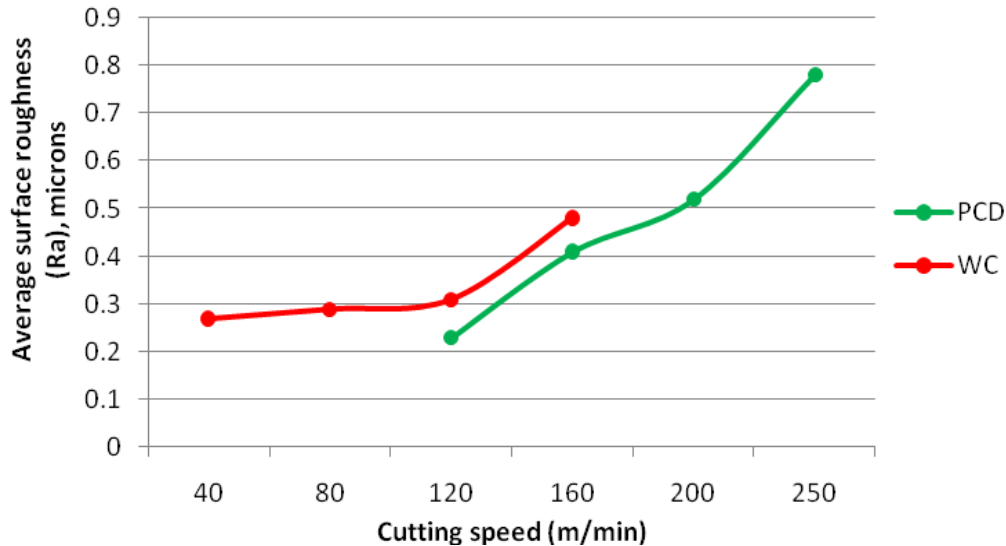


Figure 6-10: Average surface roughness (R_a) for WC and PCD inserts [101]

The effectiveness of PCD and WC inserts were tested, milling Ti-6Al-4V, by Amin et al [101]. The results (figure 6-10) indicate that the surface roughness (R_a) increased, with an increase in cutting speed at a constant feed rate ($f_z=0.1\text{mm/z}$). The average R_a is relatively low with values less than $0.4\mu\text{m}$, up to the cutting speed of 120 m/min. In the case of the PCD, the surface roughness values are almost in the range of $0.4\mu\text{m}$ up to the cutting speed of 160 m/min.

6.3.3 Vibration and machine tool factors

Vibration and tool factors are related to the tooling and setup in the operation. The vibration or chatter, deflections in the fixture, and backlash in the feed mechanism can all be minimized or eliminated. If possible, the surface roughness will be primarily determined by geometric and work material factors.



Kuljanic et al achieved a low R_a and a satisfactory geometrical accuracy milling titanium compressor blades with PCD [42] and a different study [101] indicated that the R_a of PCD inserts is lower compared to that of uncoated carbide inserts. This is due to the effect of lower wear rate and less pronounced chatter in the case of PCD inserts, especially at 120 m/min. Cutting speed up to 120 m/min in the case of carbide and 160 m/min in the case of PCD inserts produce surface finish equivalent to that obtained in polishing.

6.4 Overview of performance assessment considerations

Out of the literature [15, 56 & 101], it became evident that for a relatively low cutting speed (100m/min), the wear is low and uniform, with marks of notch wear and micro-failure due to attrition. For feed rates (f_z) below 0.051 mm, chipping becomes less of an issue [56]. Unfortunately, any reduction in f_z , results in a proportional reduction in material removal rate. At cutting speeds around 150 m/min there is some build-up and a uniform, but higher amount of flank and notch wear. The critical temperature for adhesion to occur for machining with PCD and CBN are 760°C and 900°C respectively and the nominal pressures about 0.142 and 0.146 GPa [69]. Speeds exceeding 200 m/min are associated with build-up, high flank and notch wear. The rate of this chemical attack increases with an increase in temperature. This can result in chemical reactions like oxidation [75].

Out of this was established that the main mechanisms responsible for the failure of PCD tools are diffusion, attrition, build-up and notching wear [42, 56, 66 & 101].



7. *Aims and objectives*

Information from the literature on the machining of Ti-6Al-4V indicates relative low speeds for milling this alloy. Many machining challenges limit the increase of this parameter and generally studies conclude that it is impossible to obtain an increase in cutting speed.

Tool materials able to withstand high temperatures, such as PCD, is shown to have potential to last significantly longer at higher cutting speeds. Cutting strategy is presented as potential focus area to achieve improvements. Pilot tests and studies show cutting speed (V_c) and feed rate (f_z) are key parameters to get better results.

This study explores the potential for innovative cutting materials to mill Ti-6Al-4V at high speeds. Studies of the wear modes and mechanisms were utilized to establish performance criteria.

The objective is to achieve an increase in tool life while machining at high speed, simply by avoiding the failure mechanism through an innovative milling strategy.



8. Experimental Setup and Design

8.1 Introduction

In order to establish a well defined experimental model and suitable parameters fundamental research, background work and pilot studies were conducted. The final setup and design were selected in accordance with the study objectives. The flow diagram in figure 8-1 illustrates the procedure that was followed.

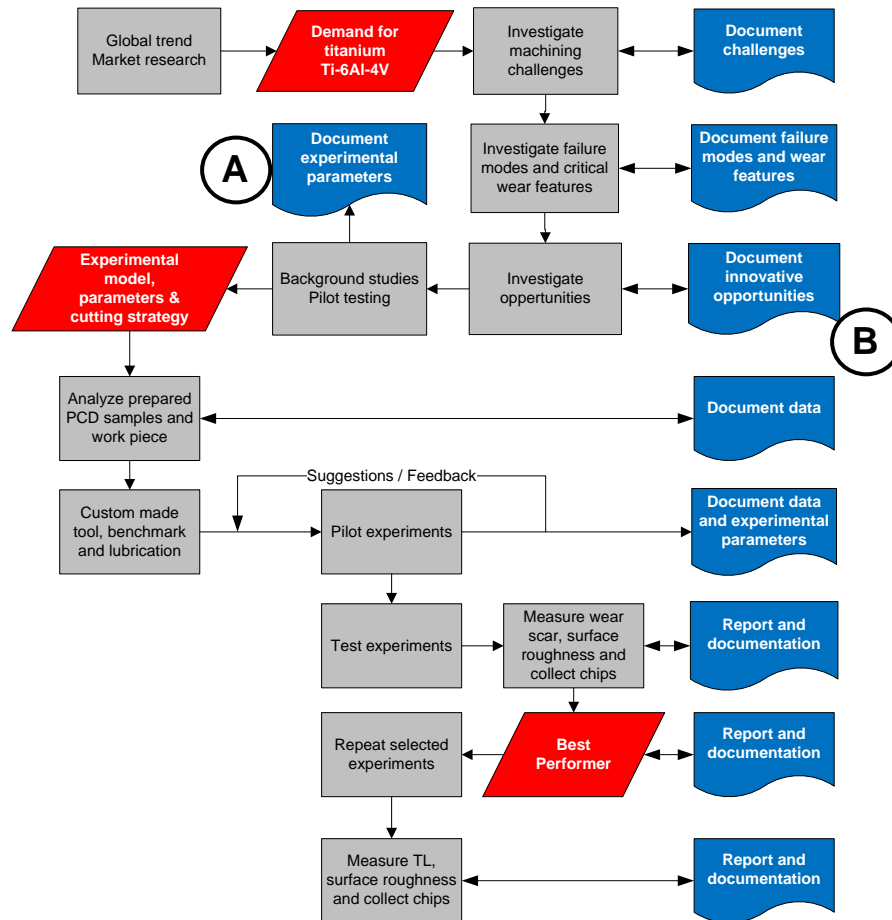


Figure 8-1: Research procedure flow diagram

A literature study and market research enabled the author to identify opportunities for improvement. Background studies and pilot test helped to set the foundation for an experimental model with cutting parameters. During the course of this study a work holding method to accommodate a 5-axis work piece in a 3-axis machine was investigated as background study (figure 8-1 A) within this predominantly cutting research. A copy of this article is included in Appendix A. The author also acted as co-



author for a paper (figure 8-1 B) presented at the South African Aerospace symposium at Spier, Stellenbosch, 2008. A copy of this article is included in Appendix B.

The results from these studies enabled the author to formulate a best practice cutting strategy, suitable for PCD. Through experimental tests the best performing cutting material and configuration were identified. This was followed with selected experiments.

8.2 Background study 1: Palletised work holding to emulate 5-axis machining

This background study presents the application of precision pallet technology, together with common 3-axis milling, to machine certain complex aerospace components, that is normally 5-axis machined. 5-axis machines are prohibitively expensive and in short supply in developing economies, like South Africa. Currently the default process for a wing section is either 5-axis machining, requiring expensive equipment, or multiple manual setups, that erodes competitiveness. In this approach however, a set of different customized precision pallets are used to present each complex plane to the 3 axis machine as a horizontal plane, requiring quick and simple face milling. After machining one surface, the pallet is exchanged with another that has been pre-set up in machining time. Trials confirm the viability of the approach with capital recovery in less than a year.

The pallet system significantly reduced the setup and changeover times, reducing production cost and lead time. This added-up to 28.6% saving in production time. The company can therefore typically supply the finished products to their clients a full 20.3 days earlier than originally planned. It is concluded that this 3-axis technique using palletised work holding is technically feasible and economically viable to machine flat surface aerospace components that would normally be machined on simultaneous 5-axis machines in the developed world.

A research article based on this work has been submitted to a research journal. A copy of this article is included in Appendix A.



8.3 Background study 2: Turning PM steels with experimental PCBN

8.3.1 Introduction

There is a definite growth in demand for PM steel parts in the automotive industry [106 & 107]. High density sintered alloys have a strength equivalent to hardened steels, but are very difficult to machine. The main critical wear mechanism, machining PM steels with PCBN, is abrasion [108]. Since different PCBN wear features, such as chipping and nose fracture exist in interrupted cutting, it is critical to have a machining operation model, that mimic the abrasion failure mode. This assures a better understanding of abrasion.

Research [108] conducted on hard turning of Vanadium 10 (V10) with PCBN samples addressed fundamental questions concerning wear mechanisms. The samples contained comparable cBN content and were all of similar grain size. The only difference among the inserts was their binder systems. Additional experimental details are confidential.

8.3.2 Background to the test

The turning test was intended as an abrasion test for PCBN grades. The work piece, V10 PM Steel, was used in the annealed condition, which generates a relatively low temperature chip to minimizing chemical wear.

The objective of the test was to measure the flank wear after known machining intervals and under constant machining conditions. Recorded data points and the wear performance of the different cutting tool materials were plotted. These figures were compared in graphical form.

8.3.3 Wear Measurement

The wear on the flank was measured and analyzed with an optical microscope and SEM. The measurement was taken at the maximal value near the leading edge of the tool. An XRD analysis helped to identify the most promising phases.

A stereoscopical microscope fitted with a digital camera was used to observe and measure wear on the tool materials. A fixture helped to keep the observation angles



constant between the analysed inserts. Different images were taken to represent flank faces of the tool at a fixed magnification.

SEM micrographs were taken of selected inserts. Images were taken using a Joel 7500F SEM and analyzed using AnalySIS software 3.2 (Build 799). The inserts were placed on a fixture which orientates samples at 45° to the horizontal for a better view.

8.3.4 Summary of results

All of the samples had a small amount of adhered work piece material on the flank, nose and crater. No early indications of cracks or prominent crater wear were discovered on the rake. The prominent grooves found in some samples could be attributed to the abrasive carbides in the work piece and the weak bonding strength of the binder system. The weak bonding enables the work piece to easily rip the insert particles out of the material.

8.3.5 Conclusion

This investigative work was done for Element Six (Pty) Ltd. The detailed results are reported in “*Wear phenomena of PCBN tools during PM steel machining, March 2008*” and are part of the company’s new application investigation body of knowledge [108].

8.4 Pilot test 1: Influence of different milling parameters

8.4.1 Background to test

The author performed these pilot tests in order to understand the influence of different cutting parameters on tool life. These experiments were used to lay a foundation for a cutting strategy developed for a missile hanger and also assisted in the development of an experimental model for the final experiments. See figure 8-1.

8.4.2 Experimental setup and procedure

The Hermle 5-Axis C40U machine was used to conduct the different pilot tests. Out of the literature it was established that cutting speed and feed rate are the most influential parameters on tool life [19, 42, 66, 75 & 56].



The author decided to also vary the depth of cut in order to gain a better understanding of the different effect of each parameter. Table 8-1 specifies the experimental equipment and machining conditions for the pilot tests with a tungsten carbide (H13A).

Table 8-1: Experimental equipment and machining specifications for pilot tests with WC

Insert type	H13A (R390-11 T3 08E-KL)
Work piece	Ti-6Al-4V (25x30x280mm)
Working engagement (a_e)	0.5 mm
Coolant	Flood (ROCOL® ULTRACUT 260) Diluted: Water : Oil 30 : 1
Machine	Hermle 5-Axis C40U
Tool	Sandvik (\varnothing 25mm) R390-025A25-11L
Wear measurement	Dell Computer with Zeiss AXIOVISION4 Software / Measuring Microscope

Measurements were taken for every cutting condition (Table 8-2) after 280mm of Ti-6Al-4V was machined with $a_e = 0.5$ mm and $a_p = 2$ mm. The author established the different test conditions based on information found in manuals of the supplier [56, 66 & 75].

Table 8-2: Experimental pilot test conditions and results

Condition	V_c (m/min)	F_z (mm/z)	DOC (a_p)	Table feed (mm/min)	Cutting time (s)	V_B (Flank)	V_B/min
A1	60	0.05	2.5	38	440	137.31	18.73
A3	140	0.05	2.5	89	188	156.2	49.72
B1	100	0.025	2.5	32	528	236.26	26.86
B3	100	0.075	2.5	95	176	127.32	43.42
C1	100	0.05	2	64	264	170.28	38.72
C3	100	0.05	3	64	264	171.6	39.02
D2	100	0.05	2.5	64	264	172.56	39.23

The shaded areas in table 8-2 for the different conditions indicate the parameter that is changed, while the other two parameters are kept constant.



8.4.3 Results

From this study it became evident that cutting speed has the largest effect on tool life, followed by feed rate. A variation in the depth of cut was associated with only a small change in wear. Figure 8-2 shows a graphical depiction of the change in tool life associated with the seven different conditions indicated in table 8-2.

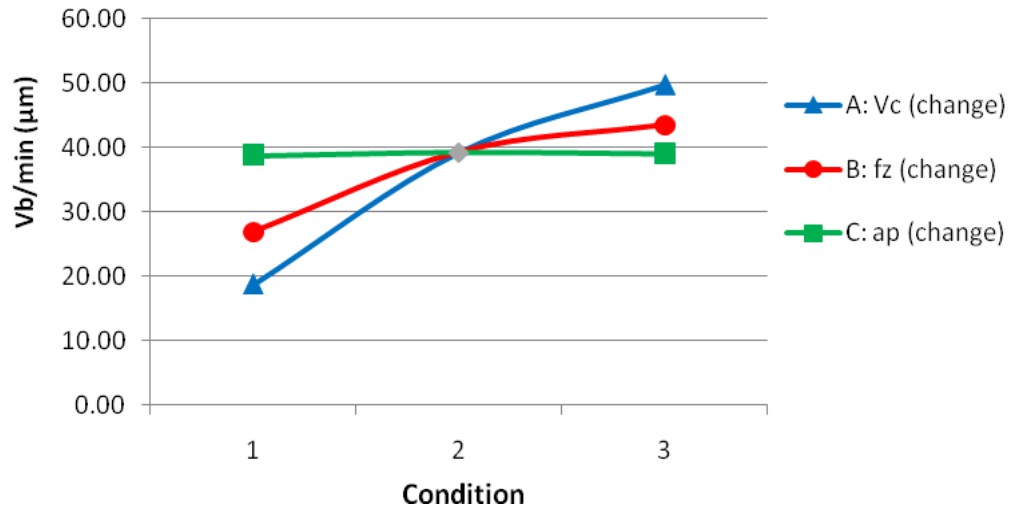


Figure 8-2: Influence of different cutting parameters on tool life

The gradient due to change in each parameter shown in figure 8-2 clearly indicates the effect on tool life for the different cutting conditions of table 8-2.

8.5 Background study 3: Cutting strategy for missile hanger

The South African government has successfully included counter trade clauses into recent aircraft acquisition transactions. To support future counter trade opportunities, Department Science and Technology (DST) has embarked on a manufacturing capability enhancement programme. The objective is to get the SA precision machining industry involved in the global aerospace supply chains.

The author and his study supervisor collaborated with Daliff Precision Engineering to redesign the manufacturing process with the emphasis on the cutting strategy employed in order to minimize the machining time of an aerospace component.

The component (figure 8-3) is the hanger fixed on a missile that slides on the launch rail. The strategy was to minimize set-ups and increase the axial immersions. The high axial



immersion cut strategy holds promise for titanium machining effective advances as a decrease in tool life is only weakly correlated with an increase in axial immersion [66].

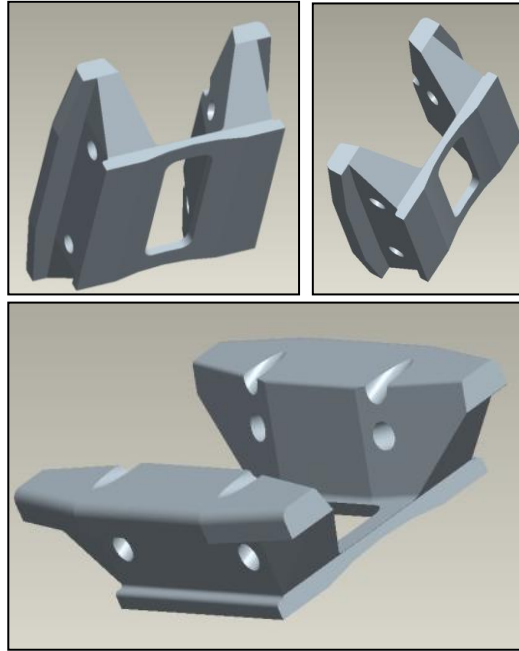


Figure 8-3: Missile hanger

The cutting strategy is at the time of the writing of this document in the final stages of implementation. Machining simulations indicate a large reduction in machining time.

8.6 Pilot study 2: Roll-in strategy for PCD materials

Technologists in the field concerned with improving performance of tungsten carbide [66 & 75] place a large emphasis on the importance of specific cutting strategies. With tungsten carbide the exit conditions of the insert from the cut into the coolant stream is of importance to avoid thermal shock [19, 22] one of the dominant failure mechanisms for carbide. This extreme emphasis led to the author to examine the applicability of this approach to PCD. In the light of PCD's failure mechanism being mechanical shock [42, 56, 78 & 79], this strategy was reconsidered.



PCD's relatively high thermal conductivity [42, 56 & 101] makes it relatively insensitive to thermal shock on cut exit (see figure 8-4).

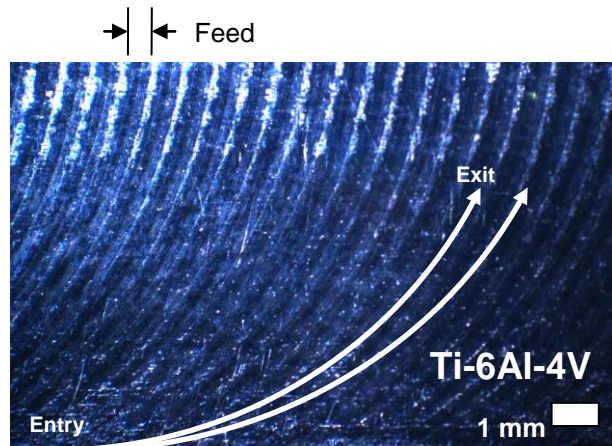


Figure 8-4: Conventional roll-in milling strategy for PCD

It's susceptibility to mechanical shock however calls for a gradual loading on cut entry (during each revolution). The author studied the influence and impact of conventional and climb milling using the roll-in strategy [66] (see Table 8-3). The author decided to use a cutting speed of 150 m/min and feed rate of 0.0375 mm/z based on previous studies [42, 56, 74, 87 & 101].

Table 8-3: Insert Specifications and cutting conditions for cutting strategy experiment

Insert type	PCD - SCMN 090308F (ISO1832)
PCD grade	CTM302 (Coarse)
Insert radius	0.8 mm
Insert clearance angle	3°
Insert rake angle	4°
Cutting edge	Sharp
Cutting Speed (V_c)	150 m/min
Feed/tooth (f_z)	0.0375 mm/z
Depth of cut (a_p)	2 mm
Working engagement (a_e)	0.5 mm
Coolant	Flood (ROCOL® ULTRACUT 260) Diluted: Water : Oil 30 : 1
Milling machine	Hermle 5-Axis C40U
Tool	Custom made (\varnothing 25mm) [see figure 8-6]
Condition (Strategies)	Conventional & Climb milling



After several test runs, results showed that conventional milling performed better for PCD, due to the relatively low transverse rupture strength of the material and reduction of mechanical shock.

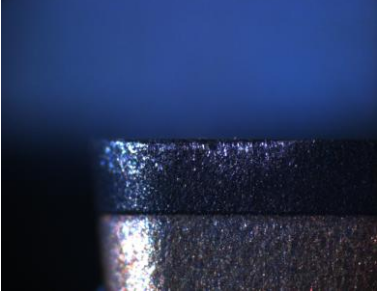
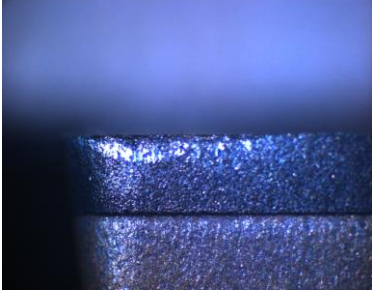
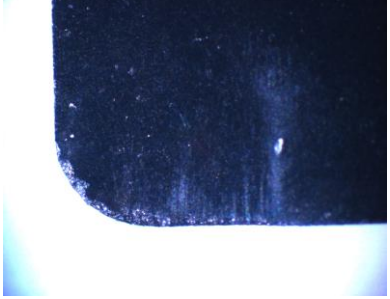
Conventional (Up)	Climb (Down)
Wear on flank	
	
Wear on crater	
	
More gradual wear with less chipping	More chipping and uneven wear

Figure 8-5: Results of cutting strategy using PCD

Down milling caused more fracture wear, due to mechanical overload [19, 22, 66 & 75] and conventional milling produced a more gradual wear scar. This is visible in figure 8-5.

Therefore it was decided to use the conventional roll-in strategy to conduct the experiments.

8.7 Experimental setup, design and procedure for final experiments

8.7.1 Experimental setup

The background studies and experimental tests (figure 8-1) helped the author establish an experimental model with feasible parameters. Conventional milling with a roll-in strategy helped the author to establish a suitable cutting condition for feasible



experimental results. Table 8-4 indicates the cutting conditions that were employed during the final experiments.

Table 8-4: Insert specifications and cutting conditions for final experiments

Insert type	PCD (SCMN 090308F) ISO1832 VP15TF (AOMT123608PEER-M) Benchmark
PCD grades	CTM302(Coarse), CTB010(Medium), CMX850(Fine)
PCD insert radius	0.8 mm
PCD insert clearance angle	3°
PCD insert rake angle	4°
Cutting edge	Sharp
Cutting Speed (V_c)	100, 150, 200 m/min
Feed/tooth (f_z)	0.025, 0.0375, 0.05 mm/z
Depth of cut (a_p)	2 mm
Working engagement (a_e)	0.5 mm
Coolant	Flood (ROCOL® ULTRACUT 260) Diluted: Water : Oil (30 : 1)
Milling machine	Hermle 5-Axis C40U
Tool	Custom made (\varnothing 25mm, 90° Shoulder mill) Mitsubishi (\varnothing 25mm) APX3000R254SA25SA

Face-milling tend to produce wear scars that are more difficult to measure the nose. Shoulder milling is more aggressive, and produces better discrimination between different PCD grades. The 90° mounting produce no chip thinning effect, whereas with the 45° the chip thinning effect will reduce the load on the insert. Milling titanium alloys that lack rigidity [19 & 32] with 45° mounting can bend the work piece due to the back force, which can lead to poor machining accuracy [75]. Although round and 45° inserts have limited depth of cut, the 90° has a cutting depth as deep as the cutter diameter and a length that allows for stable cutting [75]. The simplicity of 90° mounting and the saving of the expensive work piece material tipped the scales in favour of the 90° mounting.



The sharp PCD insert has a nose radius of 0.8 mm, and clearance and rake angle of 3° and 4° respectively. A positive rake angle enables good sharp cutting edges [75] that are critical to assist in helping to reduce the elevated temperatures generated when machining titanium [32, 42 & 56]. Mitsubishi's VP15TF was used as benchmark. The Hermle 5-Axis C40U machine was used with ROCOL® ULTRACUT 260 coolant under a flood condition. The cutting fluid is an emulsion designed specifically for superior performance in severe cutting conditions of titanium alloys. The tool was custom made in South Africa and used to test the PCD at different cutting speeds and feed rates. Generally PCD fractures through a brittle mechanism and fatigue does not play a big role [79]. Due to this brittleness of PCD, a clamp was designed to cover as large as possible area of the PCD, in order to reduce the risk of instant fracture.

The experimental CMX850 inserts were supplied in 1.6 mm thickness for the experiments. The other inserts supplied were in the standard 3.12 mm thickness. A tungsten carbide backing plate was used to enable clamping of the thinner CMX850 in the tool holder designed for standard thickness inserts.



The tools and machines used during this experimentation can be seen in figure 8-6 (A-D), showing the Hermle machine, the custom made tool with its insert and backing, the tool-fitted spindle, and the flood lubrication respectively.



Figure 8-6: Machinery and equipment for experiments

It was decided to use different cutting speeds (100, 150 & 200 m/min) and feed rates (0.025, 0.0375 & 0.05 mm/z) based on previous studies [42, 56, 74, 87 & 101]. Zoya et al also recommended a cutting speed in the range of 185 to 220 m/min for titanium alloys [59] and feed rates (f_z) below 0.051 mm/z, chipping becomes less of an issue [56].

The properties of the different PCD inserts were compared in order to identify the critical conditions and opportunities for the experiments.



Initial tests were conducted with three different PCD materials, supplied by Element Six (Pty) Ltd, in order to establish which cutting material delivers superior performance, and would thus be suitable for further experimentation. In order to identify the critical conditions and opportunities for improvement, the properties are compared relative to each other in table 3, and quantified as low, medium or high, relative to each other.

Table 8-5: Insert properties comparison [79]

Property			CMX850 (Fine)	CTB010 (Medium)	CTM302 (Coarse)
Avg. Grain size		μm	1	10	2-30
Binder		% Cobalt	15%	12%	10%
Balance			Diamond	Diamond	Diamond
Elastic					
Longitudinal SOS		m/s	Low	High	Medium
Transverse SOS		m/s	Low	High	Medium
Density	P	g/m^3	High	Medium	Low
Poisson's ratio			Low	Medium	High
Bulk modulus		GPa	Low	High	Medium
Shear modulus		GPa	Low	High	Medium
Young's Modulus	E	GPa	Low	High	Medium
Mechanical					
Transverse Rupture strength	TRS	MPa	High	Medium	Low
Fracture toughness	K_{IC}	$\text{MPa}\cdot\text{m}^{1/2}$	High	Low	Medium
Thermal					
Thermal diffusivity	Γ	mm^2/s	Low	High	Medium
Thermal Conductivity	Λ	W/m.K	Low	High	Medium
Thermal Expansion	α_{CTE}	$10^{-6}/\text{K}$	High	Medium	Low
Specific heat capacity	C_p	J/kg.K	Low	Medium	High
Thermal Shock					
Thermal Shock factor (Bulk)	R		High	Medium	Low
Thermal Shock factor (Local)	R_y		Low	High	Medium

Disclaimer

All property measurements are carried out, where possible in accordance with relevant international standards. The information quoted is for comparative purposes only and should not be viewed as a product specification. Element six limited is constantly striving to improve its products and therefore reserves the right to alter product properties without prior notice.

Although the PCD's have a 6 times higher thermal conductivity and 7-8 times higher R_y , WC has a TRS of about double that of these PCD's.



It is significant to note that the thermal conductivity for Polycrystalline diamond (PCD) is up to four times more than that of tungsten carbide. Typically PCD is significantly harder (6000 HV) than carbides (2500 HV) indicating better performance at elevated temperatures. However, PCD has lower TRS (1000-2000 MPa) versus unalloyed carbide (1500-3000 MPa) making it more susceptible to mechanical shock experienced in interrupted cutting.

It is also critical to note the following on the PCD material properties shown in table 8-5.

1. A smaller grain size requires more binder to sinter and therefore has a lower maximum temperature
2. Declining grain size leads to an improved TRS [56], but reduces the toughness of the cutting edge. Although more cobalt (binder) decreases the fracture toughness it becomes more abrasive resistant.
3. Thermal conductivity increases with E, relative to amount of cross-linking between diamond grains.
4. Density, specific heat capacity and thermal expansion may be considered constant between different grades of PCD.

8.7.2 Material specifications

The chemical composition of Ti-6Al-4V is summarized in table 8-6. It contains roughly 4 wt % vanadium and 6 wt % Aluminium, hence its name.

Table 8-6: Composition (wt %) of Ti-6Al-4V [32]

Chemical composition:								
Content	O	H	N	C	Fe	V	Al	Ti
wt %	-	0.005	0.01	0.05	0.09	4.40	6.15	Balance

Table 8-7 is a summary of the work piece physical properties at room temperature. The sample has a very high tensile strength and relatively low modulus of elasticity [16, 19 & 42]. Titanium material for aerospace applications is available in a variety of mechanical properties [30 & 32]. The material used for these experiments were in the extreme



tensile strength condition as detailed in table 8-7. This extreme hardness and tensile strength titanium being the most demanding material condition for machining was chosen for this research.

Table 8-7: Mechanical and physical properties of the Ti-6Al-4V sample at room temperature

Alpha-Beta titanium alloy	Ti-6Al-4V
Grade	5
Hardness	360 HV (37 HRC)
Ultimate tensile strength	>1080 MPa
Modulus of Elasticity	114 GPa
Test specimen	Sample cut from sheet
Material heat treatment condition	Solution heat treated and aged
Dimensions	280x32x32 mm

The Ti-6Al-4V sample is a grade 5 titanium alloy [30 & 32]. The hardness of the experimental material was measured to be around 360 HV and the ultimate tensile strength was larger than 1080 MPa. The sample was solution heat treated and aged, and supplied in a plate form (280x32x32 mm).

8.7.3 Test Equipment

Several different machine tools and pieces of equipment were used in this study. Table 7-8 specifies the function of the different machinery.

Table 8-8: Machinery and Equipment

Machinery / Equipment	Purpose
Joel SEM 7500F AnalySIS software 3.2 (Build 799)	Analyse content, composition and grain size of PCD
Hermle 5-Axis C40U	To carry out the test
Standard work holding vice	Hold titanium sample in position
Tool Holder Type SECO CSBNL 2525M09	Clamp of test Insert for machining test
Grinding Wheel	Mark test Inserts
Wear Scar Measuring Equipment Dell Computer with Zeiss AXIOVISION4 Software / Measuring Microscope	Measure wear scar
Vickers Hardness machine	Measure Hardness of work piece
Rockwell Hardness machine	Measure Hardness of work piece
Surface roughness meter	Measure surface roughness
Statistica (Version 8)	Analyze data



All the experiments were conducted on the Hermle C40U machine and the Ti-6Al-4V sample was held in position using a standard machine tool work holding vice. Due to the low modulus of elasticity of Ti-6Al-4V [16, 19 & 42], the sample was machined to a length of 280 mm to properly clamp the material, in order to minimize vibration. SEM analysis and measuring of the wear scar with an optical microscope were done at the facilities of Element Six (Springs). The Joel 7500F and AnalySIS software 3.2 (Build 799) was used for the SEM work, while the optical microscope was used with Zeiss AXIOVISION4 software. The surface roughness was measured for specific conditions and Statistica (Version 8) was used to analyze the data in detail. A Rockwell and Vickers hardness machine were used to determine the hardness of the sample. A grinding wheel was used to mark the corners of the inserts.

8.7.4 Experimental design

The aim of the experimental design is to yield conclusive experimental results for interpolation of the effectiveness of different PCD materials, tested under different cutting conditions. This design is shown in table 8-9 and repeated three times.

Table 8-9: Experimental design

Number of experiments	PCD (Grade)	Cutting Speed (m/min)	Feed (mm/z)
1	CMX850 (Fine)	100	0.025
2			0.0375
3			0.05
4		150	0.025
5			0.0375
6			0.05
7		200	0.025
8			0.0375
9			0.05
10	CTB010 (Medium)	100	0.025
11			0.0375
12			0.05
13		150	0.025
14			0.0375
15			0.05
16		200	0.025
17			0.0375
18			0.05
19	CTM302 (Coarse)	100	0.025
20			0.0375
21			0.05
22		150	0.025
23			0.0375
24			0.05
25		200	0.025
26			0.0375
27			0.05



A 3-factor, 3-level design was used in Statistica (Version 8) to analyze the data. The experiments were replicated for each condition, resulting in 81 test runs.

8.7.5 Test Procedure

A process flow diagram was developed in order to establish a test procedure. Figure 8-7 indicates the test procedure

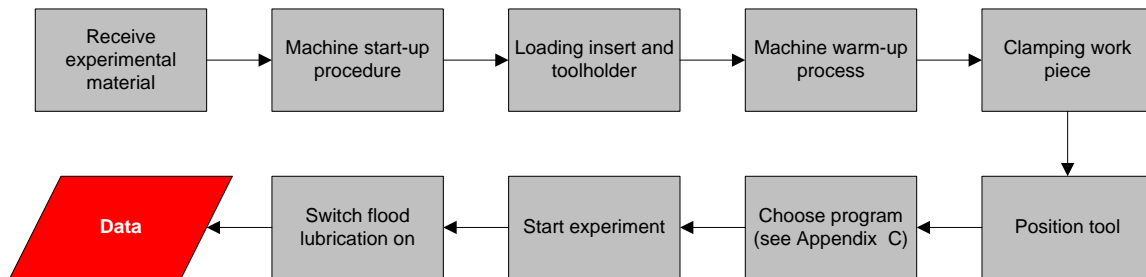


Figure 8-7: Experimental test procedure

The insert had to be reloaded after every experiment. Special caution had to be made in order to achieve repeatable results. After the inserts were properly fitted, the parameters of the program (Appendix C) were changed for the next experiment. All the experiments were conducted under flood lubrication.

8.7.6 Collected Data

Several measurements and samples were collected in order to have comparable outputs. Wear measurements were taken of the different samples at similar cutting distance intervals (560 mm) with an Optical microscope (Table 8-8). Similarly the surface roughness was measured and the chips collected. The data was used to show which test specimens are more wear resistant than others. From the literature, failure due to wear on the flank was set for a maximum flank wear (V_B) of more than 0.3 mm [101], and for surface roughness an average value (R_a) of more than 1.6 μm [79].

8.7.7 Wear Measurement

Measuring the wear on the flank (V_B) was used as primary wear criterion. Therefore, it forms a critical part of the study. This phenomenon that Ti-6Al-4V (Figure 9-14) work material builds up on the wear scar when PCD is used as cutting material was one of the forms of wear observed in these experiments. This is confirmed by Kuljanic et al [42].



The author is of opinion that this could be the case in other titanium machining research [101] as well. This suspicion is supported by the fact that analyses that would identify the deposit are not included. This leads to a significant uncertainty that the measuring of titanium deposit on the wear scar holds. It was decided that this research would have insufficient scientific grounding if only the titanium build-up on the wear scar were measured, without knowing the true geometry of the wear scar.

In order to establish the situation below the occasional built-up Ti-6Al-4V layer, the author had to acid clean several samples. Special caution had to be taken in order prevent the samples from damage. Several discussions with Element Six (Pty) Ltd researchers and technical specialists [79] were used to establish an acid cleaning method. This would reveal the true wear scar without compromising the experimental results with possible chemical reactions caused during cleaning. Ultimately the samples were cleaned with hot concentrated Hydrochloric acid [HCL (32 vol %)]. It proved to be practically impossible as no etching agent is available that would remove the Ti-6Al-4V without affecting the PCD. It was however concluded that the etching method would yield valid results. This is despite the fact that the HCL would etch the cobalt binder of the PCD [109]. The diamond particles would however define the shape of the wear scar resulting in a valid approach for the research objective. Figure 8-8 illustrates the etching process.

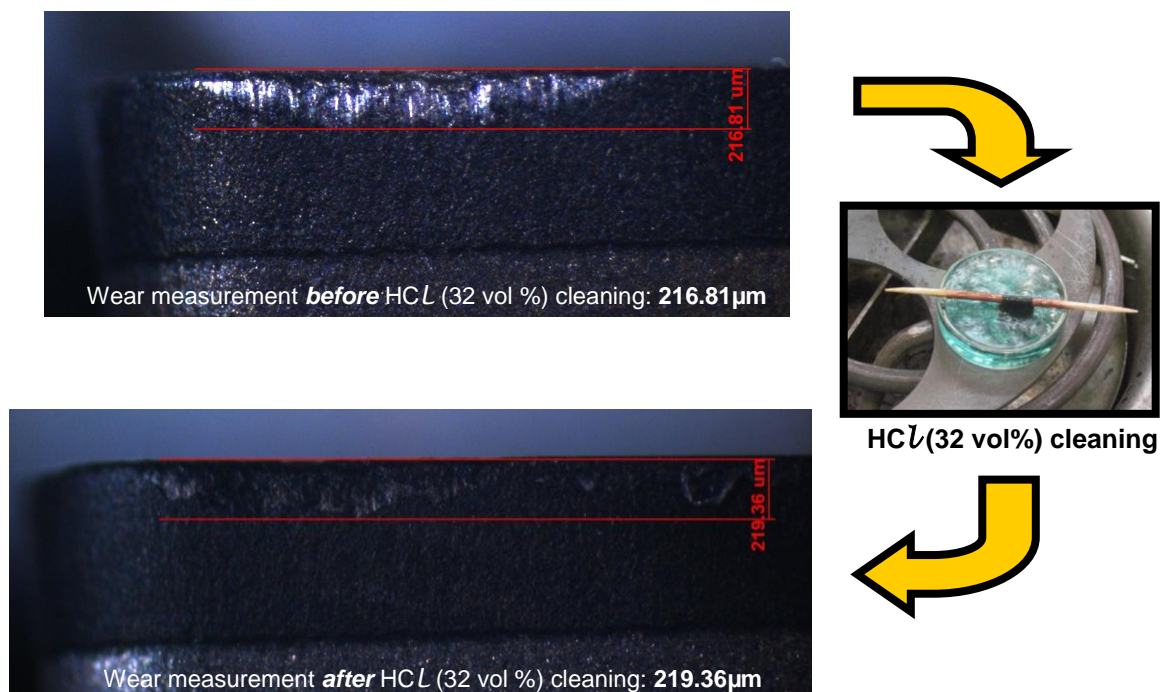
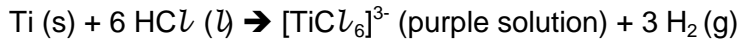


Figure 8-8: Acid (HCL - 32 vol %) cleaning process of some PCD samples



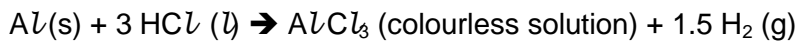
The acid cleaning reaction of the Ti-Al alloy with hot concentrated HCl (32 vol %) can be summarized as follow [109]:

a) Reaction with titanium



A hexa-chloro complex of Ti (111) is formed and has a purple-green colour. This complex only exists in the presence of excess HCl. If it is diluted with water, the soluble complex compound is hydrolyzed to form a precipitate of titanium dioxide.

b) Reaction with aluminium



c) Vanadium

Vanadium is not soluble in HCl. The dissolution of the titanium and aluminium by HCl decomposes the alloy, leaving a residue of V. This could have been removed in subsequent washing or could remain as a thin film on the wear scar area. There was also V found on the glass after the HCl vaporized from the heat treatment.

Measurements of the wear scar before and after etching confirms a direct correlation between the deposit and the size of the true wear scar as shown in figure 8-8. Therefore it was decided that acid cleaning of a limited number of samples were sufficient.



9. Results and discussion

9.1 Wear measurements

The performance of the different PCD grades was compared to that of Cemented tungsten carbide (benchmark) for different cutting conditions. The wear per time unit is used to evaluate the performance of each insert. Considering figures 9-4, 9-5 and 9-6, the ultimate would be to strive for the bottom right-hand corner, to attain a high material removal rate and minimal wear.

9.1.1 CTM302

This PCD material is a combination of coarse and fine particles [79]. The coarse particles impart excellent abrasion resistance and improve thermal stability. The fine particles improve packing density and give a low work piece surface roughness [56, 75 & 79]. Although, among the materials tested, it has the lowest TRS, the high fracture toughness of the material imparts good chipping resistance. As illustrated in figures 9-1 and 9-2, with a feed of 90 mm/min, impact related wear becomes more prominent.

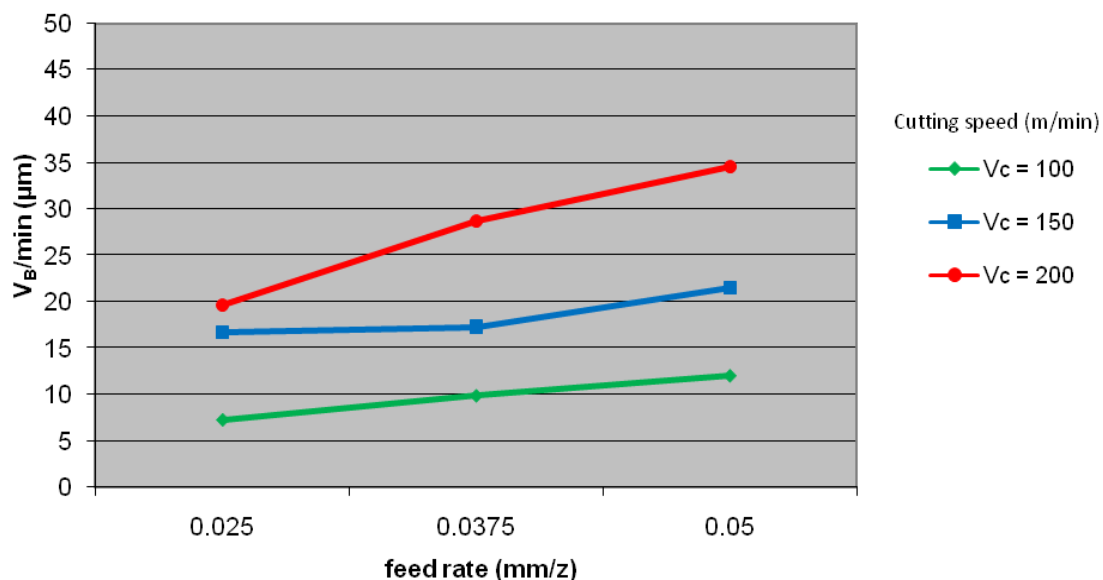


Figure 9-1: CTM302 wear (V_B) measurements for different conditions

CTM302 has a lower thermal conductivity than CTB010, but higher than CMX850. It also has higher fracture toughness than CTB010. Therefore it is not as resistant as CTB010 to crack initiation, but is more resistant to crack propagation [56]. This can be seen in the



relatively smaller chipping than for the CTB010 material at higher feeds. A feed of around 90 mm/min cause critical impact related chipping. This is shown in figure 9-2.

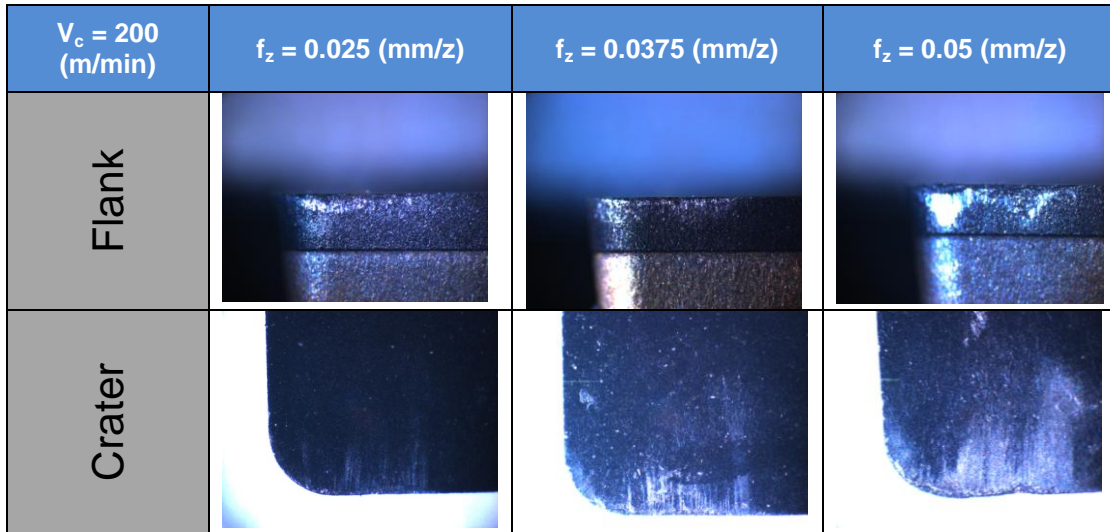


Figure 9-2: Flank and crater wear of CTM302 at high cutting speeds

A statistical prediction of the combined effect of feed rate and cutting speed was calculated using Statistica (Version 8).

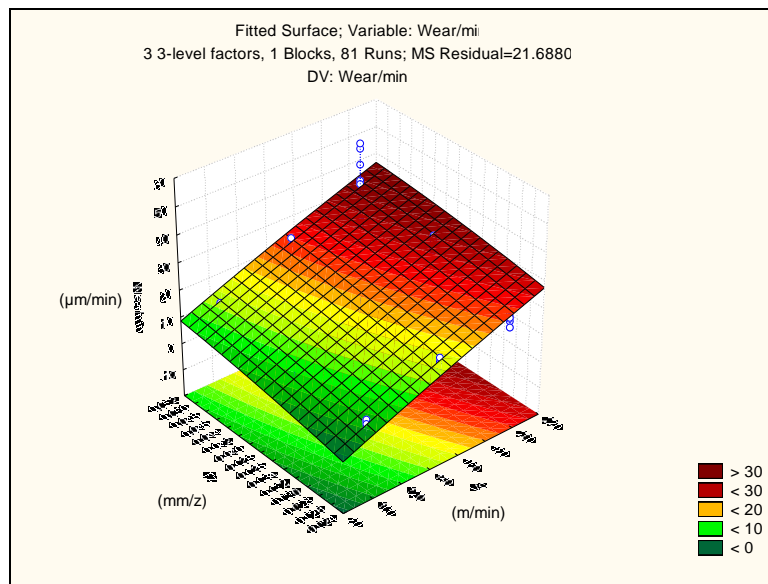


Figure 9-3: Estimated performance of CTM302 for certain conditions

It is shown in a graphical plane (Fitted surface) in figure 9-3. The program assumed the data is linear.



9.1.2 CTB010

This general purpose material has a 10 micron average grain size and is available in a range of PCD layers and overall thicknesses [79]. The performance of CTB010 is plotted in figure 9-4.

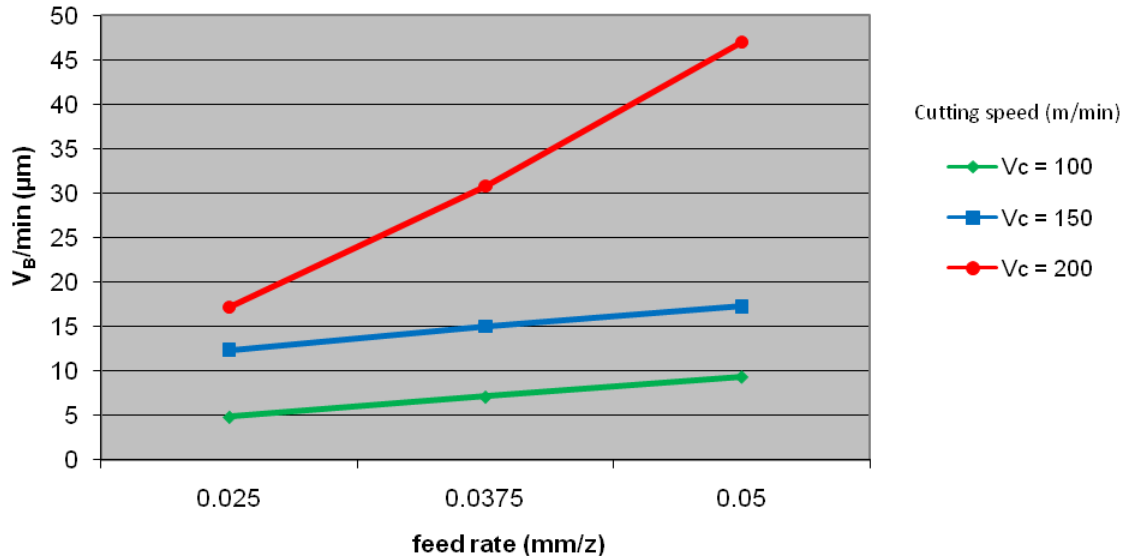


Figure 9-4: CTB010 wear (V_B) measurements for different conditions

This material has the highest thermal conductivity [79], which might have been beneficial for the material to withstand the thermally related wear at lower feeds. CTB010 has the lowest fracture toughness, although it has higher transverse rupture strength than CTM302. Therefore it can withstand the impact initially, but as soon as the cracks are initiated, the low fracture toughness cannot stop the propagation [75].

This could be one of several reasons why it fails more rapidly than the CTM302 at higher feed rates (90mm/min), where wear is more and chipping is already initiated. Increased immersion increases the exposure of the tool to high temperatures, while increased chip thickness increases the mechanical shock load on the tool [56].



A feed of around 90 mm/min also cause critical impact related chipping for CTB010. This is shown in figure 9-5.

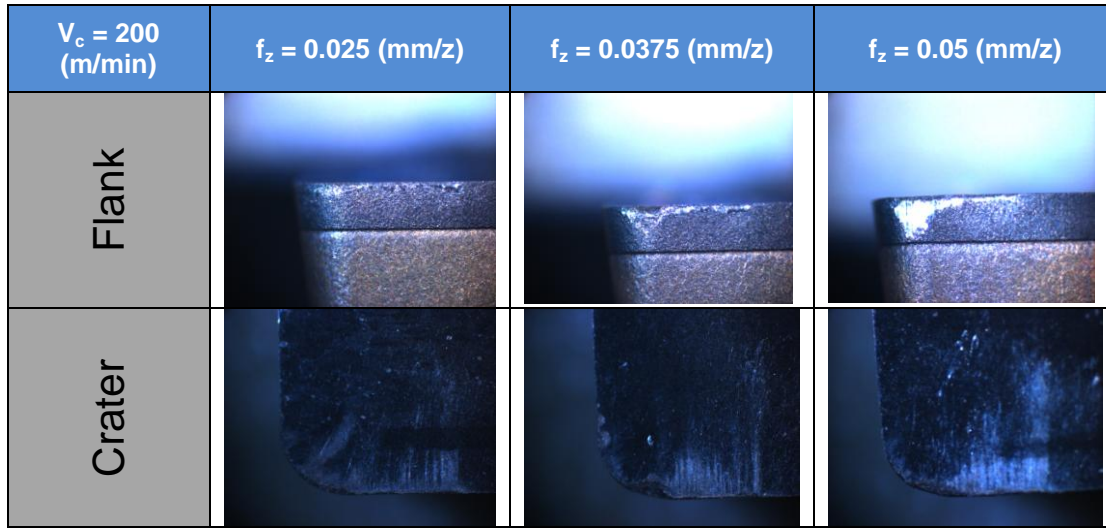


Figure 9-5: Flank and crater wear of CTB010 at high cutting speeds

A statistical prediction of the combined effect of feed rate and cutting speed was calculated using Statistica (Version 8).

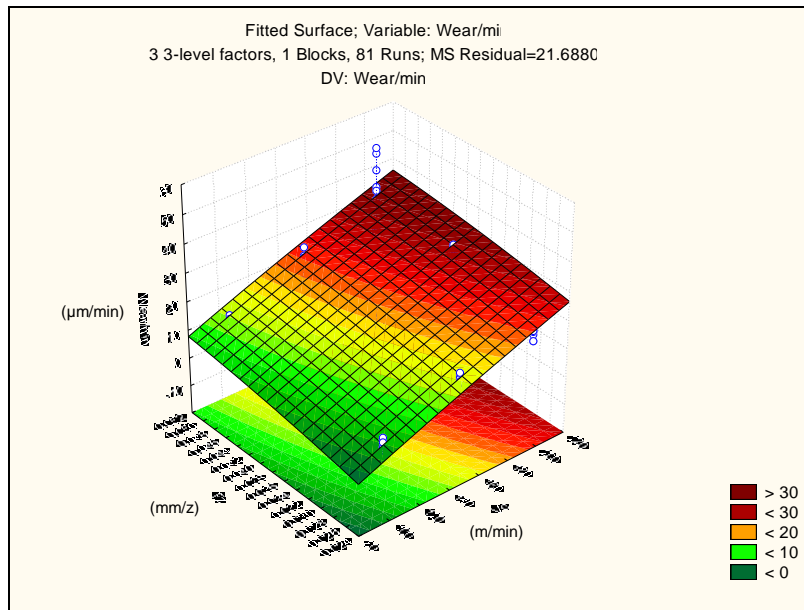


Figure 9-6: Estimated performance of CTB010 for certain conditions

It is shown in graphical format in figure 9-4. The more inclined gradient on the cutting speed (V_c) axis compared to the one of feed rate, is also a clear indication that V_c has a larger effect on the wear.



9.1.3 CMX850

Figure 9-7 indicates that CMX850 performed better than the other PCD inserts at high material removal rates.

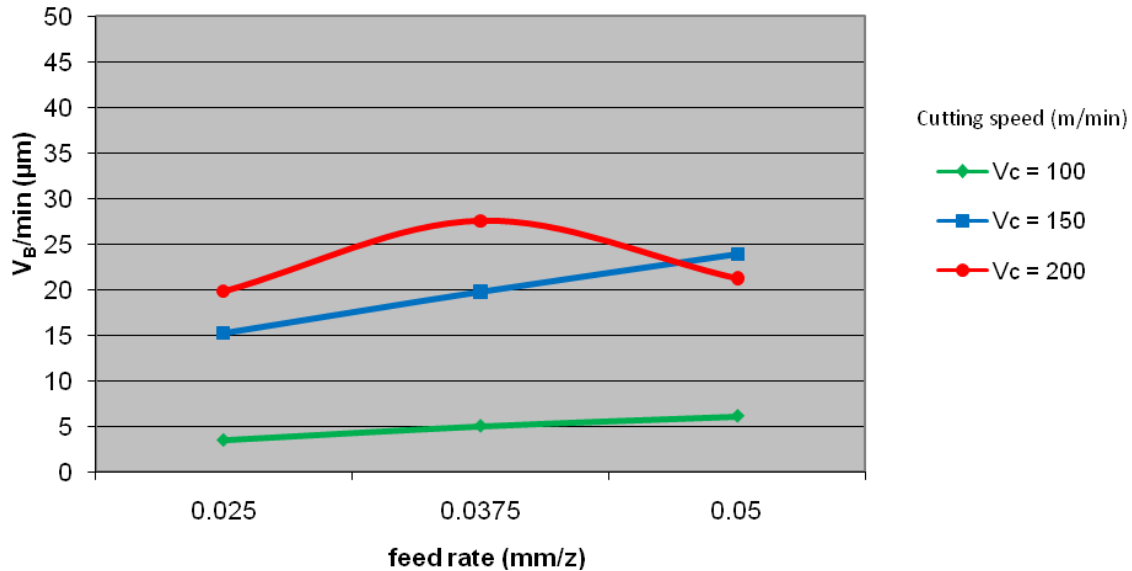


Figure 9-7: CMX850 wear (V_B) measurements for different conditions

This figure indicates that CMX850 performed better than the other PCD inserts at high material removal rates. At lower table feeds the relatively high transverse rupture strength resulted in the material to overcoming the initial micro-chipping [56, 75 & 79]. Through the results and from the literature it is evident that cutting speed is the most influential parameter. An increase in cutting speed and feed per tooth generate a higher table feed, which assures an increased material removal rate [19].

At a certain material removal rate the impact related wear (chipping), initiates sudden tool failure [31]. Out of this study it could be seen that the high transverse rupture strength of CMX850 enables the material to cut at higher material removal rates. At a cutting speed of 200 m/min and feed per tooth (f_z) of 0.05 mm/z, there is a prominent decrease in wear compared to the lower speeds (150 m/min).



This observation that goes against the normal trend of machining [19 & 22] behaviour generated a significant amount of interest among the research team. This is also clearly illustrated in table 9-3.

$V_c = 200$ (m/min)	$f_z = 0.025$ (mm/z)	$f_z = 0.0375$ (mm/z)	$f_z = 0.05$ (mm/z)
Flank			
Crater			

Figure 9-8: Flank and crater wear of CMX850 at high cutting speeds

There is less wear on the flank and rake for the CMX850 cutting with $f_z = 0.05$ mm/z compared to $f_z = 0.0375$ mm/z. A statistical forecast of the combined effect of feed rate and cutting speed was calculated using Statistica.

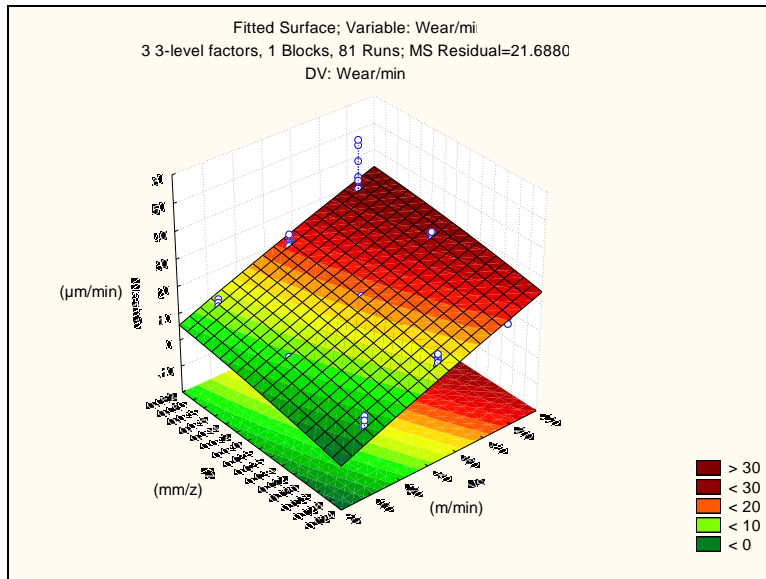


Figure 9-9: Estimated performance of CMX850 for certain conditions

A statistical forecast of the combined effect of feed rate and cutting speed was calculated using Statistica. It is shown in graphical format in figure 9-6. The darker red



colour indicates the conditions that generate more wear, while the light green specifies the less wear conditions. Although it may be expected that the graph should be lower in the corner ($V_c = 200$ m/min & $f_z = 0.05$ mm/z), the linear approximation of Statistica plots this performance forecast.

9.1.4 Summary of performance

The data from the test runs was analyzed using Statistica and the following graphs helped the author to summarize the performance for different milling conditions. Figure 9-10 illustrates the effect of the properties from different cutting materials.

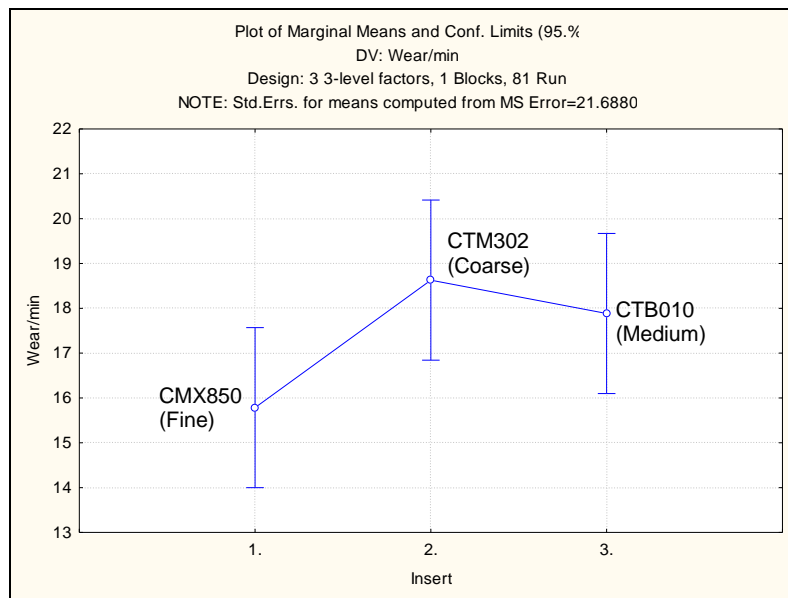


Figure 9-10: Performance of different inserts

The main effects graph clearly indicates that the fine grain CMX850 performed best overall, for the different cutting configurations. It is also interesting that there is a relationship between the performance and transverse rupture strength of the materials (see table 8-5 and figure 5-3 [56]). Similar, for a decrease in grain size (increase in density) [75], the performance improved.



Figure 9-11 and table 9-1 show the effect of cutting speed and feed rate on the performance of the insert.

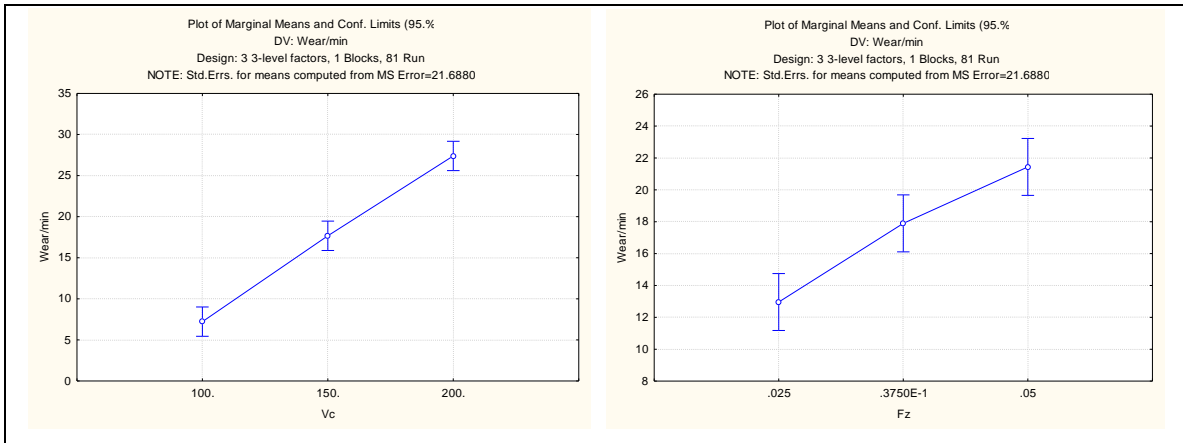


Figure 9-11: Influence of cutting speed (V_c) and feed rate (f_z)

The effect of change in cutting speed (linear approximation by Statistica) was 20.17 compared to the 7.08 for change in feed rate. This information concluded that cutting speed has a larger effect on tool life than feed rate, similar to machining with WC. A probability plot and Pareto chart was also drawn in Statistica as shown in figure 9-12.

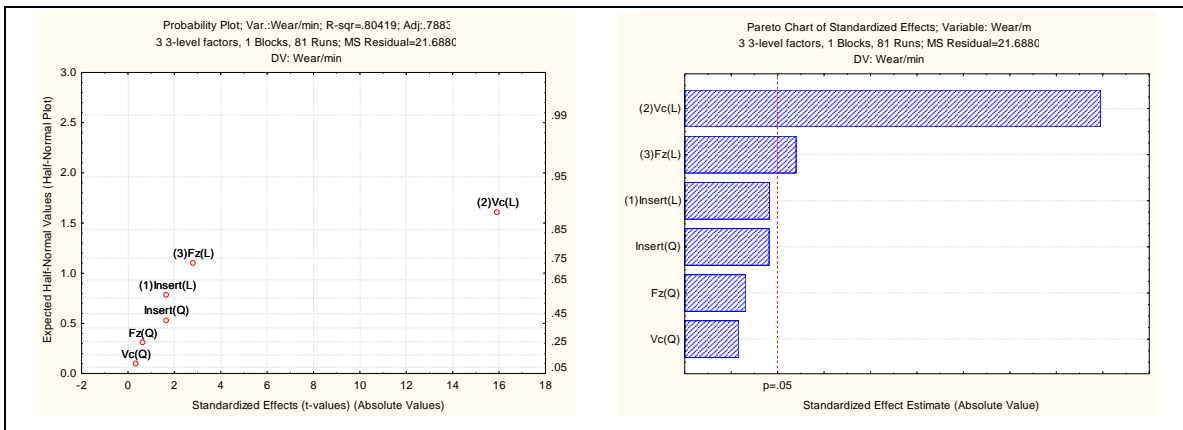


Figure 9-12: Influence of different parameters

From these figures it is also evident that cutting speed (linear approximation) has the largest influence followed by feed rate (linear approximation).



The influence of the different parameters is summarized in table 9-1.

Table 9-1: Influence of the different parameters

Factor	Effect Estimates; Var.:Wear/min; R-sqr=.80419; A 3 3-level factors, 1 Blocks, 81 Runs; MS Residua DV: Wear/min				
	Effect	Std.Err.	t(74)	p	-95.% Cnf.Lin
Mean/Interc.	16.96852	0.896249	18.93281	0.000000	15.182
(1)Insert (L)	2.10000	1.267488	1.65682	0.101790	-0.425
Insert (Q)	1.79444	1.097677	1.63477	0.106345	-0.392
(2)Vc (L)	20.17111	1.267488	15.91424	0.000000	17.645
Vc (Q)	0.36444	1.097677	0.33201	0.740817	-1.822
(3)Fz (L)	7.08444	2.534976	2.79468	0.006612	2.033
Fz (Q)	1.39222	2.195353	0.63417	0.527927	-2.982

H_0 is that a certain parameter will have no effect on the tool performance. The probability (p) indicates H_0 's likelihood. From table 9-1 it is evident that V_c (linear) and F_z (linear) will have a influence on the performance of the insert.

9.2 Wear scar

This alloy's metallic characteristics caused a high shearing angle to be formed ahead of the cutting edge. This caused the chip to contact a relatively small area on the cutting tool face and resulted in high bearing loads per unit area [53] during the milling experiments. This small contact area together with the low thermal conductivity (7 W/m.K) [42] of the work piece, resulted in a high rate of temperature increase with cutting speed.

Similar the rate of chemical wear increased with an increase in temperature [19&75]. This increased the wear closer to the tool cutting edge [31]. Together with the high pressure conditions, a Ti-6Al-4V built-up (figure 9-13) formed on the tools. Once the tool was worn, the rubbing of the edges [32] generated more heat, which increased tool failure [31].

Acid cleaning enabled the author to explore the true wear scar below the deposited Ti-6Al-4V layer. Thorough SEM analysis discovered that the scar can more or less be divided into different wear regions, with regards to the appearance and influential mechanisms [19 & 75] moving away from the cutting edge.



Moving away from the edge, the impact related mechanisms transforms into temperature and chemically related wear [75].

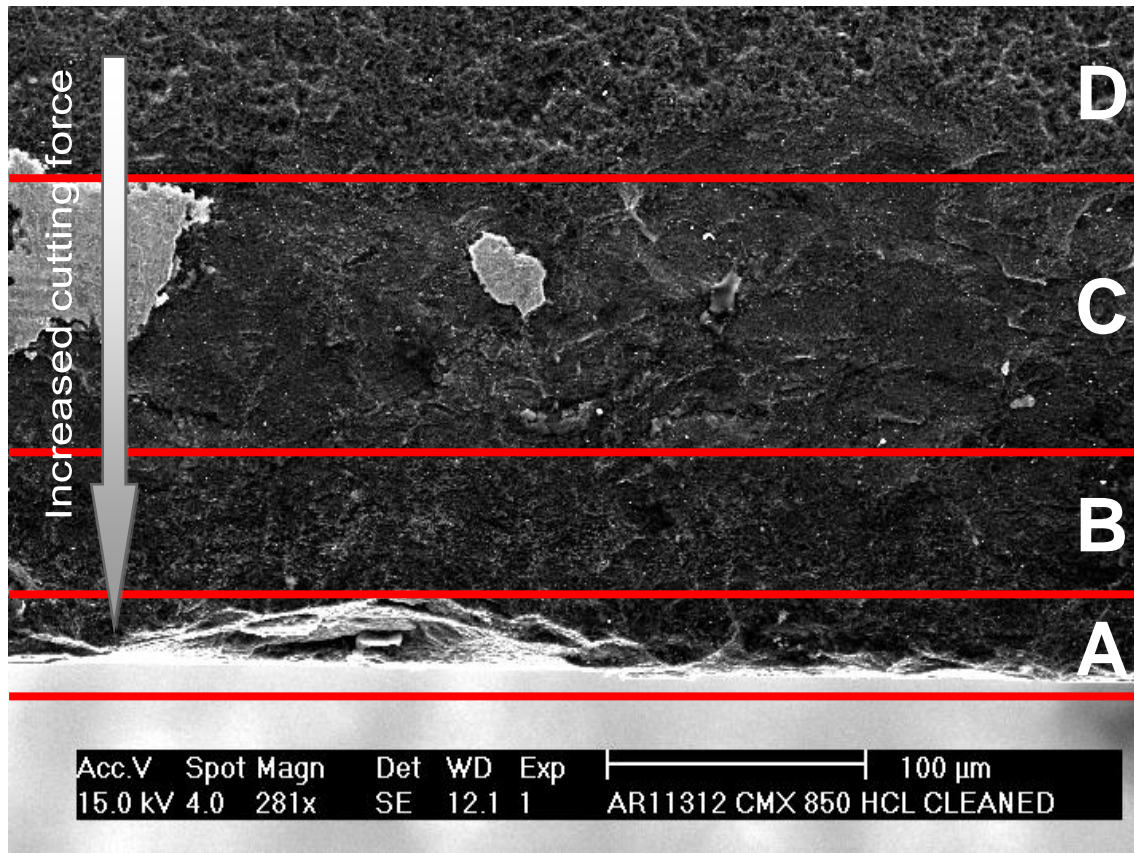


Figure 9-13: PCD wear scar

The different regions could be summarized as follows:

Region A: The highest load is exerted on the edge of the insert [19 & 53]. This is where the initial chipping occurs, due to mechanical impact and is measured to be around 45 μ m deep with the SEM.

Region B: This region is also characterized with impact related wear. The work piece material tends to stick and break away under the cutting forces [66]. This causes small particles to be gradually dislodged out of the matrix [75].

Region C: This region was covered under a Ti-6Al-4V layer. Getting below this, the region is characterized by a relatively smoother (polished) surface, due to an abrasive related wear in the form of delaminating [19, 75 & 110]. The removed layers cause more friction and the rubbing increase the cutting



temperature [30, 32, 75 & 79]. This causes the work piece to weld onto the wear scar [22, 81]. The critical temperature for adhesion to occur for machining with PCD is around 760°C and the nominal pressures about 0.142 GPa [69]. The impact forces are also lower, further away from the cutting edge [19 & 53]. Therefore the material doesn't break away in this region and is thus protected by a Ti-6Al-4V built-up (figure 9-14) layer.

Region D: From visual inspection, this region of PCD material seems to remain unaffected after cutting.

As indicated in figure 9-14 the build-up on the PCD material was found to be Ti-6Al-4V for several samples.

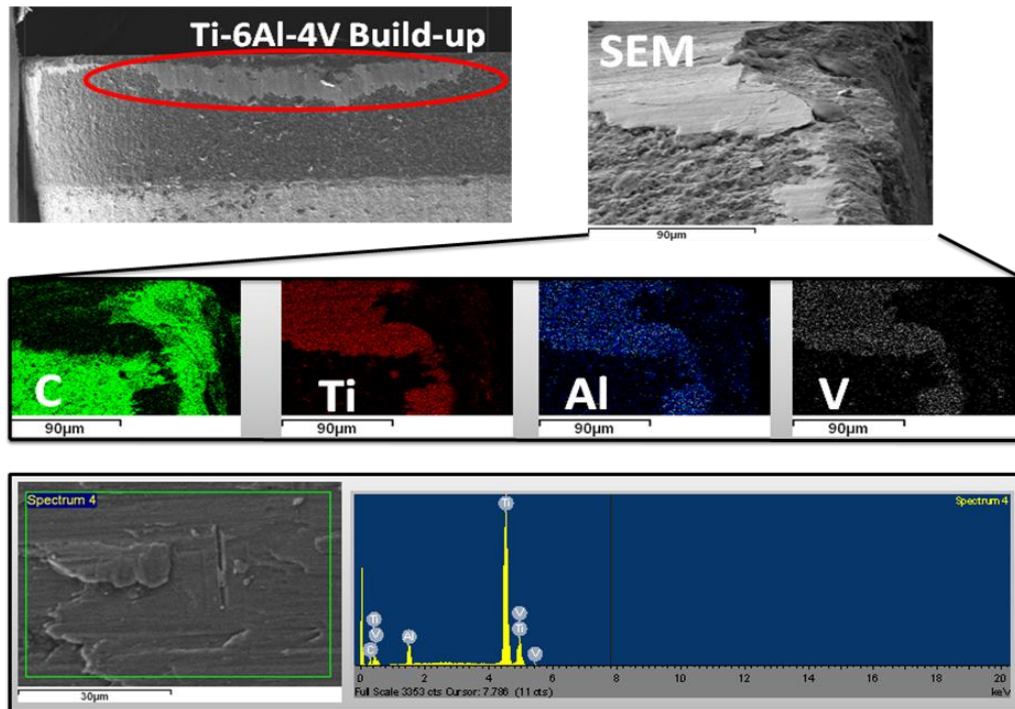


Figure 9-14: Build-up analyzed using the SEM

This deduction is supported by the breakdown per %wt for the spectrum and image mapping in figure 9-14 is shown in table 9-2.

Table 9-2: Typical breakdown (%wt) on a spectrum of the build-up on the PCD inserts

In stats.	C	O	Al	Ti	V	Total
weight%	3.95	-	5.34	86.9	3.81	100



Compared with the nominal 6% Aluminium, 4% Vanadium in table 9-2 it becomes clear that the deposit is work material.

An EDM sectioned sample gives an indication of the formed wear scar on the flank. Figure 9-15 indicates where the sample was cut and the form of the wear scar. The sample was 350x enlarged under the SEM.

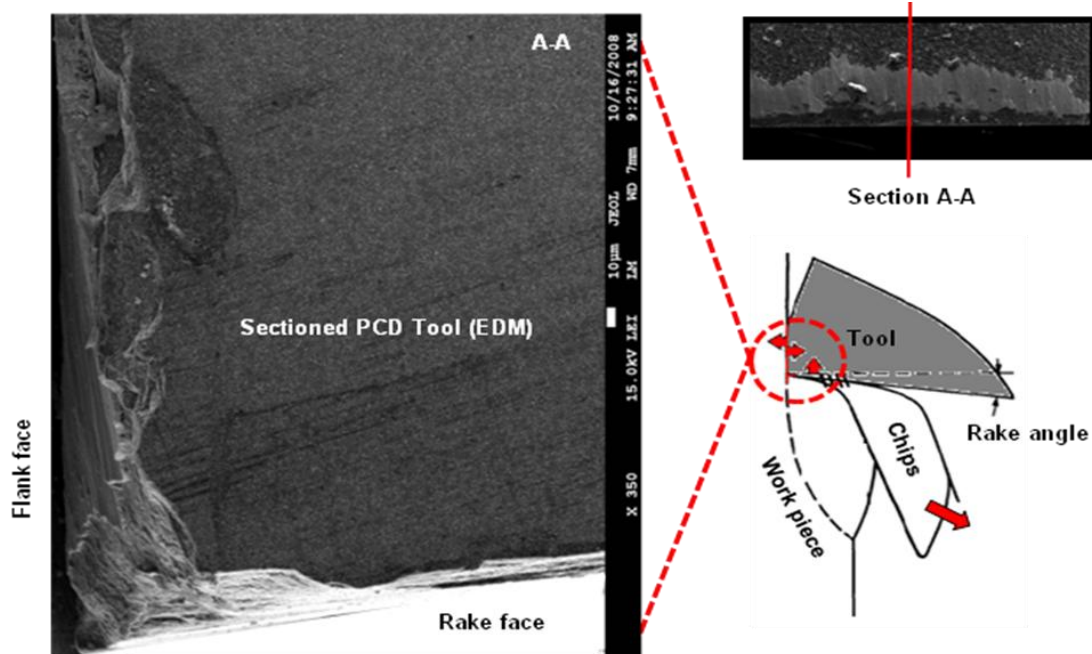


Figure 9-15: EDM sectioned wear scar

The PCD was cut through the wear scar with electric discharge machining (EDM), due to the PCD's hardness, and polished. The SEM on the sectioned sample also yielded supportive information to establish that the depth of the wear on the flank to be around 20-25 μm deep.



9.3 The performance of CMX850

Experiments using the best performing cutting tool material (CMX850) followed and results were compared to those using tungsten carbide. This PCD material (CMX 850) performed satisfactorily for cutting speeds in the range of 100-200 m/min with $f_z = 0.05$ mm/z. An increase in cutting speed resulted in sudden tool failure, because of the significant reduction in the strength and hardness of the cutting tool at elevated temperatures.

Under these conditions, the bonding strength of the tool substrate weakened, which resulted in tool wear by mechanically (abrasion) and thermally (diffusion) related mechanisms. Figure 9-16 illustrates the performance of the CMX850 at different cutting speeds. Tool life was calculated in terms of material removed, as cutting times varied for different feeds.

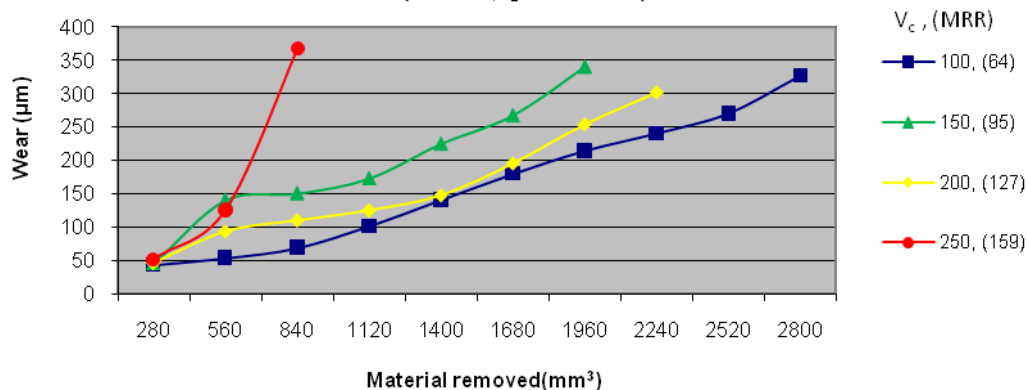


Figure 9-16: Tool life of CMX850 at different cutting speeds ($f_z=0.05$ mm/z)

CMX850's relatively high thermal conductivity and transverse rupture strength [79] enables it to make use of this high material removal opportunity.



Lowering the feed rate to 0.01 mm/z and increasing the cutting speed to 500 m/min, enabled the CMX850 to cut for long distances (2.75m, 42min 57s). Although this ensured a similar extended tool life (2.78m, 43min 25s) as when cutting at 100m/min ($f_z = 0.05$ mm/z), a distinctively better surface finish was attained. At elevated cutting speeds the PCD outperformed the benchmark cemented tungsten carbide, as shown in figure 9-17.

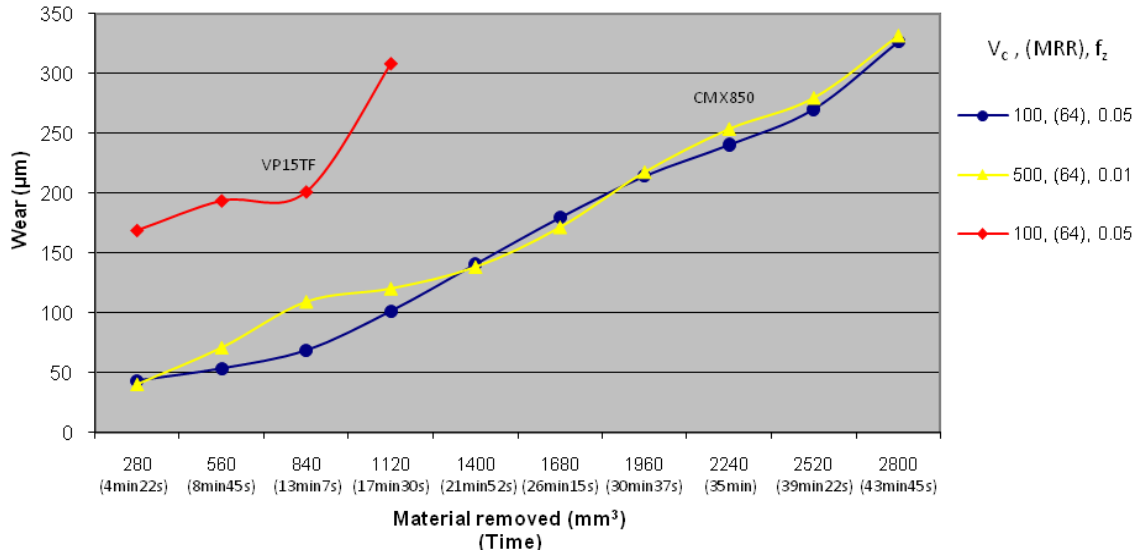


Figure 9-17: Tool life of CMX850 compared to the VP15TF at elevated cutting speeds

At elevated cutting speeds the PCD outperformed the benchmark WC as shown in figure 9-18. In this high temperature environment [74] the benchmark cemented tungsten carbide (VP15TF) failed under the thermal shock, due to its low thermal conductivity [66, 75 & 79].

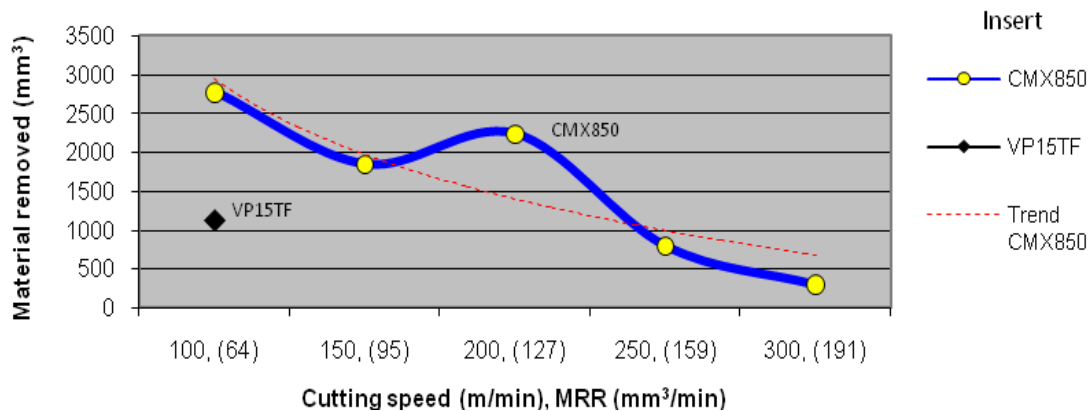


Figure 9-18: Tool life of CMX850 and VP15TF ($f_z = 0.05$ mm/z)



Figure 9-18 indicates a decreased trend in tool life, with an increase in cutting speed (feed). For inserts with low transverse rupture strength, there may be a minimum cutting speed below which mechanical overload may occur. In the same way, a local maximum tool life may exist if there is a phase change in the work piece material and the insert can withstand the harsh operating conditions [56].

For this PCD material (CMX850) there is a definite increase in tool life at a cutting speed of 200m/min ($f_z = 0.05$ mm/z). This counter-intuitive phenomenon was discussed in the literature [53 & 56]. In this temperature area the tool life is increased, with an increase in cutting speed. The tool life increased by 35% when the cutting speed is increased from 150 m/min to 200 m/min. Figure 4-5 in the literature shows that increasing the cutting speed beyond 200 m/min will increase the cutting temperature way beyond 1000°C [74].

Keeping in mind that the strength of Ti-6Al-4V already drops from 1000 MPa (room temperature) to below 550 MPa (above 500 °C) [58], the explanation for this increase in tool life could be the phase transformation which occurs at 950°C and above [29]. The Ti-6Al-4V changes from an α -phase to β -phase. The α (hexagonal close packed) is hard and brittle with strong hardening tendency, and the β (body centred cubic) is ductile, which transforms (cut) easier, but also has a strong tendency to adhere [42]. This might also be the reason for the poor chip control discussed below (figure 9-20) under these operating conditions. Therefore, this study confirmed that there is a region where the cutting zone may be heated to a sufficient temperature for significant stepwise thermal softening to occur. This thermally softened state is associated with reduced machining forces [29 & 56]. Reaping the benefits of machining in this state is only possible if the tool material can continuously withstand the elevated temperatures.

At a cutting speed of 250 m/min, the tool life dropped significantly. Although the strength of the work piece material is low [29], the chemical attack [22 & 75] on the tool is more aggressive. Together with the mechanical shock due to the higher feed, thermal softening, oxidation and chemical reactions weaken the inter-granular bonds which cause the grains to tear apart under the action of the machining shear stress [56, 66, 75 & 79].



As shown in figure 9-19 an increase in feed led to an increase in surface roughness.

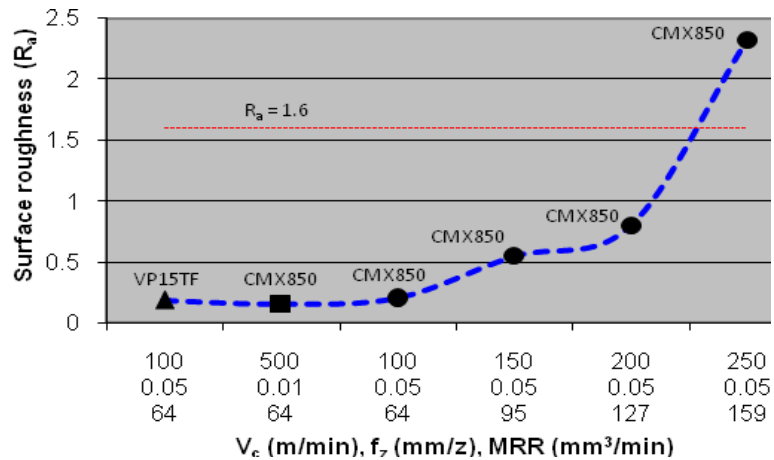


Figure 9-19: Surface roughness (R_a) produced in different conditions

Cutting speeds around 250m/min exceeded the surface roughness failure of $R_a=1.6$. At similar low material removal rates ($64 \text{ mm}^3/\text{min}$) the cutting speed and insert geometry were influential. A cutting speed of 500 m/min ensured the best surface roughness for PCD, while the innovative geometry of the WC helped to get a better surface roughness at 100 m/min. As discussed in the literature [66, 75 & 79], WC has much higher transverse rupture strength, but a lower thermal conductivity than PCD. Therefore it is common practice to use large feeds and decrease speeds when milling titanium with Cemented tungsten carbide [66].

Results from this study showed that for PCD, a decrease in feed and increase in cutting speed (V_c) produce a better surface finish, while achieving similar a tool life compared to lower speeds, higher feeds. Therefore the author established that PCD show promising results for high quality finishing at elevated cutting speeds.



Figure 9-20 illustrates the chip formation of the CMX850 produced at different cutting speeds.

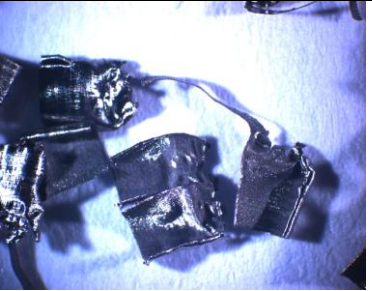
CMX850 Flood $V_c = 100$ m/min	CMX850 Flood $V_c = 150$ m/min	CMX850 Flood $V_c = 200$ m/min
$f_z = 0.05$ mm/tooth	$f_z = 0.05$ mm/tooth	$f_z = 0.05$ mm/tooth
MRR = 64 mm ³ /min	MRR = 95 mm ³ /min	MRR = 127 mm ³ /min
		
Best chip control	Good chip control	Poor chip control

Figure 9-20: Chip formation for CMX850 at different cutting speeds

An increase in cutting speed will not only reduce the cutting forces, but also a chip formation transition from continuous to segmented chips [49]. Interesting to note that the same cutting parameters ($V_c = 200$ m/min, $f_z = 0.05$ mm/z) that led to the “sweet-spot” for tool life, generated poor chip control. This might be due to the phase transformation [29]. The VP15TF produced longer, gradual chips compared to these of CMX850 (Figure 9-20). The tungsten carbide has a good designed geometry and produced a better segmented chip formation than the experimental geometry of the PCD [52].



10. Conclusion

Considering the growing market of the aerospace industry that uses more titanium and the push for reduced assembly flow time, opportunities for the advancement of the machining technology are prominent.

The work demonstrated progress over the performance reported in current literature. The performance of PCD inserts has been compared to that of WC inserts in the machining of Ti-6Al-4V at elevated cutting speeds. It has been found that the PCD performed better than the WC at these extreme thermo-environments. The study also confirmed that there is a region where sufficient temperature in the cutting zone may be generated to reduce machining forces, while keeping the operating temperature of the tool within limits.

The author explored the potential for high speed milling of Ti-6Al-4V, by investigating the fundamental causes of tool failure. The objective was to achieve an order of magnitude increase in tool life, machining at high speed, simply by reducing some of the failure mechanisms through different cutting strategies.

Tool wear for milling Ti-6Al-4V is described as a thermo-mechanical high-cycle fatigue phenomenon. Uniform and a retarded tool wear rate with the capability of higher volume of material removal per tool life are achieved in the case of PCD inserts compared to Cemented tungsten carbide. The average surface roughness produced during the experiments was relatively low and equivalent to that obtained in polishing for various conditions. The chip control for roughly all the experiments conformed to the industry requirements for practical high performance machining. The chips were found to be serrated and decreased in size as the feed was increased.

The study indicated the following issues to be important for an increase in tool life at high-speed finish milling of Ti-6Al-4V:

1. Maximising both the transverse rupture strength and thermal shock resistance factors values, will produce a robust tool.



-
2. Increased cutting speed (feed) will generally decrease tool life. For inserts with low transverse rupture strength, there may be a minimum cutting speed below which mechanical overload may occur. In the same way, a local maximum tool life may exist if there is a phase change in the work piece material and the insert can withstand the harsh operating conditions.

The best balance for a high removal rate and economic tool life need to be established for new insert entrants. Application to exactly where the heat build-up is concentrated, thermal shock and heat transfer at elevated tool temperatures are the constraint factors. Future work needs to be specific in determining the appropriate heat transfer coefficient and needs to determine relevant material property values to generate quantitative models. Comments by Boeing and their titanium supplier Timet (Titanium Metals Corporation) that Ti-54M might be the titanium alloy of the future, needs to be strongly considered in future work.

In the past, industries worked on the reduction of non-productive times. In the future we need to consider non-productive energy. Evaluating the material removal rate per kW of power (energy) required, should be considered. Considering the megatrends of our time, the author is of the opinion that the opportunity will swiftly migrate to the efficient manufacture of energy resources, like wind and water turbines.

11. References

- [1] Friedman, T. 2005. *The World is Flat: A Brief History of the Globalized World in the 21st Century*. New York: Farrar, Strauss, Giroux
- [2] Nottbohm, H. 2008. *Entwicklungstendenzen im Automobilmotorenbau*. The 5th Chemnitz Colloquim on Production technology. CPK 2008
- [3] Z_punkt GmbH. The Foresight Company. 2008. *Die 20 wichtigsten Megatrends*. http://www.zpunkt.de/fileadmin/be_user/D_Publikationen/D_Arbeitspapiere/Die_20_wichtigsten_Megatrends_x.pdf. 2007
- [4] Canton, J. 2007. *The Extreme future. The top trends that will reshape the world in the next 20 years*. Plume Printing. 2007
- [5] Saxton, B.M. 2006. *Rock the boat: Why leaders need to make waves to succeed the era of globalisation*. TerraNova. Interpak Books
- [6] Keith Campbell. 2008. *Green Skies*. Engineering News. June 27 – July 3. 2008
- [7] website: February 2008. *Airbus 2007 – 2026 Global market forecast*. http://www.airbus.com/en/presscentre/pressreleases/pressreleases_items/08_02_07
- [8] website: January 2007. *Rolls-Royce Market Outlook 2006*. http://www.rolls-royce.com/civil_aerospace/overview/market/outlook/default.jsp
- [9] website: February 2008. *Rolls-Royce Market Outlook 2007*. http://www.rolls-royce.com/civil_aerospace/overview/market/outlook/default.jsp
- [10] Segal, R. 2007. *There's no second place in aerospace*. Manufacturing Engineering. March. 2007. pp. (89-98)
- [11] website: January 2007. *Boeing Current Market Outlook 2007*.
- [12] website: Augustus 2008. IATA. http://www.iata.org/whatwedo/economics/fuel_monitor/price_development.htm
- [13] Miller, S. 1996. *Advanced materials means advanced engines*. Interdisciplinary Sci. Rev. 21 (2). pp. (117-129)
- [14] website: February 2008. *Aerostrategy*. http://www.aerostrategy.com/speeches/speech_61.pdf
- [15] Ezugwa, E.O., Bonney, J., Yamane, Y. 2002. *An overview of the machinability of aeroengine alloys*. Journal of Materials Processing Technology 134 (2003) pp. (233-253)

-
- [16] Callister, W.D. Jr. 2003. *Material Science and Engineering – An Introduction, Sixth Edition*, John Wiley and Sons. Inc. pp. (264-382)
- [17] Donachie, M.J., Donachie. S.J. 2002. *Superalloys. A Technical Guide*, Second Edition, ASM International, pp. (8-109)
- [18] Choudhury, I.A., El-Baradie, M.A. 1998. *Machinability of nickel base superalloys: a general review*. Mater, J. Process Technol. 77 (1-3) pp. (278-284)
- [19] Groover, M.P. 2002. *Fundamentals of Modern Manufacturing*. Second Edition. John Wiley & sons, Inc.
- [20] Ezugwu E.O. 2007. *Improvements in the machining of aero-engine alloys using self-propelled rotary tooling technique*. Journal of Materials Processing Technology 185 (2007) pp. (60–71)
- [21] Campbell, K. 2007. *Super Alloys: Jet Set*. Engineering News. June 22-28 p. (19)
- [22] Trent, E.M. Wright, P.K. 2000. *Metal cutting*. 3rd Edition, Butterworth Heinemann, Boston, USA
- [23] Simms, C.T., Hagel, W.C. 1972. *The Superalloys*. Wiley, New York
- [24] Z.Y. Wang, K.P. Rajurkar. *Cryogenic machining of hard-to-cut materials*, Wear 239 (2000) pp. (168–175)
- [25] Noaker, P.M. 1991. *Super speeds for superalloys*. Manufacturing Engineering. October. pp. (63-68)
- [26] Krebs, Robert E. 2006. *The History and Use of Our Earth's Chemical Elements: A Reference Guide* (2nd edition). Westport, CT: Greenwood Press
- [27] Emsley, John. 2001. *Nature's Building Blocks: An A-Z Guide to the Elements*. Oxford: Oxford University Press, pp. (451 – 453)
- [28] Department of Defense report. 2005. *China's impact on metal prices in defense aerospace*. <http://www.acq.osd.mil/ip>
- [29] Y. Honnarat. 1996. *Issues and breakthrough in the manufacture of turboengine titanium parts*. Mater. Sci. Eng. Part A213 (1996) 115-123.
- [30] Luther, G., Williams, J.C. 2003. *Titanium*. Springer-Verlag Berlin Heidelberg, New York
- [31] Kirk, D.C. 1976. *Cutting Aerospace Materials. Nickel-, Cobalt-, and Titanium-Based Alloys*. Rolls Royce (1971) Ltd, pp. (77-98)
- [32] Donachie, M.J. Jr. 2000. *Titanium. A Technical Guide*. Second Edition. ASM International. The materials information society.

-
- [33] Boyer, R.R. 1996. *An overview on the use of titanium in aerospace industry*. Journal Material Sci. Eng. Part A213 (1996) pp. (103-114)
- [34] Mantle, A.L., Aspinwall, D.K. 1998. *Tool life and workpiece surface roughness when high speed machining a gamma titanium aluminide, progress of cutting and grinding*, in: Proceedings of the Fourth International Conference on Progress of Cutting and Grinding, International Academic Publishers, Urumqi and Turpan, China, 1998, pp. (89–94)
- [35] Ezugwu, E.Q., Wang, Z.M. 1997. *Titanium alloys and their machinability - A review*. Int. J. Mater. Process. Technol. 68 (1997) pp. (262–274)
- [36] Vigneau J. 1997. *Cutting materials for machining superalloys*. International CIRP/VDI Conference on Cutting Materials and Tooling, Dusseldorf, 19-20 September 1997.
- [37] Gatto A., Luliano L. 1997. *Advanced coated ceramic tools for machining superalloys*. International Journal Machine Tools Manufacture 1997;37(5) pp. (591-605)
- [38] Maekawa, K., Kitagawa, T., Kubo, A. 1997. *Temperature and wear of cutting tools in high-speed machining of Inconel 718 and Ti-6Al- 6V-2Sn*. Wear 1997;202(2) pp.(142-8)
- [39] El-Wardany, T.I., Mohammed, E., Elbestawi MA. 1996. *Cutting temperature of ceramic tools in high speed machining of difficult-to-cut materials*. International Journal Machine Tools Manufacture 1996;36(5) pp. (611-34)
- [40] Liao, Y.S., Shiue, R.H. 1996. *Carbide tool wear mechanism in turning of Inconel 718 superalloy*. Wear 1996;193(l) pp. (16-24)
- [41] website: February 2008. Timet (Titanium Metals Corporation)
www.timet.com/pdfs/ITA_09262005.pdf
- [42] Kuljanic, E., Fioretti, M., Beltrame, L., Miani, F. 1998. *Milling Titanium Compressor Blades with PCD Cutter*. University of Udine, pp. (61-64)
- [43] Froes, F.H. 1998. *Non-Aerospace applications of Titanium*. TMS, Warrendale, USA, (1998) p.317
- [44] Breme, J.1988. *Sixth World Conference of Titanium*, Les Editions de Physique, Les Ulis, France.p.57
- [45] Brunette, D. M., Tengval P., Textor, M., Thomsen, M. 2001. *Titanium in medicine*, Springer-Verlag, Berlin, Germany. 2001
- [46] Titanium. Los Alamos National Laboratory (2004). Retrieved on 2006-12-29

-
- [47] Blenkinsop, P.A. 1995. *Titanium*, Science and Technology, The University Press, Cambridge, UK,(1996) p.41
- [48] Hong, H., Riga, A.T., Cahoon, J.M., Scott, C.G. 1993. *Machinability of steels and titanium alloys under lubrication*, Wear 162. pp. (34-39)
- [49] Schulz, H., Sahm, A. 2002. *Influence of Heat Treatment and Cutting Parameters on Chip Formation and Cutting Forces*. Metal Cutting and High Speed Machining, Kluwer Academic/Plenum Publishers, pp. (69-78)
- [50] Shaw, M.C., Dirke, S.O., Smith, P.A., Cook, N.H., Loewen E.G., Yang, C.T. 1954. *Machining titanium*. MIT Rep., 1954 (Massachusetts Institute of Technology, Cambridge, MA) (Contract AF 33-600-22674).
- [51] Cook, N.H. 1953. *Chip formation in machining titanium in Proc. Symp. on Machining and Grinding Titanium*. Watertown Arsenal, Watertown, MA, March 31, 1953, U.S. Army Ordnance Corps, 1953.
- [52] Komanduri, R., Von Turkovich, B.F. 1981. *New observations on the mechanism of chip formation when machining Titanium alloys*. Wear, 69. pp. (179-188)
- [53] Komanduri, R. 1982. *Some clarifications on the mechanism of chip formation when machining titanium alloys*. Wear 76. pp. (15-34)
- [54] Cook, N.H. 1959. *Self excited vibrations in metal cutting*. Trans. ASME, 81 (May 1959) 193.
- [55] Colwell, L.V. 1953. *Machining of titanium, in Proc. Symp. on Machining and Grinding Titanium*. Watertown Arsenal, Watertown, MA, March 31, 1953, U.S. Army Ordnance Corps, 1953, p. (16)
- [56] Barnett-Ritcey, D., Elbestawi, M.A. 2004. *High-speed finish milling of Ti6Al4V with PCD*, PhD study, MCMasters Manufacturing Research Institute (MMRI)
- [57] Dearnley, P.A., Grearson, A.N. 1986. *Evaluation of principal wear mechanisms of cemented carbides and ceramics used for machining Titanium alloy IMI 318*. Materials Science and Technology, Vol 2, No 1, pp. (47-58)
- [58] website: ATI Allvac: An Allegheny Technologies company. *ATI Titanium 6Al-4V Alloy*. <http://www.allvac.com/allvac/pages/PDF/tech/TI-020%20Ti%206-4ELI.pdf>
- [59] Zoya, Z.A., Krishnamurthy, R. 2000. *The performance of CBN tools in the machining of titanium alloys*. Mater, J. Process. Technol. (100) pg. (80-86)
- [60] Kahles, J.F., Field, M., Eylon, D., Froes. F.H. 1985. *Machining of titanium alloys*, J. Met. (1985) 27.

-
- [61] Maitre, L. 1986. *L'usinage du Titane et de Ses Alliages*, *Materiaux et Techniques*, pp. (47–53)
- [62] Machado, A.R., Wallbank, J. 1990. *Machining of titanium and its alloys*, in: Proceedings of the Institution of Mechanical Engineers, J. Eng. Manuf. B (1990), pp (204, 53)
- [63] Swinehart, H.J. 1968. *Cutting Tool Material Selection*, American Society of Tool and Manufacturing Engineers, Dearborn, MI, 1968, pp. (13-41)
- [64] Pettifor, D.G. 1995. *Bonding and Structures of Molecules and Solids*, Oxford University Press, pp. (12-13)
- [65] Altintas, Y. 2000. *Manufacturing Automation*. Metal cutting mechanics, Machine tool vibrations, and CNC design. Cambridge University Press
- [66] Sandvik Group: *Titanium Machining Application Guide*, Sandvik Coromant, Sweden, 2004
- [67] Fowler, D. 1988. *Milling with Polycrystalline Diamond*. Carbide Tool Journal Vol. 20 NO. 5, pp. (23-25)
- [68] Kitagawa, T., Kubo, A., Maekawa, K. 1997. *Temperature and wear of cutting tools in high-speed machining of Inconel 718 and Ti-6Al-6V-2Sn*. *Wear* 202 (2) pp. (142-148)
- [69] Che-Haron, C.H., Jawaid, A. 2005 *The effect of machining on surface integrity of titanium alloy Ti-6% Al-4% V*, *Journal of Materials Processing Technology* 166, pp. (188-192)
- [70] Schulz, H., Moriwaki, T. 1992. *High speed machining*. *Ann. CIRP* 41 (2) pp. (637-645)
- [71] Bhaumik, S.K. , Divakar, C. , Singh, A.K. 1995. *Machining Ti-6Al-4V Alloy with a wBN-cBN Composite Tool*, *Materials & Design* Vol. 16, No.4, pp. (221-226)
- [72] Wang, Z.Y., Sahay, C., Rajurkar, K.P., 1996. *Tool Temperatures and Crack Development in Milling Cutters*. *Int. J. Mach. Tools Manufact.* Vol. 36, No. 1, pp. (129-140)
- [73] Su, Y., He, N., Li, L., Li, X.L. 2006. *An Experimental Investigation of Effects of Cooling/Lubrication Conditions on Tool Wear in High-Speed End Milling of Ti-6Al-4V*, *Wear* Vol. 261 No. 7-8, pp. (760-766)
- [74] Kikuchi, M. 2008. *The use of cutting temperature to evaluate the machinability of titanium alloys*. Division of Dental Biomaterials, Graduate School of Dentistry, Tohoku University, 4-1 Seiryomachi, Aoba-ku, Sendai, Miyagi 980-8575, Japan.

-
- [75] Tooling Technology. *Mitsubishi Materials. Mitsubishi Tooling Technology*. April 2005
- [76] Byrne, G., Dornfeld, D., Denkena, B. 2003. *Advancing cutting technology*, Keynote Papers STC "C", Annals of CIRP, 52 (2), pp.(483-508)
- [77] Krar, S.F., Ratterman, E. 1992. *Superabrasives. Grinding and machining with cBN and Diamond*. Glencoe / McGrawHill. Chapter 10. pp. (160-180)
- [78] Lammer, A. 1988. *Mechanical Properties of Polycrystalline Diamonds*. Materials Science and Technology, 4, 1988, pp. (949-955)
- [79] Element Six (Pty) Ltd. 2008. Information from internal database and discussions with Mr. Klaus Tank and Mr. Habib Saridikmen.
- [80] Huang, B.L., Weis, C., Yao, X. Belnap, D., Rai, G. 1997. *Fracture Toughness of Sintered Polycrystalline Diamond (PCD)*. International conference on Particulate materials and processes, 5th. 1997. pp (431-438). ISBN: 1878954644
- [81] Nabhani, F. 2001. *Wear mechanisms of ultra-hard cutting tool materials*. Journal of material process technology. 115. pp. (402-412)
- [82] Tlusty, J. 1999. *Manufacturing processes and equipment*. Prentice Hall.
- [83] Ownby, P.D. 1991. *Engineering properties of diamond and graphite*. Engineered materials handbook. 4. pp. (821-831)
- [84] Flauhaut, J. *Propriétés Thermiques du Diamant*. Nouveau traité de Chimie Minérale. Tome VIII fasc. 1. pp. (131-136)
- [85] Bakon, A., Szymanski, A. 1993. Practical Uses of Diamonds, Ellis Horwood Ltd. and Polish Scientific Publishers PWN Ltd., pp. (57-60)
- [86] Wilks, J., Wilks, E. 1991. *Properties and Applications of Diamond*. Butterworth Heinemann, pp. (17-20)
- [87] Narutaki, N., Murakoshi, A., 1985. Study on Machining of Titanium Alloys, Hiroshima University, Japan, pp. (65-69)
- [88] Bundy, B., Strong, W. 1961. Journal Chem. Phys. 35. p. (383)
- [89] Konig, W., Neises, A., 1993, *Turning TiA16V4 with PCD*, IDR2: 85-88
- [90] Sharman, A.R.C., Aspinwall, D.K., Dewes, R.C., Bowen, P. 2001 *Workpiece surface integrity considerations when finish turning gamma titanium aluminide*, Wear, 249. pp. (473-481)
- [91] Ezugwu, E.O., Da Silva, R.B., Bonney J., Machado, A.R. 2005. *Evaluation of the performance of CBN tools when turning Ti-6Al-4V alloy with high pressure coolant supplies*. Int. J. Mach. Tools Manuf. 45 (9) (2005) pp. (1009-1014)

-
- [92] Li, L. Chang, H., Wang, M., Zuo, D.W., He, L. 2004. *Temperature measurement in High speed Milling Ti6Al4V*. Key Engineering Materials, Vol.259-260. pp. (804-808)
- [93] Bryant, W.A. 1998. *Cutting tool for machining titanium and titanium alloys*. US Patent, 5,718,541 (17 February 1998)
- [94] Komanduri, R., Reed, W.R. Jr. 1983. *Evaluation of carbide grades and a new cutting geometry for machining titanium alloys*, Wear 92 (1983) pp. (113–123)
- [95] Wang, Z.G. Rahman, M., Wong, Y.S. and Sun, J. 2005. *Modeling of cutting forces during the machining of Ti6Al4V with different coolant strategies*, 8th CIRP international Workshop on Modeling in Machining operations, Chemnitz, Germany, May, (2005)
- [96] Ginting, A. Nouari, M. 2007. *Optimal cutting conditions when dry end milling the aeroengine material Ti-6242S*. Journal of Materials Processing Technology (184) pp. (319–324)
- [97] Hoffmeister, H.W. 2001. *Superabrasive machining of TiAl6V4*. *Industrial Diamond Review*. 4/2001. pp. (241-246)
- [98] Nabhani, F. 2001. *Machining of aerospace titanium alloys*, Robotics and Computer Integrated Manufacturing, 17, 2001, pp. (99-106)
- [99] Kramer, B.M. 1987. *On tool materials for high speed machining*. Eng, J. Ind.(109) pp. (87-91)
- [100] Sharman, A.R.C., Aspinwall, D.K., Dewes, R.C., Bowen, P. 2000. *Tool life when turning gamma titanium aluminide using carbide and PCD tools with reduced depths of cut and high pressure fluid*. Proc. of the 28th NAMRC, 161-166
- [101] Nurul Amin, A.K.M., Ismail, A.F., Nor Khairusshima, M.K. 2007. *Effectiveness of uncoated WC-Co and PCD inserts end milling of titanium alloy—Ti-6Al-4V*. Journal of Materials Processing Technology (192–193) pp.(147–158)
- [102] Hartung, P.D., Kramer, B.M. 1982. *Tool wear in titanium machining*. Annals of CIRP. 31[1]. pp.(75-80)
- [104] Ezugwu, E.O., Bonney, J. 2003. *Surface alteration when machining Inconel 718 with ceramic and coated carbide tools under high pressure coolant supply*. Proceedings of international conference on leading edge manufacturing in 21st century. Niigata, Japan, 3-6 November 2003. pp. (595-600)

-
- [105] Thiele, J.D., Melkote, S.N. 1999. *Effect of cutting edge geometry and workpiece hardness on surface generation in the finish hard turning of AISI 52100 steel*. J Mater Process Technol 1999; 94:216-26.
- [106] Ota, M., Kukino, S., Uesaka, S., Fukaya, T. 2005. *Development of SUMIBORON PCBN tool for machining of sintered powder metal alloys and cast iron*. SEI Technical review. Number 59. January 2005
- [107] Metal Powder. 2005. *Japanese PM shows three years' growth as automotive parts make steady gains*. Metal Power Report. Volume 60, Issue 6, June 2005, pp (10-13)
- [108] Oosthuizen, G.A. 2008. *Wear phenomena of PCBN tools during PM steel machining*. Element Six (Pty) Ltd databases.
- [109] Petrucci, R.H., Harwood, W.S., Herring, F.G. 2002. *General Chemistry. Principals and modern applications*. Eighth edition. Prentice-Hall, Inc.
- [110] Bhushan, B. 2002. *Introduction to Tribology*. John Wiley & Sons, New York, pp. (332-379)

A

*Appendix A: High Performance
machining of titanium:
Charting the challenge*

HIGH PERFORMANCE MACHINING OF TITANIUM: CHARTING THE CHALLENGE

N.F. Treurnicht

Department of Industrial Engineering
University of Stellenbosch, South Africa
e-mail: nicotr@sun.ac.za

G.A. Oosthuizen

Department of Industrial Engineering
University of Stellenbosch, South Africa
e-mail: tiaan@sun.ac.za

ABSTRACT

Aircraft manufacturing is in a growth phase. High fuel prices and environmental concerns further promote the use of titanium. A growing market niche for high value titanium machined components is perceived. Machining is a major cost contributor. It creates an opportunity for a supplier to gain a competitive advantage. The most prominent cooling practice in the industry, namely flood cooling, offers room for development. Higher cutting speeds resulting in higher cutting temperatures, resulting two phase flow and delayed surface wetting on the hot insert surface, is considered. Tool materials able to withstand high temperatures, such as PCD, is shown to have potential to last significantly longer at higher cutting speeds. Cutting strategy is presented as another potential focus area to achieve effectiveness improvements. Results of an experimental pilot study indicate that current industrial practice utilises material constraints relatively well. It is concluded that new cooling techniques, new cutting materials and well designed cutting strategies will have to be developed for significant machining performance improvement.

INTRODUCTION

The aerospace and defence industries are currently experiencing huge growth, however it is questionable whether they have sufficient capacity to meet future demands. Driven by a competitive consumer market to keep airfares and shipping rates low, aerospace manufacturers need to reduce costs from 5 to 10% each year [1]. This makes the application of the materials

used in the aero-engine and efficiency of the manufacturing processes critical. The material for one of the titanium split-fan cases cost \$30 000 per part in 2007 compared to \$5 000 in 2004 [1]. Titanium and nickel-based alloys constitute the bulk of materials used in aircraft engines. For titanium-alloys the percentage content is ~ 30 wt% in commercial and 40 wt% in military gas turbines [2]. In figure 1 the breakdown of different materials in aircraft construction is shown. The specific thermal, corrosion and mechanical properties offered by titanium alloys, provide distinct advantages in engine applications. Their machinability is however poor, currently limiting their use.

The Airbus Global Market Forecast anticipates a demand for some 24,300 new passenger and freighter aircraft between 2007 and 2026, creating an average delivery rate of some 1,215 airliners annually during this 20-year period valued at US\$ 2.8 trillion [3]. Rolls Royce forecasts that engine orders will increase from 35 000 in the period 1996-2005 to about 55 000 in 2006-2015 (57% growth) [4]. The latest outlook report forecasts that engine deliveries units are estimated to be 71, 500 in 2017-2026. Engine demand over the next 20 years could be worth US\$ 701 billion [5]. Additionally, world traffic is expected to increase by 4.9% p.a. [3], [5].

Fuel is the largest cost for all airlines and a major priority for profitable airline operation. For some carriers, the fuel bill can account for up to 50% of direct operating costs. For most carriers fuel expense grew from 15% to more than 25% of total airline operating costs (2003 – 2006) [5], [6]. By 2026, the fuel consumption of the average world fleet is expected to be at three litres per 100 passenger kilometres, similar to the benchmark that the A380 set recently [3].

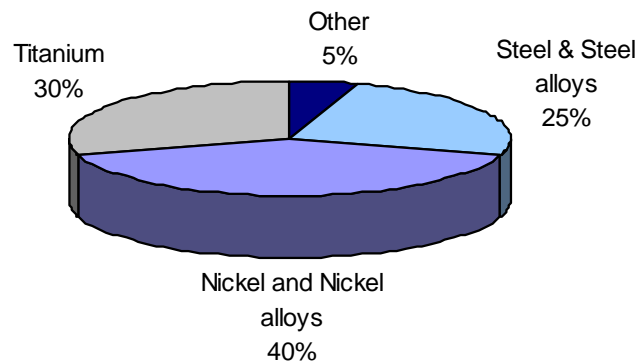


Figure 1: Typical commercial aero-engine material content

The scenario that is reported in the text above, details an aircraft market with good prospects over the foreseeable future. This creates an opportunity for a developing country like South Africa with proven technical and manufacturing expertise on an advanced enough level to be suitable for second or third tier supplier status in the global aerospace supply chains. The prospects for increased use of titanium are positive, creating niche areas for new entrants as specialist manufacturing suppliers. Given the high cost of titanium and the difficulty of machining, necessarily sets the stage for a high value part, for which the added manufacturing value could be significant as well. This is considered an export opportunity for South Africa.

1 OPPORTUNITIES RELATED TO COOLING

The thermal conductivity of Ti6Al4V (7 W/m.K) is approximately one twenty fifth of that of Aluminium (6061: 177 W/m.K), one eighth of that of steel (1018: 59 W/m.K). It is less than a third of the corresponding value for stainless steel (SS422B: 24 W/m.K) and only half of the value for even Inconel (718: 15 W/m.K). The result is a concentration of heat in the cutting zone, causing the characteristically high tool wear for which titanium is known [7]. Approximately 80% of heat generated is retained in the tool, while only 20% is removed by means of the chip [8].

Titanium machining is characterised by an unusually small contact area where the chip is in contact with tool face. Compared to steel being machined at the same rate, this contact area is only a third for titanium. The low thermal conductivity, together with the small contact area, result in a high rate of temperature increase with cutting speed and wear occurring closer to the tool cutting edge [9].

Together, the low conductivity and heat concentration on a small area account for high tool temperatures. Temperatures of 900°C have been measured at a cutting speed of 75 m/min [10].

In interrupted cutting, such as milling, the tool is subjected to cyclic heating and cooling, causing thermal shock. When the rate of cooling is increased significantly, the result is crack formation causing premature tool failure [11]. Su et al [12] connects cyclic thermal shock directly with

thermal crack initiation. It logically follows that an indiscriminate increase of cooling power will yield diminishing returns.

Further complexity is added by the fact that titanium's chemical reactivity becomes problematic at temperatures above 500 °C. Apart from diffusion wear, chips seize onto the tool cutting surface. Once a built-up edge develops, tool failure follows rapidly [9]. A practical manifestation of this problem is that chips can spontaneously ignite as they react with oxygen. Recently, a 5-axis machine was destroyed by fire in this way in Cape Town, SA.

Che-Haron [13] reports that advisable industry practice cutting speeds for titanium are limited to about 45 m/min. This is in accordance with the recommendations of Sandvik [14]. Considering that Aluminium can be cut at 20-100 times higher and hardened steel at 4-8 times higher speed, titanium machining cost could be reduced if higher speeds were possible. Cooling of the titanium machining process therefore presents an opportunity for process improvement.

Simple flood cooling, which has become standard practice, has become insufficient and at the same time too crude a technique, making cooling a frontier in titanium machining development. Application to exactly where the heat build-up is concentrated, thermal shock and heat transfer at elevated tool temperatures are the constraint factors.

Titanium machining requires high application pressures to penetrate to the localized heat generation zone. When the cutting zone is shielded from the lubricant stream such as in cutting with deeper axial immersion (roughing), the coolant needs to be focused on the cutting edge. Focused application is addressed by the relatively new technique of high pressure (10-100 bar) through spindle lubrication. Barnett-Ritcey [15] doubled tool life at an experimental cutting speed of 150 m/min.

At high tool temperatures, typically above 500°C, the heat transfer mechanism between the cooling fluid and the tool surface changes to two phase high speed flow. The coolant is vaporised on contact with the heated tool surface, forming an isolating boundary layer on the tool surface.

Quantifying the phenomenon, the heat transfer coefficient for water is reduced almost tenfold from a value of 13 500 W/m²K at 380°C to 1470 W/m²K above 830°C [15], [16]. The phenomenon is also described as delayed surface wetting or constrained coolant jet impingement in the heat transfer literature. The relevance to titanium machining is that cooling becomes ineffective at higher heat loading on the tool surface. The design of efficient cooling systems specifically for titanium machining is considered an area that holds potential for significant improvement.

Cooling of titanium machining is not a challenge with a single boundary, where more (cooling) is not automatically better. Implementing a cooling system with too high a cooling power will promote thermal shock. Even with the low, unpredictable power of flood cooling thermal shock has been described often in the literature as well as encountered in practice. We are of the opinion that through spindle application, high pressures (50 bar +) as well as customized, possibly even under dynamic control, of gas / fluid mixtures for “soft” or controlled heat exchange rate cooling holds the first key to significantly increased machining effectiveness.

2 SOFTENING / EASY MACHINING AT ELEVATED SPEEDS / TEMPERATURES

At elevated temperatures titanium becomes softer and therefore easier to machine. If a cutting material can be found that can withstand these elevated temperatures dynamically (cyclic heat input), this could yield a local optimum condition at which machining cost and lead time can be reduced.

Figure 2 shows that a cutting material able of withstanding temperatures in the region of 1000 to 1500°C will be able support cutting speeds in excess of 200 m/min. Withstanding elevated temperatures, especially of fast cyclic thermal loading, such as in intermittent cutting, will depend fundamentally on the thermal diffusivity. It is significant to note that that the thermal conductivity for Polycrystalline diamond or PCD ($\lambda = 500\text{W/mK}$) is five times more than that of tungsten carbide ($\lambda = 100\text{W/mK}$). Typically PCD is significantly harder (6000 HV) than carbides (2500 HV) indicating better performance at elevated temperatures. PCD also has lower transverse rupture

strength (1350-2500 MPa) versus unalloyed carbide (2500-3500 MPa) making it more susceptible to mechanical shock experienced in interrupted cutting. Thermal conductivity when divided by specific heat capacity yields a thermal diffusivity for PCD that is practically 10 times greater than for tungsten carbide, which indicates vastly better performance under thermal shock.

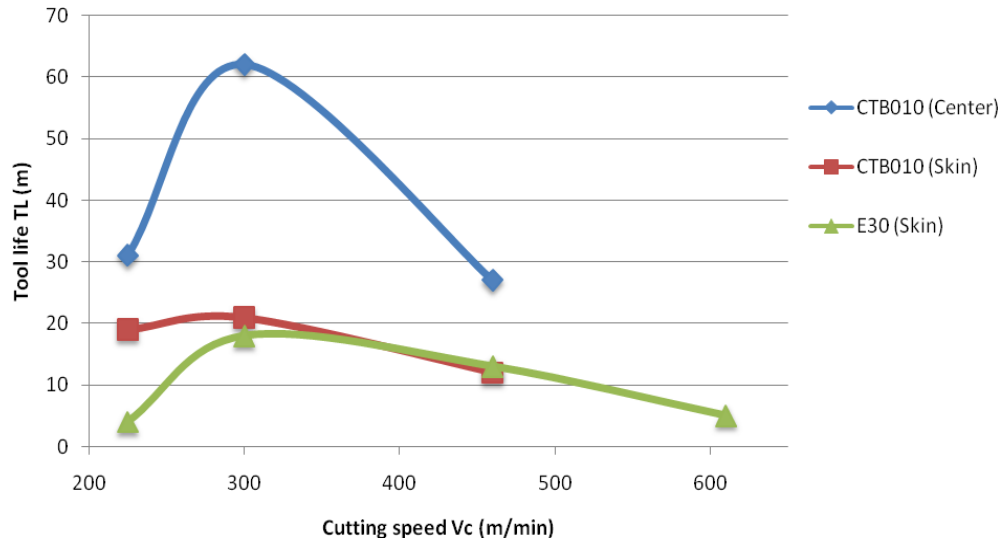


Figure 2: Effect of cutting speed on tool life ($h_x = 0.025\text{mm}$, $a_e = 0.25\text{mm}$, forged Ti6Al4V, A50) [17]

The completely counter-intuitive phenomenon that the tool life is increased, when the cutting speed is also increased, is shown in Figure 2. The tool life recorded with the CTB 010 PCD insert is doubled when the cutting speed is increased from 229 m/min to 305 m/min. From figure 3 it can be seen that increasing the cutting speed beyond 250 m/min will increase the cutting temperature to significantly over 1000°C. This phenomenon could be explained by the phase transformation at 995 °C when Ti6Al4V changes from an α -phase to a β phase that is easier to transform.

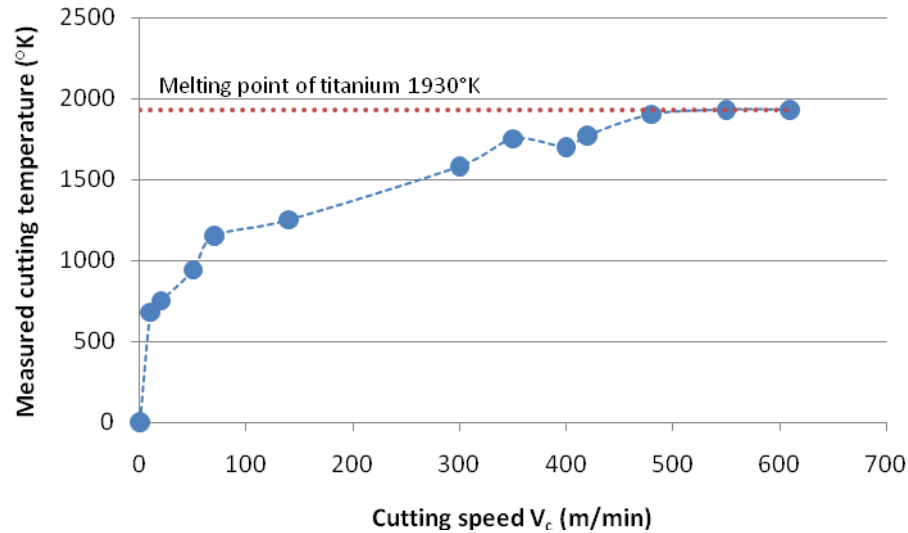


Figure 3: Area-weighted average cutting temperature as a function of cutting speed for K68 carbide insert (chip load, 0.127 mm/rev) [17]

Up to now, tool materials that can these extreme temperatures were not available. In the same figure it can be seen that tool material E30 which is a more conventional tungsten carbide did not perform well at all.

The titanium machinability research group at Stellenbosch is investigating a new experimental PCD grade manufactured by Element Six (Pty) Ltd. This PCD material combines a high chipping and abrasion resistance with good processability. This creates a distinct potential for withstanding high temperatures combined with increased mechanical shock resistance. Its fine grain size gives the new material both relatively high fracture toughness as well as high transverse rupture strength, which is an ideal combination for interrupted cut milling of titanium. The material is expected to be suitable for roughing and finishing applications.

4 MACHINING STRATEGY FOR TITANIUM

The potential for significant advances in titanium machining is perceived to exist utilising the material characteristics of superhard cutting materials. These include the synthetic diamond family and new improved carbide grades. Carbides in their extreme hard form are rather susceptible to thermal shock. Due to relatively high transverse rupture strength the carbides are however relatively less sensitive to mechanical shock loading. The combination of these two

parameters lead to the machining strategy focus that should minimise both forms of shock but placing an emphasis on reducing thermal shock if it is a trade-off between the two factors. Figure 4 shows a roll-in strategy to minimise shock loading on the cutting edge. This work needs to be analysed fundamentally and applied to the new generation PCD tool materials. PCD is for example relatively more susceptible to mechanical shock due to lower TRS values than those for carbides, but much more resistant to thermal shock due to high thermal diffusivity characteristics.

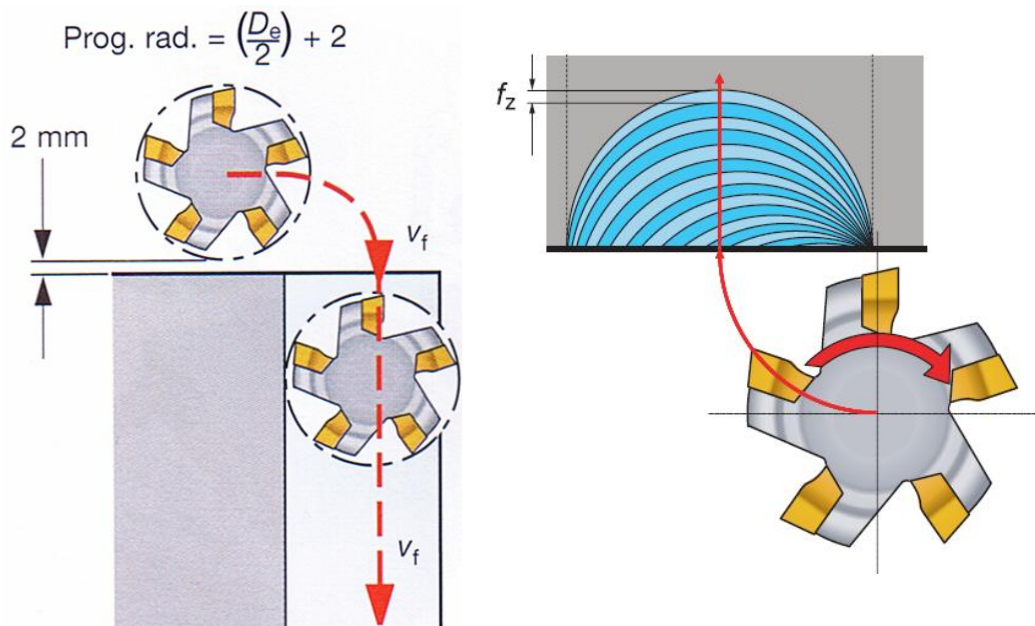


Fig 4: Roll-in machining strategy [14]

High axial immersion cut strategies also holds promise for titanium machining effectiveness advances. Research by Sandvik [14] has shown that a decrease in tool life is only weakly correlated with an increase in axial immersion. The negative correlation of tool life with maximum chip thickness is stronger, while the also negative correlation with cutting speed is extremely strong. It therefore seems theoretically possible to tailor the cutting process parameters to maintain tool life while increasing the material removal rate. This strategy will require an increase of axial immersion. There are further possibilities to apply these principles to the considerably different set of material characteristics of the synthetic diamond family of cutting materials.

5 EXPERIMENTAL WORK

A range of experiments were performed to establish a baseline for envisaged experimenting with new PCD materials. The goal was to establish which cutting speeds and feeds could be achieved with industry standard cooling techniques.

Experiments were conducted at a machining specialist manufacturer using a Leadwell 3-axis milling machine. The work piece was a 30 mm square bar of Ti6Al4V in the solution heat treated and aged condition. Hardness tests confirmed the specified 1080 MPa yield strength. Face milling was used. The tool used was a toroidal insert carrier with three cutting surface curved inserts. The carbide insert material used was F40M grade.

6 RESULTS AND DISCUSSION

Experiments were conducted with the aim that insert life should exceed 4 min. Each insert was inspected after 2 min and 4 min to determine wear progression. Three lubrication strategies, dry machining, air lubrication and flood lubrication were tested.

Table 1: Cutting parameters

	Suggested Cutting Parameters	Experimental Cutting Parameters	
vc	60	90	m/min
ae	32	30	mm
ap	3	0.5	mm
Dc	50	32	mm
fz	0.2	0.6	feed/tooth
z	1	1	
n	381.97	895.25	rpm
vf	76.39	537.15	mm/min
Q	7.33	8.06	cm³/min

7 CONCLUSIONS

The experiments indicated that the speeds, feeds and depths of cut recommended by the tool manufacturers can be exceeded to a certain extent. The gains that can be achieved along this route, is however limited. The cutting recommendations are relatively accurate. New techniques and / or cutting materials will have to be found to substantially improve machining speed and effectiveness of titanium.

8 RECOMMENDATIONS

The following research strategies could be fruitful for further improvements:

Increase of cooling effectiveness: Advanced technology techniques beyond simple flood cooling will be necessary.

New generation PCD materials have significant potential for improvements.

Carefully planned cutting strategies taking the tool material strengths and weaknesses into consideration, holds improvement potential.

9 REFERENCES

- [1] Segal, R., There's no second place in aerospace. *Manufacturing Engineering*. March. pp. 89-98, 2007.
- [2] Ezugwu, E.O., Bonney, J., Y.Yamane, Y., An overview of the machinability of aerospace alloys, *Journal of Materials Processing Technology*, 134, pp 233-253, 2003.
- [3] website: February 2008. Airbus 2007 – 2026 Global market forecast. http://www.airbus.com/en/presscentre/pressreleases/pressreleases_items/08_02_07
- [4] website: January 2007. Rolls-Royce Market Outlook 2006, http://www.rolls-royce.com/civil_aerospace/overview/market/outlook/default.jsp
- [5] website: February 2008. Rolls-Royce Market Outlook 2007, http://www.rolls-royce.com/civil_aerospace/overview/market/outlook/default.jsp
- [6] Boeing Current Market Outlook, 2007.
- [7] Kuljanic, E., Fioretti, M., Beltrame, L., Miani, F., Milling Titanium Compressor Blades with PCD Cutter, University of Udine, pp. 61-64, 1998.
- [8] Bhaumik, S.K. , Divakar, C. , Singh, A.K., Machining Ti-6Al-4V Alloy with a wBN-cBN Composite Tool, *Materials & Design* Vol. 16, No.4, pp. 221-226, 1995.
- [9] Kirk, D.C., Cutting Aerospace Materials (Nickel-, Cobalt-, and Titanium-Based Alloys), Rolls Royce (1971) Ltd, pp. 77-98, 1976.

-
- [10] Dearnley, P.A., Grearson, A.N., Evaluation of principal wear mechanisms of cemented carbides and ceramics used for machining Titanium alloy IMI 318, *Materials Science and Technology*, Vol 2, No 1, pp. 47-58, 1986.
- [11] Wang, Z.Y., Sahay, C., Rajurkar, K.P., Tool Temperatures and Crack Development in Milling Cutters, *Int. J. Mach. Tools Manufact.* Vol. 36, No. 1, pp. 129-140, 1996.
- [12] Su, Y., He, N., Li, L., Li, X.L., An Experimental Investigation of Effects of Cooling/Lubrication Conditions on Tool Wear in High-Speed End Milling of Ti-6Al-4V, *Wear* Vol. 261 No. 7-8, pp. 760-766, 2006.
- [13] Che-Haron, C.H., Jawaid, A., The effect of machining on surface integrity of titanium alloy Ti-6% Al-4% V, *Journal of Materials Processing Technology* 166, pp. 188-192, 2005.
- [14] *Titanium Machining Application Guide*, Sandvik Coromant, Sweden, 2004.
- [15] Barnett-Ritcey, D.D., M.A. Elbestawi, M.A., Tool Performance in High Speed Finish Milling of Ti6Al4V, *Proceedings of IMECE'02*, November 17-22, IMECE-MED-33655, pp. 1-9, 2002.
- [16] Price, R.F., Fletcher, A.J., Determination of surface heat-transfer coefficients during quenching of steel plates, *Metals Technology*, May, pp. 203-211, 1980.
- [17] Barnett-Ritcey, D.D., High-Speed Milling of Titanium and Gamma-Titanium Aluminide: An Experimental Investigation, Ph.D. thesis, McMaster University, Canada, 2004.

B

Appendix B: Work holding

USING PALLETISED WORK HOLDING TO EMULATE 5-AXIS MACHINING OF AEROSPACE COMPONENTS IN THE DEVELOPING WORLD

G.A. Oosthuizen¹, H.J. Joubert² and N.F. Treurnicht³

¹Department of Industrial Engineering
University of Stellenbosch, South Africa
tiaan@sun.ac.za

²Department of Industrial Engineering
University of Stellenbosch, South Africa
h2j@sun.ac.za

³Department of Industrial Engineering
University of Stellenbosch, South Africa
nicotr@sun.ac.za

ABSTRACT

This paper proposes the application of precision pallet technology, together with common 3-axis milling, to machine certain complex aerospace components, that is normally 5-axis machined. In this approach however, a set of different customized precision pallets are used to present each complex plane to the 3 axis machine as a horizontal plane, requiring quick and simple face milling. After machining one surface, the pallet is exchanged with another that has been pre-set up in machining time. Trials confirm the viability of the approach with capital recovery in less than a year.

1. Introduction

Many developing countries, in this case specifically South Africa, have a significant technology base in certain fields. Projects like a space observation telescope, satellite launches and new nuclear power generation concepts require an advanced manufacturing capability as a prerequisite. A common factor among developing nations is that their exchange rate is favourable for exports rather than for imports (€ 1 = 12 SARand, Feb 2009). Being fully imported, advanced machine tools therefore represent a large investment in local currency. According to Byrne et al [1], machine tool developers are expected to not mainly concentrate on maximum speeds and acceleration of machine axes, but to concentrate on other non-productive time aspects, like set-up time of machines. This includes work in the area of machine accuracy and flexibility.

The objective of this study addressed this scarcity of simultaneous 5-axis machines through exploring the use of precision palletised work holding, to emulate 5-axis machining on a 3 axis machine for flat surfaces. To provide a suitable context, the subject is introduced from a flexible manufacturing perspective.

The company where this approach was studied manufactures short run components, prototypes and tools on demand, to typical aerospace specifications. The 5-axis CNC machines are fully occupied mostly for 24 shifts, 7 days per week, while the 3-axis machines have reserve capacity.

2. Background

Nagarjuna et al [2] mentioned that manufacturing industries are rapidly changing from economies of scale to economies of scope. These industries are characterized by short product life cycles and increased product varieties in a similar manner to the situation at the company where the concept was tested. This implies a need to improve the efficiency of job shops while still maintaining their flexibility. Manufacturing speeds together with minimised secondary times, process stability and machining quality continuously increase production efficiency [3]. A flexible manufacturing system (FMS) can be defined as an integrated computer-controlled configuration of numerical control machine tools, as well as work holding and a material handling system designed to simultaneously manufacture a low to medium volume of a wide variety of high quality products at low cost [4]. The pallet work holding system proposed to the company allows for different operations on the standardized pallet chuck. This significantly reduces change over- and setup times, making it a very adaptable and flexible process. All proposed setup adjustments take place outside the milling machine, within the machining cycle time of other parts undergoing similar machining operations. This is the case for 3-axis machining. Should 5-axis machining be available change over and setup times can be reduced significantly.

2.1 Flexible work holding

The company manufactures on a strictly make-to-order basis. Therefore the work holding method should compensate for a wide range of different part sizes and cutting strategies. As mentioned, extreme flexibility is required of the work holding technique. From the ten desirable characteristics of work holders examined by Fellers et al [5], holding, supporting, part location and tool approach accessibility are applicable.

Figure 1 [6] shows the different flexible work holding strategies, and indicates the manually assembled work holding strategy used by this company.

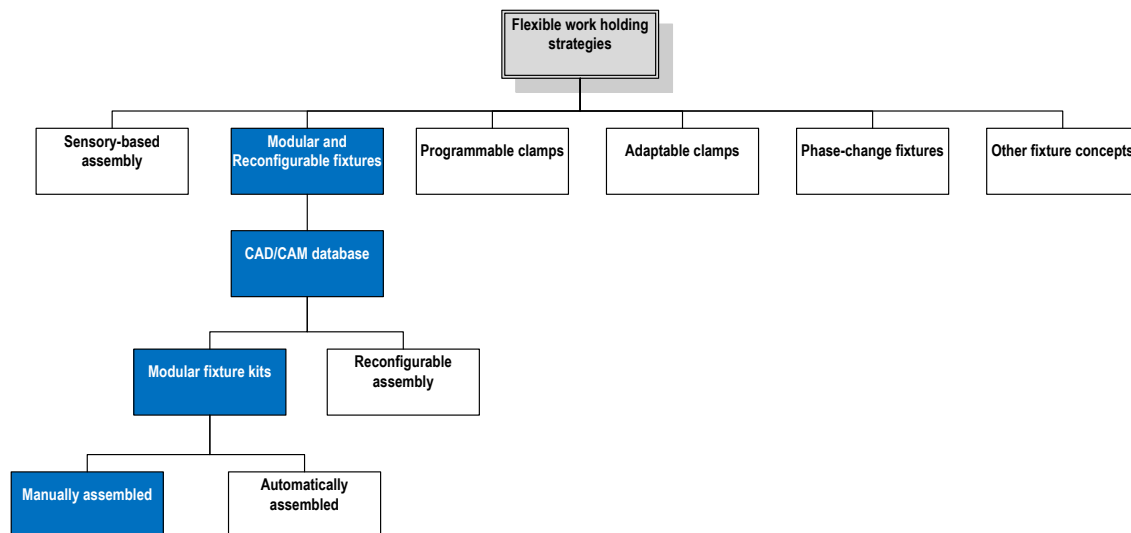


Figure 1: Flexible work holding strategies [6]

Choi et al [7] mentioned that if the part could be magnetically suspended in the air, all sides could be machined without changing the set-up. The result would be a single machine set-up that often called Complete Machining. Integration of various machining processes into one machine tool and six side machining process strategies have transformed the classical process chains with sequential and dedicated machine applications in one clamping [1]. In addition, process designs have been further optimised regarding productivity by introducing parallel processing and hybrid, also known as assisted machining, processes (e.g. laser aided turning).

All these approaches have one main goal: To reduce non-value adding processing times due to transportation and part handling. Usually, this goes along with an elimination of re-clamping operations, which has positive effects on the part accuracy [8].

2.2 Machine flexibility

Machine flexibility is the fundamental building block of the other manufacturing flexibilities. As the machine flexibility increases, a machine tends to be capable of performing a larger number of operations as suggested by Koste and Malhotra [9]. A higher level of product mix flexibility, process flexibility, operation flexibility and routing flexibility are resulting gains [10]. Chen and Chung [11] and Wahab [12] measure machine flexibility as the weighted sum of machine-operation efficiencies.

The different machining operations for this relative complex work piece are done on the same machine, and therefore, as mentioned by Groover [13], the setup/changeover time is used as the measure. Setup time is considered inversely proportional to machining flexibility. The proposed pallet system illustrated in figure 2 offers the capability to adapt a given machine to a wide range of production operations and part styles.



Figure 2: An example of a pallet being mounted on a chuck

The greater the range of operations and part styles, the greater the machining flexibility. The figure clearly illustrates how the different pallets are placed onto the chuck.

2.3 Production flexibility

Production is facing the need for higher productivity, flexibility and quality due to the on-going progress of customisation and global competitive markets. Over the last decade, new manufacturing strategies like high speed and high performance cutting, hard and dry machining, process-integration, complete machining and new tool materials influenced machine tool developments, or have been made possible by it [14]. As a consequence, productive as well as non-productive times could be drastically reduced. Production flexibility also depends on the machine flexibility of the individual machines [13]. If it is economically viable for the company, investing in standardized pallet chucks (receivers) for each machine will be a way to increase the production flexibility. Customized work holding pallet platforms could then be designed for the different complex operations of the parts, which will fit onto these standardized chucks at the different machines as illustrated in figure 2. This will in turn make all the machines more flexible, which will lead to an increase in production flexibility. The designed workholding pallets will also help the company to respond swiftly to demand variation as mentioned by Theodorou [15].

2.4 Flexibility and this study

Other benefits of flexibility include the increase in machine utilization, lower manufacturing lead time and higher labour productivity. In this study precision pallet technology was proposed to re-route some of the work that could only be done on the capital intensive 5-axis machine, to one of the freely available 3-axis machines. Designing processes to perform work on more generic, freely available machines (3-axis) is an application of production flexibility in itself. The method is compared to a method using successive manual setups by means of a time study, as the 5-axis machine was not available.

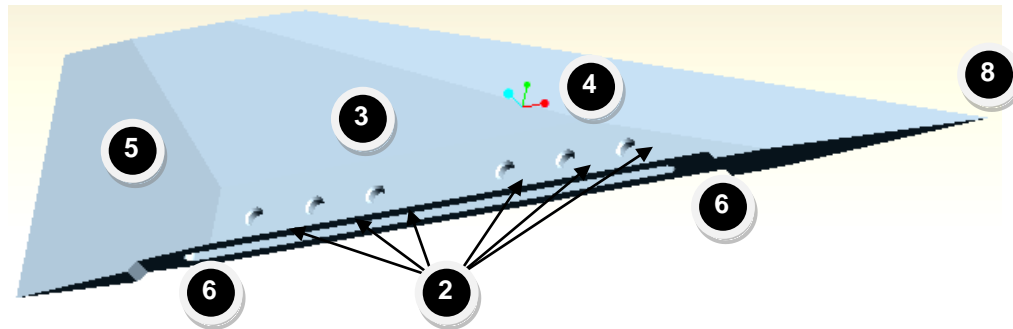
3. Experimental Method

The research method followed consisted of the mapping of the current process, interviews with technical staff on the current and proposed process, as well as a time study. The current process was largely mapped through interviews conducted with the technical staff together with data collection from company records. This information was used as the benchmark. Interviews

throughout the time study served to obtain a better understanding of the problem, to identify opportunities for improvement and to establish a better working relationship with the technical staff.

3.1 Operations to machine missile wing

The technology demonstrator that was suggested by the company is a missile wing. For this component aerodynamic requirements result in a complex geometry, as shown in figure 3. It needs to undergo different machining operations in order to achieve the required shape.



Operation	Description
1	Pre-operation and clean-up cut
2	Drill set-up and counter sunk holes
3	Mill 3° angle face
4	Mill 12° angle face
5	Mill 4° angle face
6	Cut step, 45° angle and slot
7	Final cut and positioning holes are cut off
8	Handwork on leading edge and corners

Figure 3: Different missile wing operations

Similar face milling operations had to be done at different angles, as shown in figure 4. Using a set of different precision pallets, customized to the correct angle, each complex plane is presented to the 3-axis machine as a horizontal plane, resulting in quick machining and a high quality surface finish.

After machining one surface, the pallet is exchanged with another that has been pre-set up. The different cutting operations are indicated in figure 4.

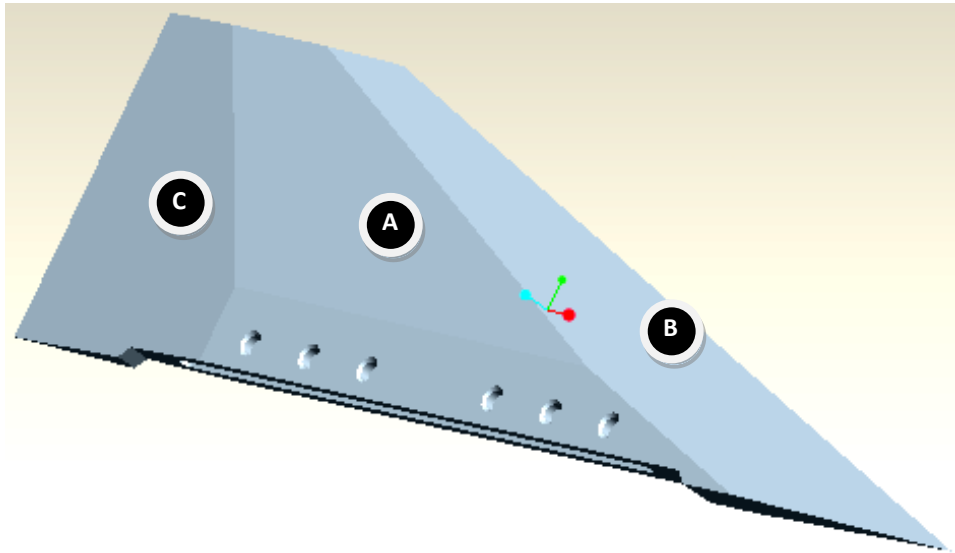


Figure 4: Different milling operations

Cut A is a 3° operation, cut B a 12° operation and cut C a 4° milling operation. Therefore pallets with different angles had to be manufactured to fit on the chuck base of the pallet system.

3.2 Current work clamping process

The established method used at the company to machine these parts was to clamp the work piece into the vice mounted on the bed of the 3-axis milling machine. When loading a new work piece into the machine it is important to establish accurate location of the tool prior to the machining cycle. This is usually done with a touch probe or gauge block which is time consuming. The time spent on this operation contributes to a major part of the setup time.

Traditionally, when loading a new work piece onto a machine, accurate location of the blank must be determined prior to the machining cycle. This increases the setup-time significantly. Likewise, when moving a work piece from one machine tool to another, it is necessary to reload the partially machined part into a fixture or vice and then establish a datum point from which to continue the machining. This transfer process can be time consuming because of the need to re-establish

location of the work piece on the second machine tool. This is also a major potential cause of inaccuracy.

3.3 Proposed pallet process

A systematic approach to part loading and unloading is available to the machining industry through pallet technology. Although this technique is primarily designed for part loading and unloading, it was proposed in this case to emulate 5-axis machining on a 3-axis machine. Using this chuck and pallet system, a work piece reference location only needs to be established once.

Figure 5 illustrates how the different pallets are placed onto the chuck.

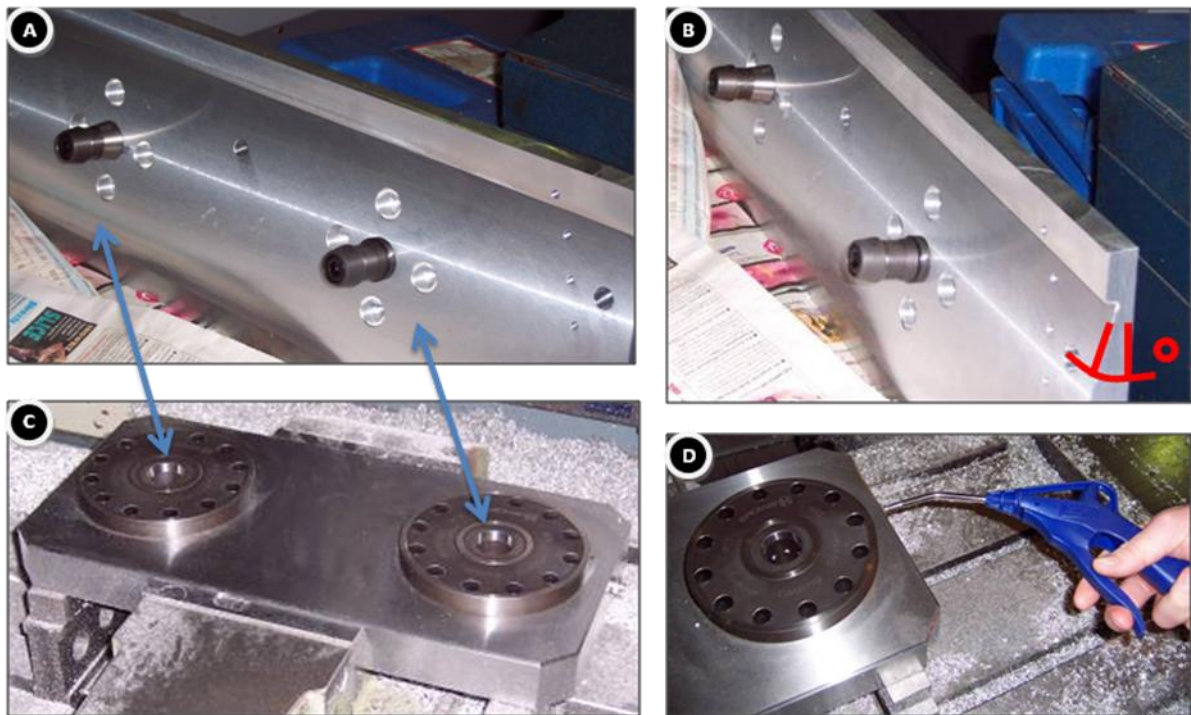


Figure 5: Pallet and Chuck system

Figure 5C shows how this chuck is kept in position by a machine vice. The chuck stays in this position throughout the entire process. All the different cuts are made on this chuck or base assembly. Different pallets are machined with different angles as depicted in figure 5B. These pallets are changed for the different cutting processes as indicated by the arrows in figure 5A. Figure 5D indicates how the pallet is released from the chuck by supplying air at a pressure of about 8 bar. The next pallet is subsequently clicked into position. Research also shows that

palletized work holding systems also offer a unique opportunity to address the problem of vibration control for milling operations from another perspective as described by Rashid et al [16].

Using this setup technology, five sides of the part are accessible to the machine tool cutter. Clamping is achieved using a ball lock mechanism. The lock is positive. It is pneumatically actuated and designed to be fail-safe. Air actuates the opening of the chuck only. It closes mechanically, therefore if the air supply is cut off, the chuck remains securely clamped. It takes only a few seconds to remove a pallet and replace it with the next that has been pre-setup during the machine's operation time. In this way, more time is saved by the elimination of the need to re-establish a datum for each part. Locating and securing pallets and then unloading finished parts takes a significant amount of setup time. Palletizing parts off-line within machining time and then positioning and securing them in common chucks achieve a significant reduction of setup time. In the developed world it is perceived to be common practice for operators to be assigned to more than one machine. In the developing world however, this practice is rare, allowing the possibility to use machining time for setup without having a cost implication.

With the increasing pressure of competition, demands made on flexibility in the workshops are extreme. The production of one-off parts and small series is under particular pressure from the cost spiral. Especially in this area, many plants still have a large cost reduction potential. This could be put to good use, to enhance competitiveness directly, but also by releasing capital intensive 5-axis capacity, indirectly.

4. Results

After experimentation and a time study the following results were recorded. The machining time of the current process was compared to the proposed (improved) process in terms of the first-off machined parts and machining time of all the parts.

The graphs below give a graphical representation of the current process compared to the proposed (improved) process. As indicated in figure 6 the machining of the missile wing consisted of eight different operations. From the figure it can be seen that the time to set-up the first part of the batch for each operation and time to do a quality inspection is also minimized. These results are due to the standard pallet work holding method used for all operations. This standardization also gave the machine shop the ability to interchange work between machines as well as shifts efficiently. Thereby, the machining time is reduced as shown per operation.

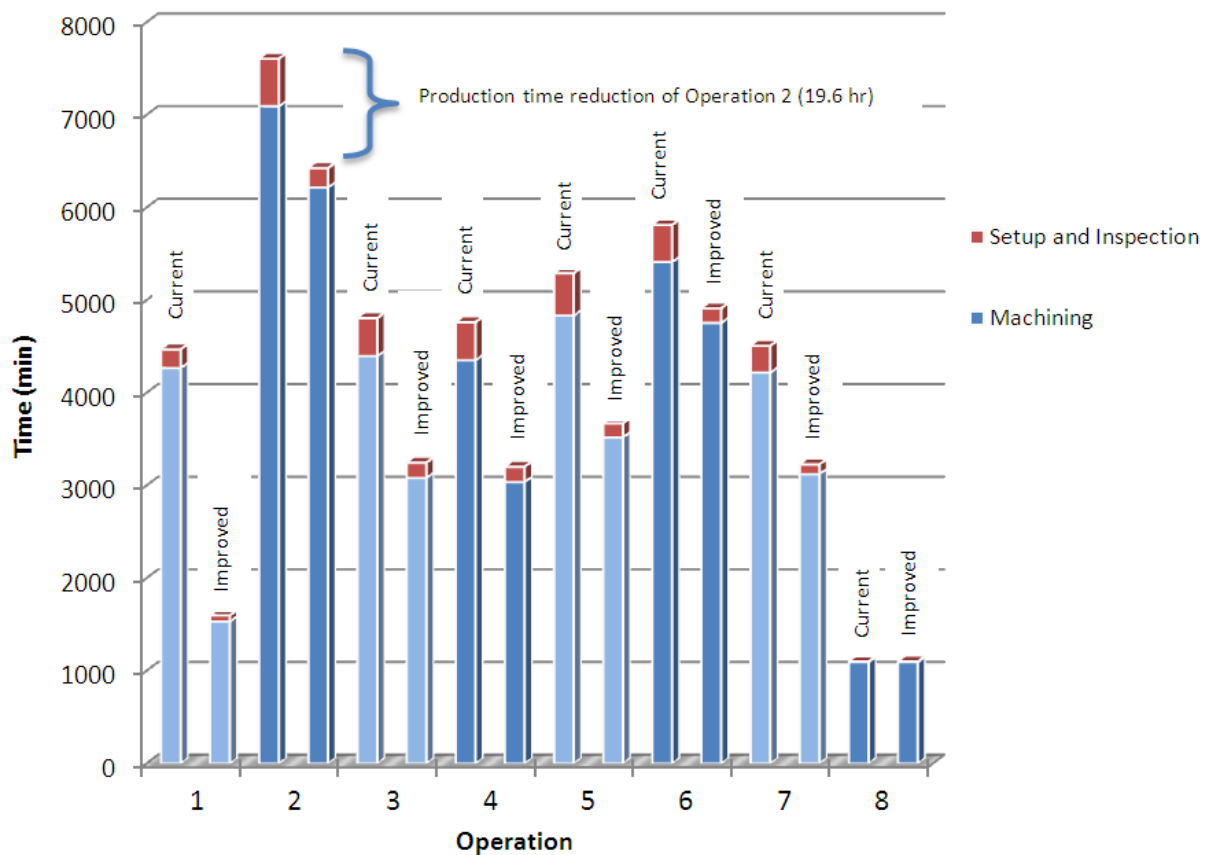


Figure 6: A comparison between the old and improved process for the individual machining times for each operation in the process

From the figures it became evident that the pallet work holding technique decreased the time it took to physically do the set-up and inspection of each operation significantly, and led to a decrease in machining time for each operation. This improved process led to a saving of 183 production hours as shown in figure 7.

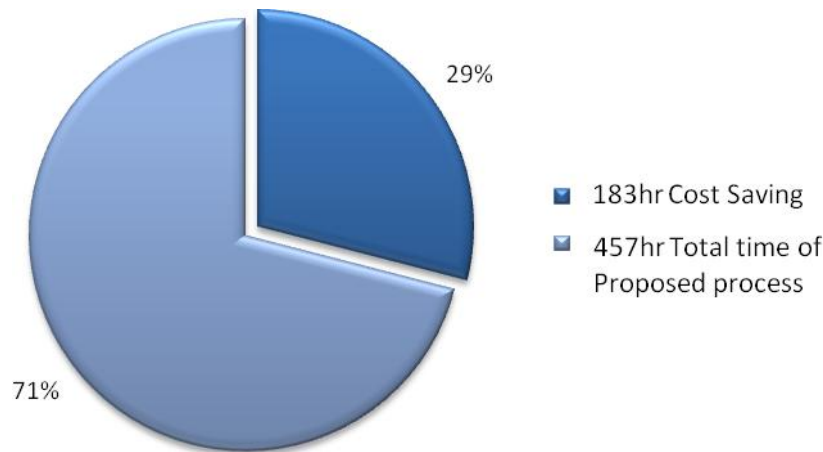


Figure 7: Cost reduction for proposed pallet process (full circle or 640hr represents the existing process)

This cost reduction represents a saving of approximately 20.3 working shifts of 9 hours.

4.1 Return on investment

It is critical for similar enterprises to know how the expected investment compares to the costs. If the 3-axis milling machine that was investigated is occupied with the same type of work, the following calculation of return on investment (ROI) is applicable. It could be argued that the machine will do simple 3-axis work for a significant percentage of its time, in which case this projection of ROI will not be as favourable. For the ROI calculation the conservative assumption was made that the machine will perform similar 5-axis work on the 3-axis machine for 50% of the time. The owner of the machining company argued that it is his objective to increase high complexity work and rather decrease the percentage of simple machining work. The effect of this policy is already reflected in the fact that utilisation of the 5 axis machine has grown to 7 days a week, 24 hours per day. It is therefore not surprising that the owner implemented the technology on several of his 3-axis machines. The ROI is expressed in terms of payback period.

Investment: Chuck: € 4 400, Pallet € 400 x 3.

Expenses: 3-Axis milling machine operates at € 24 / hr with 50% of work to be similar.

Savings: Similar projects can be completed 29 % earlier, resulting in significant savings.

Payback period:

Using $P = A \left[\frac{1 - (1+i)^{-n}}{i} \right]$, [17] and the cash flow diagram below [Figure 9] the payback period was calculated.

where

P (Present value) = € 5 600 loaned at $i = 14\%$ (annually)

A (Annual savings) = € 24 /hr x 50% x 29% x 9(hr/day) x 5(days/week) x 4.2(weeks)
= € 657.72 savings per month

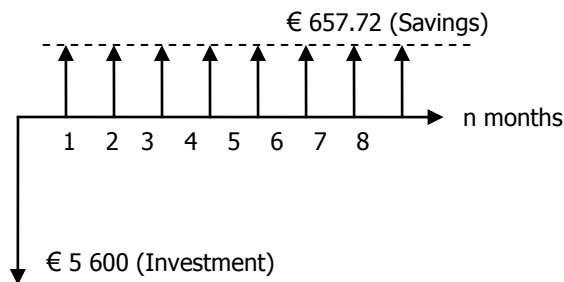


Figure 8: Cash flow diagram of investment

Using a discrete cash flow table [17] with a 1% discrete interest rate, the payback period is 186 days or 8.85 months as illustrated in figure 9.

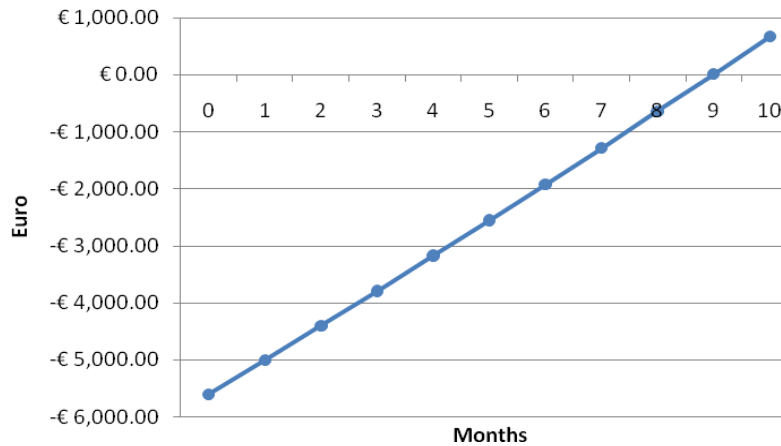


Figure 9: Payback period for initial investment (ROI progression – year 1)

Hours of work per year: = 2250 hr (250 days x 9 hrs)

Cost savings per year: = € 7 830-00 (50% x € 24 x 2250 hr x 29%)

According to the calculation above the company is saving € 7 830-00 per year by investing in this work holding system.

4.2 Discussion

Although it becomes clear that the proposed pallet process shows a significant reduction in time, as well as enabling 5-axis work on a 3-axis machine, there are several other benefits the palletized process introduced.

In the machining sector, standards among equipment makers have mostly been kept as brand specific specifications. Reluctance to establish compatibility between unlike machines and accessories carries over into both hardware and software. Therefore, standardization becomes the individual company's own responsibility. Once the work piece is palletized, it is standardized and can be placed securely on any machine equipped with a compatible receiver or chuck. With this standard work holding method the operator easily reduces his first-off's setup time and also minimized the total time per operation to a large extent. This standardization gave the machine

shop the ability to interchange work between machines as well as shifts efficiently. The design of the pallet and its chuck assured consistent placement of a work piece in a machine tool. These supplementary factors on their own present a strong case for using a palletizing system.

However, it was the proposed process' modularity that gave the machine shop a method of dealing with various applications in an easier, more straightforward way. Modularity is important to processing different sizes and shapes of work piece blanks. The chuck is designed to accept a very large selection of pallet configurations.

5. Conclusion

The implementation of the palletizing system led to a large reduction in the production time. The time study compared the current against the proposed, improved process. The improved process decreased the production hours of 640 hours by 183 hours. This represents a saving of approximately 20.3 working shifts of 9 hours. The current process required approximately 71 working shifts, while the proposed process would require only 50.7 working shifts. This is a 28.6% saving in production time. The company can therefore supply the finished products to their clients a full 20.3 days earlier than originally planned. This amounts to a saving of €7 830-00 per year by investing in this work holding system. Seen from an investment perspective, the capital expenditure will be recovered after a payback period of approximately 9 months.

The pallet system significantly reduced the setup and changeover times, reducing production cost and lead time. If the pallet system is deployed on a larger scale in the company it will contribute to flexibility in a significant way. This project was chosen for its potential to yield cost and lead time improvements. There is little doubt that this level of improvements will not be able to be sustained if the system should be deployed on a larger scale. It however yields improvements that will make a significant contribution to competitiveness. The next step will be to select follow-up jobs that can make use of the technology and gradually implement the technology on a larger scale to simultaneously keep the ROI on the pallet equipment on a profitable level.

It is concluded that this 3-axis technique using palletised work holding is technically feasible and economically viable to machine flat surface aerospace components that would normally be machined on simultaneous 5-axis machines in the developed world.

6. Acknowledgements

Mr Norbert Leicher, Daliff Precision Engineering (Pty) Ltd, for hosting the study.

Mr Zaid Fakier, Daliff Precision Engineering (Pty) Ltd, for his excellent technical inputs.

Mr Aubrey Simon and Mr Werner Lombard, Rheinmetall Denel Systems (Western Cape), for permission to use their product as the test bed for the concept study.

7. References

- [1] **Byrne, G. Dornfeld, D. Denkena, B.** 2003. *Advancing cutting technology*, Keynote Papers STC "C", Annals of CIRP, 52 (2), pp.(483-508)
- [2] **Nagarjuna, N., Mahesh, O., Rajagopal, K.** 2006 *A heuristic based on multi-stage programming approach for machine-loading problem in a flexible manufacturing system*. Robotics and Computer-Integrated Manufacturing 22. pp. 342–352
- [3] **Die Deutsche Werkzeugmaschinenindustrie.** 2001. VDW. Frankfurt/Main. January 2002.
- [4] **Viswanadham, N., Narahari Y.** 1992. *Performance modeling of automated manufacturing systems*. India: Prentice-Hall.
- [5] **William O. Fellers, William W. Hunt.** 2001. *Manufacturing Processes for Technology*, Second Edition, Prentice Hall
- [6] **Shirinzadeh, B.** 1995. *Flexible and automated workholding systems*. Industrial Robot. Vol. 22 No. 2. pp. 29-34. MCB University Press
- [7] **Choi, D.S. Lee, S.H. Shin, B.S. Whang, K.H. Yoon, K.K. Sanjay, E. Sarma** 2001. 'A new rapid prototyping system using universal automated fixturing with feature-based CAD/CAM',

Journal of Materials Processing Technology, 113. pp. 285-290.

- [8] **Grundler, E.** 2002. Weg vom einfachen Drehteil – hin zur Komplettbearbeitung, *VDI-Z Integrierte Produktion*. 144/11-12:29-31.
- [9] **Koste, L.L., Malhotra, M.K.**, 1999. 'A theoretical framework for analyzing the dimensions of manufacturing flexibility. 'Journal of Operations Management 18, 75–93.].
- [10] **Sarker, B.R., Krishnamurthy, S., Kuthethur, S.G.** 1994. *A survey and critical review of flexibility measures in manufacturing systems*. Production Planning and Control 5 (6). pp.512–523
- [11] **Chen, I.J., Chung, C.H.** 1996. 'An examination of flexibility measurements and performance of flexible manufacturing systems.' International Journal of Production Research 34. pp. 379–394.
- [12] **Wahab, M.I.M.** 2005. 'Measuring machine and product mix flexibilities of a manufacturing system'. International Journal of Production Research 43. pp. 3773–3786.
- [13] **Groover, Mikell P.** 2001. *Automation, Production systems, and computer-integrated manufacturing*, Second Edition, Prentic Hall.
- [14] **Weck, M.** 2002. Werkzeugmaschinen für die Produktion von morgen im Spannungsfeld, Proceedings of the Aachener Werkzeugmaschinen Kolloquium 2002, pp. 373-409
- [15] **Theodorou, P.** 1996. The restructuring of production in SME's: the strategy of manufacturing flexibility. In: Papis I, Siskos I, Zopounidis C, editors. Management of SME's. ITE: University Press of Creta. Pp. 47–56.
- [16] **Rashid, A. Mihai Nicolescu, C.** 2006. 'Active Vibration control in Palletized workholding systems for milling', *International Journal of Machine Tools & Manufacture* 46. Pp. 1626–1636.
- [17] **Blank, L. Tarquin, A.** 1985 'Engineering Economy.' Second Edition, McGraw-Hill international book company.

C

*Appendix C: Experimental
machine
programmes*

Program for PCD:

```
0 BEGIN PGM PCD MM
1 BLK FORM 0.1 Z X+0 Y+0 Z-26
2 BLK FORM 0.2 X+310 Y+12 Z+0
3 TOOL CALL 6 Z S2547 F1000
4 L X+0 Y-41.5 F5000 M3
5 L Z+0 F5000
6 APPR LCT X+0 Y+0 Z+0 R14.5 RR F96
7 L X+280 F96
8 DEP LCT X+280 Y-41.5 Z+0 R14.5 F96 M5
9 L Z+200 FMAX
10 L X+0 Y-41 F5000 M3
11 L Z+0 F5000
12 APPR LCT X+0 Y+0.5 Z+0 R14.5 RR F96
13 L X+280 F96
14 DEP LCT X+280 Y-41 Z+0 R14.5 F96
15 L Z+200 FMAX
16 TOOL CALL 0
17 END PGM PCD MM
```

Program for VP15TF:

```
0 BEGIN PGM VP15TF MM
1 BLK FORM 0.1 Z X+0 Y+0 Z-26
2 BLK FORM 0.2 X+310 Y+12 Z+0
3 TOOL CALL 6 Z S2547 F1000
4 L X+0 Y-41.5 F5000 M3
5 L Z+0 F5000 M8
6 APPR LCT X+0 Y+0 Z+0 R14.5 RL F64
7 L X-280 F64
8 DEP LCT X-280 Y-41.5 Z+0 R14.5 F64
9 L Z+200 F5000
10 L X+0 Y-41 F5000
11 L Z+0 F5000 M8
12 APPR LCT X+0 Y+0.5 Z+0 R14.5 RL F64
13 L X-280 F64
14 DEP LCT X-280 Y-41 Z+0 R14.5 F64
15 L Z+200 FMAX M5
16 END PGM VP15TF MM
```